DIGITAL ACCESS TO SCHOLARSHIP AT HARVARD
DASH.HARVARD.EDU

HARVARD LIBRARY
Office for Scholarly Communication

Neural Mechanisms of Gait Regulation and Olfactory Plasticity in Caenorhabditis elegans

Citation
Shen, Yu. 2015. Neural Mechanisms of Gait Regulation and Olfactory Plasticity in Caenorhabditis elegans. Doctoral dissertation, Harvard University, Graduate School of Arts & Sciences.

Permanent link
http://nrs.harvard.edu/urn-3:HUL.InstRepos:14226051

Terms of Use
This article was downloaded from Harvard University's DASH repository, and is made available under the terms and conditions applicable to Other Posted Material, as set forth at http://nrs.harvard.edu/urn-3:HUL.InstRepos:dash.current.terms-of-use#LAA

Share Your Story

The Harvard community has made this article openly available.
Please share how this access benefits you. Submit a story .

Accessibility

Neural Mechanisms of Gait Regulation and Olfactory Plasticity in *Caenorhabditis elegans*

A dissertation presented

by

Yu Shen

to

The Department of Organismic and Evolutionary Biology

in partial fulfillment of the requirements
for the degree of
Doctor of Philosophy
in the subject of

Biology

Harvard University
Cambridge, Massachusetts
September 2014

©2014 – *Yu Shen*

All rights reserved

Professor Yun Zhang Yu Shen

Neural Mechanisms of Gait Regulation and Olfactory Plasticity in *Caenorhabditis elegans*

Abstract

One of the fundamental questions in biological science is to understand how the nervous system functions to generate behavior. The past decades have witnessed much progress in behavioral neuroscience, but it is often challenging to gain mechanistic insights at the molecular and cellular level. The small nervous system and experimental accessibility of the nematode *Caenorhabditis elegans* offer an opportunity to study neural mechanisms underlying behavior in greater detail. Because many of the genes and proteins are conserved across species, studies in *C. elegans* provide useful information to the broad research community. In this dissertation, I use the locomotory gait regulation and olfactory aversive learning as two examples to demonstrate that *C. elegans* neurobiology can offer unique insights into the organization of behavior in more complex organisms.

Chapter 2 of this dissertation characterizes a small neuronal circuit that modulates the amplitude of head deflection in *C. elegans*. *C. elegans* moves its head rhythmically along the dorsal-ventral axis during forward movement. By quantifying local head curvature, I found the cholinergic SMD neurons facilitate head deflection, whereas the GABAergic RME neurons restrain head deflection. I then examined the calcium dynamics in RME and found the activity is

correlated with, but not dependent on, dorsal-ventral head movement. Using a combination of neurophysiological, behavioral and optogenetic approaches, I found that the SMD neurons drive the calcium oscillation in RME via cholinergic neurotransmission. In return, the activated RME releases GABA, tuning down SMD activity via the B-type GABA receptor, and negatively regulates the head bending amplitude. The interaction between SMD and RME contributes to an excitation-inhibition balance in the motor system, which fine-tunes the bending angle and thus optimizes the phase velocity during forward movement. This oscillatory circuit suggests a parsimonious model for a small neural network to regulate the locomotory gait.

The SMD motor neurons are also implicated in a sensori-motor circuit underlying olfactory learning. In Chapter 3, I investigate the plasticity of the circuit in pathogen-induced learning behavior. *C. elegans* learns to avoid the smell of pathogenic bacteria after being infected by the pathogen. I characterize a mutant that displays enhanced olfactory learning, *eol-1*, isolated from a forward genetic screen. *eol-1* acts in the URX sensory neurons to inhibit learning. The protein product of *eol-1* has many homologs in eukaryotes, including the mammalian protein Dom3Z implicated in pre-mRNA quality control. Expressing the mouse *Dom3z* in *eol-1*-expressing cells fully rescues the learning phenotype in *eol-1* mutants, indicating that EOL-1 shares functional similarities with Dom3Z in regulating learning. Mutating the residues that are critical for the enzymatic activity of Dom3Z, and the equivalent residues in EOL-1, abolishes the function of these molecules in learning. These results provide insights into the function of a conserved protein in regulating experience-dependent behavioral plasticity.

In summary, this dissertation aims to understand how a small nervous system regulates complex behavior in *C. elegans*. I show that the neural circuits underlying rhythmic locomotion share common properties, and evolutionarily conserved molecules have similar functions in

regulating neural plasticity. Some of the principles uncovered in *C. elegans* may be generalizable and informative to our understanding of the human brain.

Table of Contents

Acknowledgements

My six years in graduate school has been a wonderful experience. While research has its ups and downs, I have always been surrounded by a fantastic group of people. I could not thank them enough for being excellent company on the joyful journey and for their lasting contribution to my professional and personal growth.

First and foremost, I would like to express my sincere gratitude to my Ph.D. advisor Dr. Yun Zhang. None of the work presented in this dissertation would have been possible had it not been for Yun's support, inspiration and guidance. As a scientist, Yun embraces the uncertainty of scientific research and enjoys exploring the unknown. Instead of following fashion for low-hanging fruits, she has been systematically extending the depth and breadth of the research area of her group, and I am proud of being involved in such endeavors. During my six years in the Zhang lab, I had a great fortune to learn everything from her, from cloning my first ever construct to designing experiments to test my own hypothesis, from writing my proposal for the Ph.D. candidacy exam to drafting correspondence letters to the journal editors. Her door is always open when I need advice or help, but she also leaves enough space for her trainees. In the last two years of my graduate study, I worked rather independently on a project I initiated out of interest. Yun was very open-minded to my random ideas, even though some were proved wrong or unrealistic in retrospect. She shared with me every little excitement from unexpected findings, guided me to forge through puzzling situations, and handled our occasionally different opinions in a very democratic manner. She has an extraordinary mind and many invaluable qualities of a woman scientist: intellectual and exact, yet humble and caring. I deeply appreciate the values and skills she has taught me, and I will benefit from them for a lifetime.

I am very grateful for my thesis committee who guided me through my graduate study. Dr. Colleen Cavanaugh is extremely enthusiastic about my research and is always responsive in our communication. She read my proposal and progress reports page by page and handed them back with hand-written comments. I thank her for all the heart-warming advice and tips she shared, from grant writing to thesis exam scheduling. I thank Dr. Catherine Dulac for offering insightful comments on my research. Every single meeting with her was intellectually stimulating and refreshing. Dr. Bence Ölveczky is not only a brilliant scientist, but also a dedicated teacher. I enjoyed taking his class on the neurobiology of motor control, which set the knowledge basis for one of my research projects. My sincere appreciation also goes to Dr. Sam Kunes, who is one of the most friendly and composed. I thank him for the thoughtful questions he raised at my thesis conferences, and his genuine care about students' professional growth.

Ever since I started my first experiment in the Zhang lab, I have benefited tremendously from my collaborators and colleagues, who are among my very best friends in graduate school. Dr. Quan Wen is my close collaborator in the project on motor neurons. Trained as a physicist, his superb skills in engineering and programming complement mine perfectly. We exchange and debate ideas, share the very first 'Eureka' moments, and encourage each other over the difficult times. For my project on EOL-1, Dr. Jiangwen Zhang analyzed the whole-genome sequencing data, and Dr. John Calarco trained me with great patience on the biochemistry experiments. John also offered generous help with editing my manuscript. I thank them all for being the best collaborators I could ask for. Inside the Zhang lab, I started with a group of fantastic colleagues: Dr. Heonick Ha passed to me her dexterous skills in behavioral assay, Dr. Michael Hendricks shared with me his experience in calcium imaging, and Dr. Adam Bahrami was my fun company on the nights that I spent screening mutants. I benefit greatly from Dr. Gareth Harris's

exceptional knowledge in science and his unparalleled enthusiasm for discussion. I appreciate the contribution of my friend and colleague Dr. Yuqi Qin to the project on motor neurons, and the assistance of a very talented Harvard College student Connie Zhong in my research. My sincere gratitude goes to all the other members of the Zhang lab: my fellow graduate students Dr. Xiaodong Zhang, Dr. ZhunAn Chen, Jingyi Yu and Bicheng Han, our postdoc researchers Dr. Jing Ren and Dr. Konstantinos Kagias, our technicians Chris Meehan, Petra Kubikova, Flavia Chen and Shane Smith, our lab manager Shuli Bigelow, lab alumni Colleen Carlston, Alessandra Donato, and all those who have worked in the Zhang lab. I am incredibly grateful for their friendship and the collegial environment they have created.

My graduate school experience would not have been as enjoyable without the Harvard research community. Dr. Aravi Samuel is a longtime friend and collaborator of the Zhang lab. I thank him for generously sharing research equipment, his insights and humor. I am grateful to Dr. Jeff Lichtman for the wonderful classes he offered on connectomics and scientific presentation. I enjoyed every minute of his lectures filled by passion and wisdom. I thank Dr. Joshua Sanes and Dr. Kenneth Blum for their leadership at the Center for Brain Science, Dr. Edward Soucy, Dr. Joel Greenwood and Steve Turney for offering technical support, and the staff members of the CBS core facility. OEB faculty member Dr. Kirsten Bomblies is my HGWISE mentor for the past four years. A gifted plant biologist and a passionate artist, she shared with me amazing stories from her research, teaching as well as her leisure activities. I am grateful for being able to talk to her about everything like a friend. I also thank other people in the *C. elegans* research community for sharing reagents, protocols and tips, in particular, Dr. Mei Zhen who generously sent us their unpublished transgenic strain. More detailed lists of their names and the funding agencies are included in Chapter 2 and 3.

I have had the fortune to go to graduate school at Harvard thanks to my undergraduate education at Peking University. My undergraduate thesis advisor Dr. Long-Chuan Yu guided the 20-year-old me into the fascinating world of neuroscience and shaped my lab habits and work ethics. Dr. Yi Rao offered me insightful advice on choosing the field of research. Dr. Hongya Gu, Dr. Yan Zhang and Dr. Guo Lu provided strong support for my application to graduate school. I thank the faculty and schoolmates at PKU for instilling in me a sense of rightness and independent thinking. My life abroad is enriched by a number of student groups, including the Harvard Chinese Students and Scholars Association, Peking University Alumni Association, and Harvard Asian American Dance Troupe. My classmates in the department of OEB, in particular Hsiao-Han Chang, Oleg Dmytrenko, Ben Ewen-Campen and Xuemei Zhai, have offered me their warm help in scientific discussion and personal development. I would miss the days we wandered together in the Harvard Forest and the nights we spent curling, chatting and playing skits. I am deeply grateful to my friends in the Chinese student community, who have created for me a home away from home. I would like to give special thanks to Hubo Li, Ting Liu, Dongxing Wang, Fei Wu, and Haifei Zhang for their trust and genuine friendship.

Last but not least, I owe everything to my loving family. I thank my parents Yingxiang Shen and Qingjuan Hua for raising me in a nurturing and caring household. They are self-made man and woman of integrity. Having suffered from the Cultural Revolution in their youth, they value education more than anything else and have made every effort to offer me the best without asking for anything in return. I thank my husband Xiang Ma, who is a passionate neuroscientist and also my best friend. We share so many interests in science and humanities that a lifetime is not enough to spend together. I am very grateful to my grandfather Shoumin Hua, who offered me home education in my childhood and greatly influenced my values. My maternal grand-

mother Jiazhen Xu and paternal grandmother Minshu Wu passed away when I was abroad for graduate school, but their unconditioned love never left me. It is my family who taught me to stay true to myself, to strive for excellence, and to pursue a life with meaning. My deepest gratitude goes to them for their continued support.

Chapter 1. Introduction

I. Neural circuits underlying locomotory behavior

One of the major challenges in neuroscience is to understand the organization of behavior in the language of dynamic activity embedded in a neural circuit. Animals interact with the external world via two interfaces: sensory neurons encode the environmental stimuli into dynamic neuronal activity, and motor neurons innervate the muscle system, translating neural inputs from the upstream processor to behavior outputs. The signal encoding process of sensory neurons has been extensively studied, whereas the motor program has yet to be examined in sufficient detail. However, it is equally important, if not more, to decompose the behavior of an animal into the dynamic activity of its motor neurons, because only by converting both sensory inputs and motor outputs into the same language of neuronal activity can we explain the stimulus-response algorithm of animals by the function of neural circuitry. Rhythmic repeated movement can serve as a promising experimental model in this pursuit. In the past decades, remarkable progress has been made to understand the structural and functional organization of neural circuits that control locomotory behavior in both vertebrate and invertebrate systems (Grillner, 2003; Kiehn, 2006). As an introduction, I will discuss our understanding of the motor circuit underlying the swimming behavior in lampreys, the walking behavior in mammals and the forward/backward locomotion in the nematode *C. elegans*. Some properties, such as reciprocal inhibition and negative feedback, are conserved in the neural circuits of different systems.

The motor circuit for undulatory swimming in lampreys

Lampreys are an order of jawless fish and their central nervous systems are regarded as a vertebrate prototype. Because of its relative simplicity, the undulatory swimming behavior in

lampreys has been well dissected at network and cellular levels (Grillner, 2003). Lampreys swim by propagating a mechanical, laterally directed wave (with a frequency from 0.25 Hz to 10 Hz) along the body, which pushes the rostral end of the animal forward in the water. The whole body of a lamprey consists of about 100 segments. In each segment, the alternating bursts of activity of motor neurons contract the muscles on the left and right side alternatively (Grillner et al., 1991). In isolated brainstem-spinal cord preparation, brainstem stimulation or application of glutamate agonists in the bath solution elicits similar patterns of motor neuron activity, suggesting that the undulatory movement in swimming is controlled by central pattern generators (CPG), i.e. neural networks that can generate rhythmic patterned outputs without sensory feedback (Grillner and Wallen, 2002). The lamprey CPG in the spinal cord, upstream control and sensory feedback of CPG are described below.

Central pattern generators

Central pattern generators (CPG) can produce an organized pattern of motor output independent of sensory inputs, although sensory feedback plays an important role in regulating motor behavior (Marder and Bucher, 2001). The CPG controlling swimming behavior in lampreys consists of three types of interneurons (Fig. 1. 1), one type of excitatory glutamatergic interneurons and two types of inhibitory glycinergic interneurons. The excitatory interneurons (EIN), which possess spontaneous rhythmic activity, activate motor neurons as well as the inhibitory interneurons on the ipsilateral side (Buchanan and Grillner, 1987; Buchanan et al., 1989). One type of inhibitory interneurons, referred to as contralateral crossing inhibitory interneuron (CCIN), inhibits all the three types of interneurons and motor neuron on the contralateral side (Buchanan, 1982). The other type of inhibitory interneurons, named as lateral

inhibitory interneuron (LIN), inhibit the ipsilateral CCINs and occasionally motor neurons (Rovainen, 1974; Buchanan, 1982). In this microcircuit, each side of the spinal cord can generate bursting activity itself, and the cross inhibition mediated by CCIN between the two sides contributes to the alternating left-right rhythmic bursting activity.

Previous research has investigated molecular and cellular mechanisms that underlie the rhythmic activity in the lamprey CPG. In one intact hemisegment, the bursting activity can still be elicited even when glycinergic synaptic transmission is blocked, suggesting the bursting activity is initiated by the ipsilateral excitatory interneurons (EIN) (Cangiano and Grillner, 2002). EINs can receive upstream excitatory inputs or excite each other within the EIN population (Grillner, 2003). During the initiation phase of CPG activity, the voltage-dependent NMDA (N-methyl-D-aspartate) receptor, low-voltage-activated calcium channels (LVA-Ca^{2+}), and sodium channels might be activated (Cohen and Wallen, 1980; McClellan and Grillner, 1984). The activation of NMDA receptors results in plateau-like depolarization and contributes to the maintenance of the depolarizing phase. Calcium ions that enter through the NMDAR and LVA-Ca^{2+} channel or N- and P/Q-type calcium channels during the action potential activate calcium-dependent potassium channels, which contribute to the termination of the depolarizing phase (Grillner, 2003). The interaction of different types of ion channels provides a molecular basis for the rhythmic bursting activity in the neural circuit, which then innervates muscles to control undulatory swimming behavior.

DLR, MLR and RS neurons

In lampreys, the diencephalic locomotor region (DLR) and the mesencephalic locomotor region (MLR) are two locomotory command centers. The lamprey DLR and MLR project

monosynaptically to the reticulospinal (RS) neurons in the middle and posterior rhombencephalic reticular nuclei (MRRN and PRRN), which then activate the spinal CPG (Grillner, 2003). In *in vitro* brain slices, high- frequency stimulation of the DLR elicits rhythmic burst firing of the RS neurons as well as rhythmic excitation in neurons of spinal cord ventral roots (El Manira et al., 1997). In semi-intact preparation with exposed brain stem, where the animal's brain is held immobile and the body free to move, the rhythmic burst firing of the RS neurons generated by stimulating the DLR results in well-coordinated swimming (Menard and Grillner, 2008). Electrical stimulation of the MLR also elicits rhythmic activity of the RS neurons and well-coordinated swimming throughout the stimulation period in semi-intact preparation (Sirota et al., 2000).

Unilateral stimulation of the MLR produces symmetrical bilateral locomotion in all vertebrates, including lampreys (Sirota et al., 2000). Previous studies have shown that the RS neurons receive symmetrical bilateral inputs from the MLR. In semi-intact preparations, electrical stimulation of the MLR or microinjection of AMPA into the MLR induces similar synaptic responses in both sides of the homologous RS cells (Brocard et al., 2010). Retrograde tracing shows that the effect is not mediated by one single cell in the MLR that projects to the RS cells on both sides; instead, some neurons in the MLR project ipsilaterally and others contralaterally, and both types signal to the RS neurons (Brocard et al., 2010). Interestingly, the majority of the DLR neurons project to the MRRN RS neurons ipsilaterally (El Manira et al., 1997) and unilateral stimulation of the DLR also produces symmetrical bilateral locomotion (Menard and Grillner, 2008). The mechanisms underlying such bilateral control remain unclear.

Inputs to DLR and MLR

The diencephalic locomotor region (DLR) and mesencephalic locomotor region (MLR) receive inputs from the basal ganglia, midbrain as well as several sensory processing centers. Retrograde labeling studies reveal that the DLR receives GABAergic projection from the caudoventral, lateral, and dorsal pallium, as well as the striatal region in the basal ganglia (Menard and Grillner, 2008). Injection of GABAergic antagonists facilitates the induction of locomotory movement, suggesting that the GABAergic projections provide tonic inhibition and disinhibition of these projections should release locomotion (Menard and Grillner, 2008). The majority of the GABAergic inputs to the MLR are originated from the medal pallium; a small population of the GABAergic inputs to the MLR comes from the lateral pallium, striatum, thalamus and hypothalamus. These GABAergic inputs also provide tonic inhibition onto the MLR neurons (Menard et al., 2007).

In addition to the GABAergic projections, dopaminergic neurons in the posterior tuberculum (PT) also project to the MLR. PT stimulation evokes DA release in the MLR, activates the MLR and RS neurons and elicits locomotory movement (Ryczko et al., 2013). Some sensory stimuli may evoke locomotion in lampreys by engaging this circuit; for example, olfactory stimuli activate the MLR and DLR via PT and then activate the RS neurons (Derjean et al., 2010). In contrast, visual stimuli and mechanical stimuli can bypass the MLR/DLR to initiate locomotion. Visual stimuli activate the RS neurons via the optic tectum (superior colliculus), sending steering/turning commands to the motor system (Kozlov et al., 2014). Mechanical stimuli delivered on the lamprey's body activate sensory neurons in the primary dorsal root ganglion (DRG); DRG then activate the dorsal column nuclei neurons that project directly to the RS neurons (Dubuc et al., 1993b, a). Mechanical stimulation on the head skin activates trigeminal nerves, which project to the RS neurons indirectly via relay neurons distributed in the

alar plate (Northcutt, 1979; Viana Di Prisco et al., 2005). By taking different paths in the neural network, sensory signals converge to the RS neurons, which then activate the spinal cord CPG to elicit locomotion.

Sensory feedback to the CPG

By definition, a CPG generates rhythmic patterns of output even if no sensory input is present. But in functioning organisms, CPG and its activity are rarely in isolation. A well-known example in lampreys is that passive movement of the isolated spinal cord preparation mimicking a swimming-like pattern can entrain the rhythmic activity of the spinal motor neurons (Andersson et al., 1981). It suggests that sensory feedback produced by the passive movement can effectively modulate the activity of spinal cord CPG. In swimming lampreys, mechanosensation is mediated by a group of neurons called edge cells in the lateral margin of the spinal cord (Grillner et al., 1984). Edge cells express intraspinal stretch receptors. When muscles on one side contract, the edge cells on the contralateral side are activated as their lateral margin is extended, providing stretch signal to the CPG network. There are two types of edge cells: the glutamatergic excitatory neurons (SRE) activate the ipsilateral neurons, and the inhibitory glycinergic neurons (SRI) suppress the activity of the contralateral neurons (Di Prisco et al., 1990). The joint effect of SRE and SRI reduces the activity of the contralateral part of the CPG and enhances the activity of the ipsilateral part. When the input to the CPG is strong enough, the endogenous rhythmic activity is entrained by the exogenous rhythmic activation imposed by passive movement.

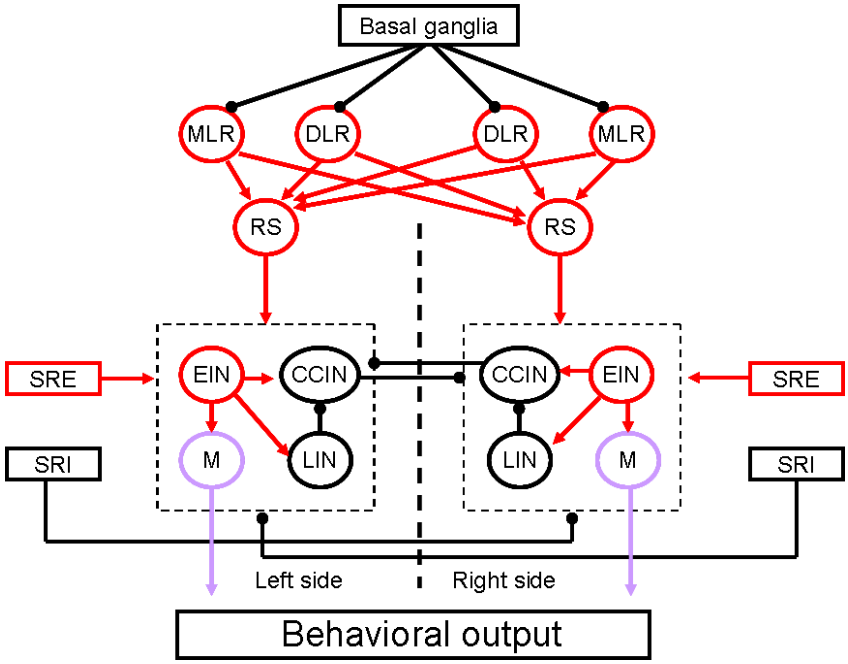

Figure 1. 1 Neural circuit for swimming in lampreys. Schematic representation of the spinal cord CPG, the upstream input and sensory feedback. The CPG consists of three types of interneurons, EIN, CCIN, and LIN. EIN excites ipsilateral motor neurons, LIN and CCIN. LIN inhibits ipsilateral CCIN, which inhibits all cell types in the contrallateral part of the CPG. The CPG receives ipsilateral excitatory sensory feedback from SRE and contrallateral inhibitory feedback from SRI. CPG receives excitatory input from RS. RS are activated by MLR and DLR, which receive input from basal ganglia and other regions. Abbreviation: CPG, central pattern generators; CCIN, contralateral crossing inhibitiory interneurons; DLR, diencephalic locomotor region; EIN, excitatory interneurons; LIN, lateral inhibitory interneurons; M, motor neurons; MLR, mesencephalic locomotor regions; RS, reticulospinal neurons; SRI, inhibitory stretch receptor neurons; SRE, excitatory stretch receptor neurons (Modified from Grillner & Wallen 2002).

The motor circuit for walking in mammals

Although the motor circuit underlying walking in mammals was first studied more than 100 years ago and the concept of 'central pattern generator' was proposed based on these studies (Brown, 1911; Brown, 1914), less is known about its functional organization than about the neural circuit for swimming in lampreys. The large number of neurons in the mammalian spinal cord hinders the progress in mapping the motor circuit by classical electrophysiological and anatomical studies, which have been used in simpler motor systems successfully. Instead, *in vitro* studies of rhythmic neural activity on the isolated rodent spinal cord preparation and powerful genetic approaches in mice contribute significantly to the recent advances in our understanding of the motor circuit for walking in mammals. To generate smooth walking behavior, a motor circuit needs to secure three key functions: rhythm generation, flexor-extensor coordination in a limb, and left-right coordination between limbs. Our current understanding of the neural circuits underlying these basic functions is discussed below.

Central pattern generators and rhythm generation

More than 100 years ago, Thomas Graham Brown proposed a 'half-center' model of CPG organization for flexor-extensor alteration. In this model, he postulated that each CPG contains two half-centers that control flexor and extensor motor neurons in a limb, respectively. The mutual inhibitory connections between the half-centers ensure the rhythmic activity pattern. This model was challenged by the finding that rhythmic activity of the flexor and extensor motor neurons can be evoked after blocking the inhibitory synaptic transmission between the half-centers (Kiehn, 2006). An alternative model proposed by Sten Grillner postulated that extensor and flexor are controlled by "unit burst generators" (Grillner, 1981). Each unit burst generator

(unit CPG) produces the rhythmic activity by itself, and the output pattern of the limb is a result of the combined activity of the different CPGs (Grillner, 1981). To date, multiple lines of evidence support this hypothesis and indicate that the rhythmic activity pattern is generated by the ipsilaterally glutamatergic neurons (Talpalar and Kiehn, 2010). In rodents, the cervical enlargement contains the CPG involved in forelimb movement, and the lower thoracic and lumbar spinal cord contains the hind-limb CPG (Kiehn, 2006). In genetically engineered mice expressing channelrhodopsin in the gluatmatergic neurons, photo-stimulation of the lumbar spinal cord can initiate and maintain the rhythmic activity in isolated spinal cords (Hagglund et al., 2010), suggesting that the glutamatergic neurons are sufficient for rhythmic pattern generation.

Studies using genetic approaches have identified at least three types of glutamatergic neurons involved in the rodent CPG, including the EphA4-positive interneurons, the V2a interneurons, and the Hb9 interneurons in the mouse spinal cord (Kiehn, 2011). The ephrin receptor A4 (EphA4) and ephrin ligand B3 (ephrin B3) knockout mice display a rabbit-like hopping gait rather than alternating walking gaits (Dottori et al., 1998; Kullander et al., 2001; Yokoyama et al., 2001). In both knockout mice, the axon of EphA4-positive spinal interneurons aberrantly crosses the midline barrier formed by ephrin B3, resulting in synchronous neuronal activity on the left and right sides. These findings indicate that at least a subset of the EphA4-poistive spinal interneurons belongs to excitatory CPG neurons, and it is supported by recent results based on intersectional genetics (Borgius et al., 2014). Second, based on the dynamic expression of transcription factors, interneurons in the rodent CPG region in the spinal cord can be divided into five subclasses, V0, V1, V2, V3 and Hb9 (Goulding, 2009). Among them, the ventrally located V2a interneurons are found to directly control left-right CPG circuits (Kiehn,

2011). V2a neurons project to motor neurons ipsilaterally (Dougherty and Kiehn, 2010; Ziskind-Conhaim et al., 2010). However, ablation of V2a neurons disturbs left-right coordination (Crone et al., 2008), suggesting that V2a neurons provide the upstream excitatory input to the commissural neurons responsible for left-right coordination. Thirdly, the homeobox 9 (Hb9) interneurons located close to the midline of the upper lumbar spinal cord are proposed to be involved in rhythm generation (Kiehn, 2011). Hb9 neurons show synchronized firing pattern and rhythmic activity during each locomotor cycle, and they have putative synaptic connections with motor neurons (Kwan et al., 2009; Ziskind-Conhaim et al., 2010). However, because Hb9 neurons share similar transcription factors with motor neurons, they have not been ablated selectively in the spinal cord (Kiehn, 2011). Thus, although Hb9 neurons are hypothesized to provide direct excitation to the motor neurons, there is no direct evidence for their essential role in a rhythm-generation CPG.

Flexor-extensor coordination

One of the challenges for the neural network of limbed animals is to coordinate the activity of flexor and extensor in one limb during walking. To ensure precise timing for activation of the flexor and extensor around individual joints, the CPG network may send alternating excitatory and inhibitory commands to the motor neurons (Kiehn, 2011). The inhibition is usually mediated by GABA or glycine in mammals. Blocking fast inhibitory transmission with GABAA receptor antagonist and glycine receptor antagonist in the rat spinal cord transforms the alternating flexor-extensor activity to synchronous rhythmic activation (Cowley and Schmidt, 1995; Cazalets et al., 1998; Beato and Nistri, 1999), suggesting that inhibitory neurotransmission plays a critical role in flexor-extensor coordination. In addition, the

alternating activation pattern of flexor-extensor persists in hemisected spinal cord (Kjaerulff and Kiehn, 1997), indicating that the crossing interconnections are not required and the flexor-extensor coordination is ipsilateral.

Three types of inhibitory interneurons are implicated in the ipsilateral coordination of flexors and extensors in a limb: Renshaw cells (RCs), reciprocal Ia inhibitory interneurons (rIa-IN) and non-reciprocal group I interneurons, all of which form monosynapses onto motor neurons (Kiehn, 2011). Both the Renshaw cells and rIa-INs show rhythmic activity during walking, in which RCs are activated in phase with the related motor neurons and rIa-INs are activated out of phase (McCrea et al., 1980; Pratt and Jordan, 1987). Anatomical evidence shows that RCs receive collateral inputs from the motor neurons and project to the same population of motor neurons that activate them, whereas the flexor- and extensor-related rIa-INs reciprocally inhibit motor neurons in the other group [Fig. 1. 2A, (Kiehn, 2006)]. Flexor and extensor rIa-INs inhibit each other reciprocally and both receive inhibition from the ipsilateral RCs [Fig. 1. 2A, (Hultborn et al., 1971)], which together contribute to the flexor-extensor coordination. Genetic and molecular studies suggest that RCs and rIa-INs belong to the V1 population of interneurons (Goulding, 2009), which can be labeled by the transcription factor En1 (Alvarez et al., 2005). However, rhythmic inhibition of the motor neurons is not eliminated by complete removal of V1 neurons, suggesting that additional sources exist to generate the reciprocal inhibition. Aside from the V1 origin, part of the rIa-INs may be generated from the Gata2/3-expressing V2b population, which are also inhibitory neurons with ipsilateral projection (Goulding, 2009; Kiehn, 2011). With a better understanding of the developmental origin and molecular markers of these key neurons, future research may utilize optogenetic tools to acutely manipulate neuronal activity and analyze the functional consequence.

Left-right coordination

For animals with a certain degree of left-right symmetry, the other task of the neural circuit is to coordinate the motor behavior of the left and right limbs during walking. Lesion studies have found the left-right coordination of rodent hind limbs is mediated by commissural interneurons (CIN) located in the ventral regions of the spinal cord with their projections crossing the midline (Kjaerulff and Kiehn, 1996; Kiehn, 2011). The CINs are distributed along the hind-limb spinal cord and can be divided into two major categories, intersegmental and intrasegmental CINs, depending on their axonal projections (Cowley and Schmidt, 1997). The intersegmental CINs can be subdivided into ascending, descending, and bifurcating CINs (Bannatyne et al., 2003), and the intrasegmental CINs include three types, CINei, CINi, and CINe [Fig. 1. 2B, (Kiehn, 2011)]. The glutamatergic commissural interneurons CINei provide indirect inhibition of motor neurons via inhibitory interneurons including RC and rIa-INs; CINi projects monosynaptically to motor neurons via inhibitory synapses; CINe projects directly to motor neurons via excitatory glutamatergic synapses. Among them, CINei and CINi contribute to the alternating activation pattern during walking and CINe contributes to the synchronous activity during hopping (Kiehn, 2011).

Genetic studies have revealed that CINei and CINi belong to the V0 group of interneurons marked by the transcription factor Dbx1, and CINe belongs to V3 interneurons (Stepien and Arber, 2008). Further, CINei are Evx-positive and CINi are Evx-negative, allowing potential separation of the two subtypes. CINei neurons also express Sim1, a marker for V3 interneurons (Kiehn, 2011). These genetic markers provide a basis for further study on the development and organization of the microcircuit involved in left-right coordination.

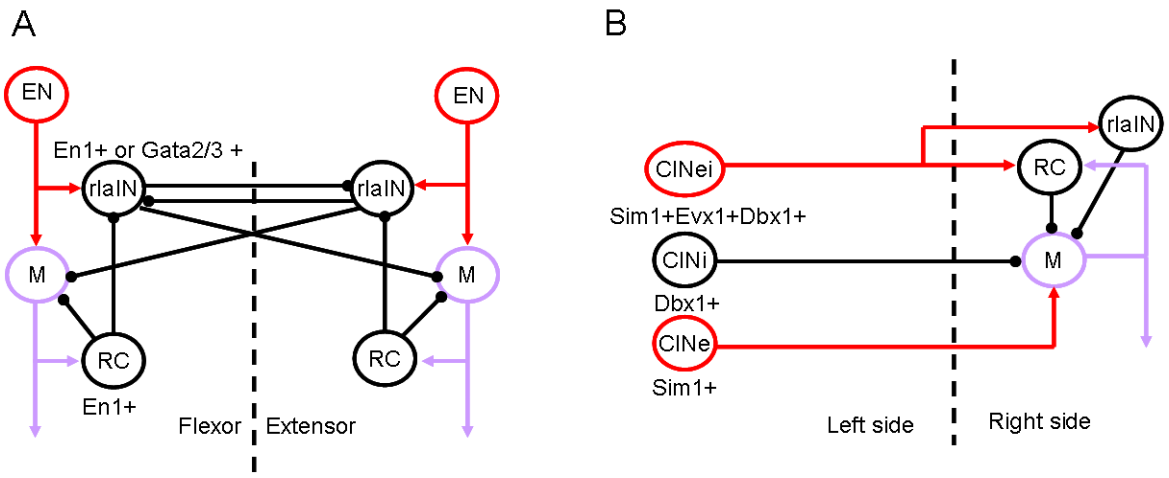

Figure 1. 2 Neural circuit underlying walking in mammals. In the microcircuit for flexor-extensor coordination (A), flexor and extensor rIa-INs receive excitatory inputs and form inhibitory synapses onto the rIa-IN and motor neurons in the other group. RC receives projections from collateral axons of motor neurons, provides negative feedback to motor neurons and inhibits rIa-IN in the same group. RCs are En1-positive. Some of the rIa-INs are En1-positive and others are Gata2/3 positive. In the microcircuit for left-right coordination (B), there are three types of CIN. Among them, CINei express Sim1, Evx1, and Dbx1. They provide indirect inhibition of motor neurons via RC and rIa-IN. CINi express Dbx1 and provide direct inhibition onto motor neurons. CINe express Sim1 and activate motor neurons. Abbreviation: CIN, commissural interneurons; EN, excitatory interneurons; M, motor neurons; rIa-IN, reciprocal Ia inhibitory interneurons; RC, Renshaw cells (Modified from Kiehn 2011).

The motor system in *C. elegans*

The nematode *Caenorhabditis elegans* has several advantages for studying the neural circuit underlying locomotion in a non-limbed model system. First, the connectivity of the 302 neurons in hermaphrodite animals is well defined (White et al., 1986), allowing identification of individual neurons and structure-guided construction of functional circuits. Second, *C. elegans* is highly accessible by both forward and reverse genetic tools, and many of the genes are evolutionarily conserved in mammals. The cloning and sequencing of the *unc-54* gene in *C. elegans* in the 1980s provided crucial information about the myosin heavy chain protein (MacLeod et al., 1981; MacLeod and Talbot, 1983), and many other *unc* mutants identified in genetic screens uncovered useful information about their mammalian homologs (Chalfie and Jorgensen, 1998). Thirdly, on the ground of the first two advantages, recent advancement in biotechnology has offered an unparalleled opportunity in *C. elegans*. It is now feasible to monitor and to manipulate neuronal activity in a freely behaving animal, and the imaging can be performed on a selective set of neurons or the whole brain (Leifer et al., 2011; Schrodel et al., 2013; Tokunaga et al., 2014). With these advantages, *C. elegans* provides a unique system to study how the interaction between specific neurons in a structurally well-defined circuit transforms dynamic neural activities to precise, yet flexible, motor patterns.

On a solid agar surface, the basic locomotory program in *C. elegans* is displayed as rhythmic undulatory forward movement interrupted by backward movement (reversals) and turns (Brenner, 1974; Pierce-Shimomura et al., 1999), all of which are controlled by specific neurons in its sensori-motor circuit (Gray et al., 2005). The motor circuit for undulatory movement has three major components: the command interneurons, motor neurons and body wall muscles. The command interneurons integrate information from upstream interneurons and sensory neurons,

project to four major types of motor neurons that innervate the body wall muscle (Altun and Hall, 2011). Under standard culture conditions, *C. elegans* has an innate bias for forward movement (Brenner, 1974; Pierce-Shimomura et al., 1999). The decision of forward or backward movement depends on the selective activation of different populations of command interneurons and motor neurons.

The command interneurons

The motor neurons in the ventral nerve cord (VNC) of *C. elegans* are driven by five types of command interneurons, or pre-motor interneurons, including AVA, AVB, AVD, AVE and PVC (White et al., 1986). In the touch-induced locomotory behavior, anterior touch induces backward movement and posterior touch induces forward movement. Ablation studies have shown that killing the AVA and AVD interneurons reduces anterior touch response and blocks backward movement; ablation of AVB and PVC reduces posterior touch response and blocks forward movement; single ablation of these interneurons results in uncoordinated forward or backward movement (Chalfie et al., 1985). These findings suggest that the sinusoidal forward or backward moves are coordinated by multiple command interneurons in *C. elegans*.

Based on the *C. elegans* neuronal connectome, AVA, AVD and AVE project to the DA and VA motor neurons, whereas AVB and PVC project to the DB and VB motor neurons (White et al., 1986). Although AVE shares the same connections with motor neurons as AVA and AVD, ablation of AVE has no detectable effect on the spontaneous and tap-induced backward movement (Wicks and Rankin, 1995), suggesting that AVE is not essential in the circuit for reversal. Calcium imaging of multiple neurons shows that AVA and AVE, but not AVD, exhibit synchronized activation during spontaneous reversals, whereas AVB activity is correlated with

forward movement (Kawano et al., 2011). However, optogenetic stimulation of the sensory neuron ASH or interneuron RIM activates both AVA and AVD in the induced avoidance behavior (Guo et al., 2009), suggesting that different command interneurons may be involved during spontaneous or stimuli-induced reversals.

The ventral nerve cord (VNC) motor neurons

The command interneurons innervate motor neurons in the ventral nerve cord. Among the 113 motor neurons in *C. elegans*, seventy-five innervate the body wall muscles. These VNC motor neurons are classified into eight distinct cell types: AS, DA, DB, DD, VA, VB, VC, and VD. The primary target of VC is vulvar muscle; in the other seven classes involved in undulatory movement, VA, VB, DA, DB, AS neurons are cholinergic and excitatory, whereas VD and DD are GABAergic inhibitory neurons (White et al., 1986; Altun and Hall, 2011). The D- and V-motoneurons innerve different groups of the body wall muscles: DA, DB, DD, and AS neurons innervate dorsal muscles, and VA, VB, and VD neurons innervate ventral muscles.

The VNC motor neurons have distinct locomotory functions (Fig. 1. 3). A-type neurons receive projections from AVA/D/E and mediate backward movement; in contrast, B-type neurons receive projections from AVB/PVC and mediate forward movement. The identity of A-type neurons VA and DA requires a paired-class homeodomain protein UNC-4 (Miller et al., 1992). In *unc-4* mutants, VA neurons receive projection from AVB rather than AVA, thus the animals show defects in backward movement (White et al., 1992). Calcium imaging studies found that the activity of VB neurons is higher than VA neurons during forward movement, whereas the activity of VA neurons exceeds VB during backward movement (Kawano et al., 2011). It suggests that imbalanced activity of the two motoneuron circuits underlies the

directionality of locomotory behavior. Interestingly, the coupling between the command interneuron AVA and the A-type motor neurons is found to be mediated by gap junctions, specifically, the UNC-7 and UNC-9 innexins in *C. elegans*. The UNC-7/UNC-9 gap junctions between AVA and A-type neurons suppress the activity of reversal-mediating A-type neurons when AVA is silenced, thus maintain the backward microcircuit at a low output state and promote forward movement (Kawano et al., 2011). The forward-promoting AVB and B-type neurons are also connected by gap junctions, but their roles remain unclear. A recent study has proposed that the B-type motor neurons in VNC transduce proprioceptive signals to couple adjacent body regions, propagating the undulatory wave from head to tail during forward movement (Wen et al., 2012). This newly identified function of B-type motor neurons agrees with the cellular economy of the *C. elegans* wiring diagram, in which many neurons have a high level of complexity and often multiple functions (Wen et al., 2012).

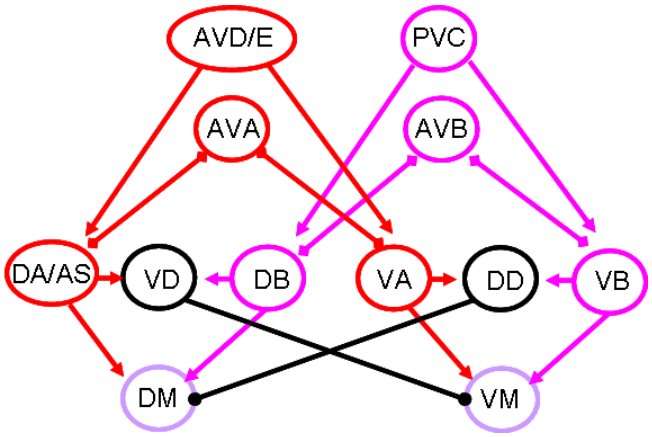

Figure 1. 3 Neural circuit underlying *C. elegans* undulatory movement. The command interneurons for backward movement are AVA, AVD, AVE, which project to VA, DA and AS motor neurons. The command interneurons for forward movement are AVB and PVC, which project to VB and DB motor neurons. Dorsal muscles (DM) receive excitatory inputs from DA, DB, and AS motor neurons; ventral muscles (VM) receive excitatory inputs from VA and VB. DM and VM receive inhibitory inputs from D-type motor neurons, DD and VD, which are activated by A- and B-type motor neurons. The activation of dorsal muscles by DA/DB motor neurons is coupled with the inhibition of ventral muscles mediated by VD motor neurons; the activation of ventral muscles by VA/VB motor neurons is coupled with the inhibition of dorsal muscles mediated by DD motor neurons.

In addition to the command interneurons and VNC motor neurons, the head motor neurons also play key roles in the motor system of *C. elegans*. The anteriormost head muscles are mainly innervated by head motor neurons SMD, RME, RMD and SMB; the neck muscles are mainly innervated by head motor neurons SMD, RME, RMD, SMB, RIV, RIM and the ventral nerve cord (White et al., 1986; Gray et al., 2005; Altun and Hall, 2009). The roles of individual neurons in locomotion have been probed into both experimentally and computationally (Sakata and Shingai, 2004; Gray et al., 2005; Kocabas et al., 2012), but it remains unclear how the excitatory and inhibitory activities are coordinated to generate the initial wave that is propagated into the forward locomotory gait. In Chapter 2, I will discuss a small motoneuron circuit that regulates the amplitude of head deflection bidirectionally. Furthermore, pre-motor and motor neurons in *C. elegans* are involved in more than simple locomotory behavior. Previous studies in the lab have shown that the command interneuron AVA secrets a *C. elegans* TGF-beta ligand DBL-1 to regulate olfactory aversive learning induced by pathogenic bacteria (Zhang and Zhang, 2012). The head motor neuron SMD not only regulates the motor output of learned olfactory preference, but also modulates the neurophysiological properties of a key interneuron required for neural plasticity (Ha et al., 2010; Hendricks et al., 2012). In the next section of Chapter 1, I will introduce olfactory learning as a behavioral paradigm to investigate the mechanisms underlying neural plasticity.

II. Neural mechanisms of olfactory learning

Olfactory memory: a neuroscience perspective

Scents can be powerful triggers of memories. The scent of a pine tree is a reminder of Christmas, whereas smells of chlorine bring one back to summer vacation spent beside a swimming pool. In the well-known novel *Remembrance of things past* (Proust, 1932), the flavor of a madeleine biscuit dipped in a cup of tea unwillingly triggered detailed memory of the author's childhood. The experience, later referred to as the "Proust phenomenon" (Chu and Downes, 2000), implies that olfactory memory has unique autobiographical content and strong emotional potency upon retrieval (Herz and Schooler, 2002; Herz et al., 2004). This fascinating nature of olfactory memory has been noted in literature and discussed frequently in psychology, anthropology, medicine, and neuroscience. Recent neuropsychological studies have shown that odor-cued memories are often more emotional and vivid than memories evoked by visual or audial stimuli (Herz and Cupchik, 1995; Chu and Downes, 2002), causing a stronger feeling of being brought back to the circumstance remembered (Herz and Schooler, 2002; Willander and Larsson, 2006). Brain imaging studies have also provided neurobiological evidence for the emotional saliency of olfactory memory (Herz et al., 2004; Vermetten et al., 2007).

In the past two decades, increasing efforts have been devoted to understanding the neural mechanisms of acquisition, storage and retrieval of olfactory memory (Wilson et al., 2004; Tong et al., 2014). In humans or non-human primates, olfactory learning and memory are usually studied by psychophysics test on healthy individuals or subjects with brain lesion or resection. Olfactory function is evaluated from two main aspects, namely "peripheral" and "central", referring to the basic ability to detect an odor and higher-level processing such as odor

identification, discrimination and recognition, respectively (Martzke et al., 1997; Atanasova et al., 2008). Among many test types, odor recognition is often used to assess olfactory learning and memory (Dade et al., 2002); other tests include odor discrimination after aversive conditioning, perceptual learning or more complex cross-modal tasks (Gottfried et al., 2004; Li et al., 2006b; Atanasova et al., 2008; Li et al., 2008). These behavioral procedures are often combined with functional brain imaging such as Positron emission tomography (PET) and functional magnetic resonance imaging (fMRI) to examine the activity of brain areas during memory processing (Dade et al., 2002; Gottfried et al., 2004; Herz et al., 2004).

Neural substrates of olfactory learning and memory

In the main olfactory system of the human brain, an odor is processed in a neural circuit that consists of three primary stages: the olfactory epithelium, bulb and cortex (Yeshurun and Sobel, 2010). Both the epithelium and the bulb play essential roles in odor processing: about 350 functional receptor types are expressed within ~12 million olfactory receptor neurons (ORNs) in the epithelium (Moran et al., 1982; Glusman et al., 2001); each ORN is believed to express only one of the receptor types (Vassar et al., 1993; Chess et al., 1994), and all ORNs expressing a particular type of olfactory receptor converge on the same glomerulus and project to the olfactory bulb (Yeshurun and Sobel, 2010). The primary olfactory cortex mainly refers to the piriform cortex (Haberly, 2001; Yeshurun and Sobel, 2010); beyond that, olfactory information is also projected to the orbitofrontal gyri, the insular cortex and the amygdala (Small and Prescott, 2005; Kadohisa, 2013).

Lesion and functional imaging studies have evaluated the roles of the piriform cortex, orbitofrontal cortex (OFC) and amygdala in olfactory learning. Using an odor learning and

recognition task, Dade et al. found that epilepsy patients who had undergone resection of a temporal lobe (including primary olfactory cortex) performed significantly less well than control subjects (Dade et al., 2002). By PET imaging on healthy individuals, the study also found that the activity in the piriform cortex increased during odor recognition but not odor encoding, suggesting that piriform cortex may have an active role in olfactory memory processing instead of acquisition (Dade et al., 2002). The result is consistent with another finding based on fMRI and a cross-modal memory task, which showed that the piriform cortex was activated during memory retrieval (Gottfried et al., 2004). The piriform cortex has also been implied in aversive olfactory learning. Combining multivariate fMRI and an olfactory psychophysics procedure, Li et al. found that the spatial divergence of ensemble activity patterns in the piriform cortex paralleled the enhancement of odor enantiomer discrimination after aversive conditioning (Li et al., 2008). The study demonstrates interesting correlation between aversive olfactory learning and piriform neural plasticity, but whether a causal relationship exists needs to be verified.

The function of the orbitofrontal cortex (OFC) has been studied in odor recognition memory. An early study on 121 patients with cerebral excision from different areas found that excision from the right temporal or orbitofrontal cortex caused impairment in the odor recognition task (Jones-Gotman and Zatorre, 1993), suggesting OFC is required for normal odor memory. Another study based on an fMRI paradigm of odor habituation reported that olfactory perceptual learning experience induced neural plasticity in OFC, and the magnitude of changes in OFC activity predicted behavioral improvement (Li et al., 2006b). However, because of limited control for lesion study and the temporal insensitivity of functional neuroimaging, it remains unclear in which step of memory processing OFC is required (Gottfried et al., 2004).

The amygdala receives direct projection from the olfactory system in non-human primates (Carmichael et al., 1994; Kadohisa, 2013). It is well established that amygdala has a critical role in human emotional memory (Cahill et al., 1995; LeDoux, 2000), thus the anatomy supports the emotional salience of olfactory memory. A psychophysics study on patients with temporal lobectomy showed that bilateral amygdala damage severely impaired odor recognition memory (Buchanan et al., 2003). Further, behavioral test and fMRI imaging revealed specific activation patterns in the amygdala during recall of personally meaningful odors (Herz et al., 2004), providing neurobiological evidence that amygdala activity underlies the emotional potency of olfactory memory. As technologies advance, structural and functional connectome at higher resolution will help understanding how the odor information is processed and integrated with the emotional meaning in the amygdala or additional brain regions.

Olfactory memory study in neuropsychiatric diseases

The acquisition and storage of olfactory memory share common neural substrates with many of the human neuropsychiatric disorders (Martzke et al., 1997; Atanasova et al., 2008). The brain areas that play key roles in olfactory recognition, such as OFC and amygdala, are also implied in altered cognitive function in schizophrenia, depression and dementia caused by neural degeneration (Mesholam et al., 1998; Pause et al., 2003; Lombion-Pouthier et al., 2006; Atanasova et al., 2008). For example, schizophrenia patients show defects in odor sensitivity, identification, discrimination and memory (Moberg et al., 1999; Hudry et al., 2002; Moberg et al., 2003). Patients with neurodegenerative disorders such as Alzheimer's disease (AD) and Parkinson's disease (PD) have altered odor identification and recognition abilities, and the olfactory deficit reflects the likelihood of clinical conversion from mild cognitive impairment to dementia (Mesholam et al., 1998; Conti et al., 2013). Therefore, olfactory processing may be

used as an early functional readout of key brain regions and provide diagnostic potential in clinical settings (Moberg et al., 2003; Conti et al., 2013).

The emotional potency and long-term retention of olfactory memory are also implicated in neuropsychiatric disorders. Several studies have reported that specific smells associated with traumatic experience can precipitate emotional memories in patients with posttraumatic stress disorder (PTSD) or induce panic attack in refugees (Kline and Rausch, 1985; Vermetten and Bremner, 2003; Hinton et al., 2004). By combining PET imaging and psychophysics test, Vermetten et al. found that combat veterans with PTSD showed increased anxiety to the trauma-associated odor diesel and increased regional blood flow in amygdala, insula and selected cortical areas (Vermetten et al., 2007), supporting that trauma-associated odor cues are effective reminders of the pathological memory in PTSD. Understanding how the information is integrated by the olfactory system and peripheral brain areas may offer hints to develop new cue-exposure therapy or pharmacological intervention.

Olfactory learning in rodent and insect model systems

Although psychophysics studies of olfactory memory in human subjects have been fruitful, the approach is limited by the availability of qualified patients, the resolution of brain imaging and other ethical considerations related to human subject research. Recent initiatives have started to probe into the genetic underpinnings of human olfaction (Keller et al., 2007; Knaapila et al., 2012; Jaeger et al., 2013; McRae et al., 2013), but not all the issues can be resolved. So far, most of our knowledge about human olfactory memory at the molecular and cellular level is based on neuroscience research in model organisms, in particular, rodents and insects.

Several reasons explain the advantages of using model organisms to study olfactory learning and memory. First, the structural and functional organization of the olfactory system shares remarkable similarity in different organisms. Both insects and mammals use a hierarchical path of odor processing that comprises the 1st layer of olfactory neurons (ORNs), the 2nd layer of projection neurons (PNs, in insects) or mitral/tufted neurons (M/T cells, in mammals), and the 3rd layer of central olfactory organ, namely the mushroom body (MB) and lateral horn (LH) in insects and the primary olfactory cortex in mammals (Davis, 2004). Rodent or insect ORNs that express the same olfactory receptor type project their axons to the same glomeruli, and the PNs or M/T cells directly project to the central olfactory organs. Second, olfaction is a highly developed sensory modality in rodents and insects, often associated with salient values like food, mate or predator threat. Odorants can be paired with food reward or unpleasant punishment to establish robust appetitive or aversive learning, and the memory can be long-lasting (Waddell and Quinn, 2001). Third, some model organisms like mice and the fruit fly *Drosophila* are highly accessible by genetic and neurophysiological tools. It is now possible to generate animals with conditioned gene-knockout in a particular group of neurons, monitor the neuronal activity in real-time during olfactory learning task, and use optogenetic tools to manipulate neuronal activity and even falsify memory (Rebollo et al., 2014; Wu et al., 2014). Lastly, many genes involved in the olfactory system, especially those required for higher-level functions such as learning and memory, are conserved from insects to mammals (Waddell and Quinn, 2001). Therefore, important molecular components identified in model organisms can be mapped back to the human genome for comparative study of gene function. Below I will discuss a few examples from mouse and fly models of olfactory learning.

Mouse model of olfactory learning

One of the most commonly used olfactory assessments in mice is the odor discrimination task. As in other learning paradigms, the task can be performed with two general categories of olfactory conditioning procedures, classical conditioning and instrumental conditioning (Bodyak and Slotnick, 1999; Mihalick et al., 2000; Schellinck et al., 2001; Pavesi et al., 2013). In the appetitive training procedure, two odors are paired with or without an attractive unconditioned stimulus such as sugar; during test period, the animal's olfactory preference represented by digging time or discrimination reversal is measured (Mihalick et al., 2000; Schellinck et al., 2001). In the aversive training procedure, odors are associated with harmful stimulus such as electric foot shock, and animals acquire fear response to the odor after conditioning (Otto et al., 2000; Paschall and Davis, 2002; Jones et al., 2005). The instrumental conditioning is applied with food or water reinforcement to enhance animal's ability of odor discrimination (Bodyak and Slotnick, 1999).

Because trauma-associated odor cues have been shown to precipitate emotional memory in PTSD (Vermetten et al., 2007), it is of particular interest to model odor-mediated fear conditioning in mice. Multiple lines of evidence show that mice are able to develop olfactory-cued fear (Otto et al., 2000; Paschall and Davis, 2002). Freezing and startle responses are increased after olfactory conditioning, and animals can discriminate the odor paired with shock from a neutral odor (Jones et al., 2005). Human studies have suggested that aversive conditioning alters odorant-evoked neural activity in the piriform cortex (Li et al., 2008). Using a GFP-based calcium indicator to measure the activity in mouse glomeruli, Fletcher reported that foot shock-based aversive training enhanced (M/T) cell glomerular representation to the conditioned odor, especially by increasing the activity level of initially weakly activated

glomeruli in which the odor was delivered with foot shock (Fletcher, 2012). The results resonate with a previous study based on electrophysiological recording (Doucette et al., 2011), which shows mitral cells respond differently to the rewarded and unrewarded odors as mice learned to discriminate between them. Together, it suggests that the associative plasticity occurs in cortical and limbic brain areas, and the information about rewarded stimulus is located at the (M/T) cell level (Doucette et al., 2011).

Interestingly, one recent study suggests the plasticity could happen even earlier. Using a trial-based, discriminative olfactory fear-conditioning paradigm, Kass et al. performed optical imaging on the mouse olfactory sensory neurons (OSNs). Instead of calcium indicators, the study used a fluorescent exocytosis indicator to allow *in vivo* visualization of odorant-evoked signals, which indicates neurotransmitter release from the OSN axon terminals to glomeruli in the olfactory bulb (Kass et al., 2013). By imaging individual mice before and after odor-cued aversive training, the authors found that fear conditioning selectively facilitated the OSN output evoked by the shock-predictive odor (Kass et al., 2013). It suggests that fear learning altered the early representation of odors associated with aversive experience by modulating the synaptic output of the OSNs, which may enhance the olfactory system's sensitivity to the threat-predictive odor signal (Kass et al., 2013). This proposed mechanism supplements to a previous report of structural plasticity, which described enlargement of specific glomeruli and increase in olfactory sensory neurons induced by odor-cued fear conditioning (Jones et al., 2008). Whether the peripheral neural plasticity can be generalized to other sensory modality or in other organisms remains a curious question.

Drosophila olfactory learning

The fruit fly has proved to be more intelligent than expected. Since the first olfactory conditioning assay was established in 1974, *Drosophila* has become one of the most favored invertebrate model organisms to study the molecular genetics of learning and memory (Quinn et al., 1974; Waddell and Quinn, 2001). Paradigms of habituation, sensitization, classical conditioning and instrumental conditioning are now available, in which *Drosophila* modifies its response to a variety of stimulus, including odor, taste, touch, light and context based on experience (Quinn et al., 1974; Tully and Quinn, 1985; Corfas and Dudai, 1989; Liu et al., 1999; Waddell and Quinn, 2001). The olfactory conditioning can be appetitive or aversive: flies learn to avoid an odor that was paired with an electric shock, or learn to approach an odor that was presented together with a food reward (Tempel et al., 1983; Tully and Quinn, 1985; Waddell and Quinn, 2001). In either case, the odor information as conditioned stimulus is integrated and associated with the unconditioned stimulus. The acquisition of learned odor preference depends on the stimulus intensity and training interval; the learned behavior decays gradually within the first several hours, but a long-term memory is still present after 24 hours (Tully and Quinn, 1985).

Because of its robustness and efficiency, the olfactory conditioning procedure in *Drosophila* turns out to be extremely useful in neurogenetics research of learning and memory. Many mutants isolated in genetic screens show deficiency in different stages of the assay, and analysis of these mutants has revealed the role of intracellular signal transduction cascades in distinct phases of olfactory memory [Fig. 1. 4, (Dudai, 2002)]. The first mutant isolated, *dunce*, is defective in forming short-term memory after three training trials, although its ability to sense the odorants is unimpaired (Dudai et al., 1976). Another mutant *rutabaga* shows the same

deficiency, and a third mutant, *amnesiac*, has fairly normal learning but retains memory poorly (Quinn et al., 1979). Molecular cloning and characterization of these genes unveiled that they all participate in the cAMP signaling pathway: *dunce* encodes a cAMP-specific phosphodiesterase, *rutabaga* encodes a Ca^{2+}/calmodulin-dependent adenylyl cyclase, and the product of the *amnesiac* gene is a pre-proneuropeptide neurotransmitter that stimulates the cAMP cascade (Chen et al., 1986; Levin et al., 1992; Feany and Quinn, 1995; Waddell and Quinn, 2001). It provides independent evidence in support of the critical role of the cAMP signaling pathway, first identified in the sea slug *Aplysia*, in learning and memory (Kandel, 2001). Further, transgenic *Drosophila* expressing an antagonist of the transcription factor CREB, dCREBb, is devoid of protein synthesis-dependent long-term memory (Yin et al., 1994). Additional learning mutants isolated from behavioral screens are mapped to genes include *radish*, *latheo*, *nalyot*, *linotte*, and more, which either alter the brain structure or specifically disrupt a certain phase of memory (Waddell and Quinn, 2001; Dudai, 2002). Many of the genetic regulators of olfactory memory formation and processing are found to be evolutionarily conserved from insects to mammals (Kandel, 2001; Waddell and Quinn, 2001). The genetic amenability and easiness of screen in *Drosophila* offer an advantage in identifying enhancers, suppressors or other components in the existing pathway or unveil novel molecular mechanisms of olfactory learning.

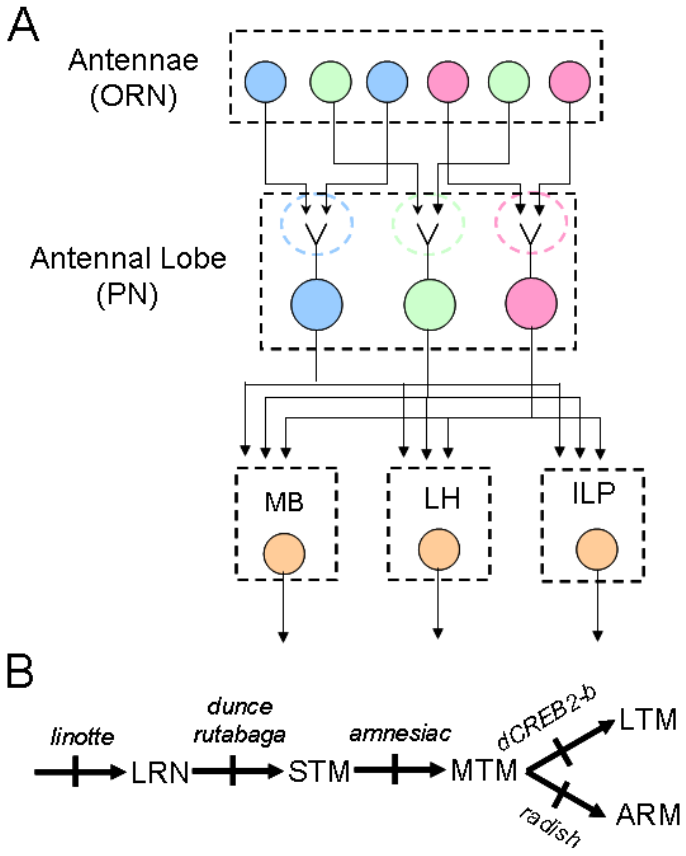

Figure 1. 4 Anatomical organization of *Drosophila* olfactory nervous system and genetic dissection of *Drosophila* olfactory memory. A, In *Drosophila*, the olfactory receptor neurons (ORNs) are located in the antennae and project to the antennal lobe, where they terminate in the glomeruli and target on the projection neurons (PNs). ORNs that express the same olfactory receptor project to the same glomeruli. PNs project to three regions: mushroom bodies (MB), lateral horn (LH) and the inferior lateral protocerebrum (ILP) (Modified from Davis 2004). B, Olfactory memory mutants. *linotte*, a mutant defective in learning (LRN); *dunce* and *rutabaga*, mutants defective in short-term memory (STM); *amnesiac*, mutant defective in middle-term memory (MTM); Transgenic animals expressing dCREB2-b are defective in long-term memory (LTM); *radish*, a mutant defective in memory that is resistant to anesthesia (ARM) (Modified from Dudai 2002).

To bridge the gap between genes and behavior, remarkable progress has been made in *Drosophila* to understand the neuronal basis of olfactory learning and memory. In regard of the hierarchy in the olfactory system, the mushroom body (MB) and lateral horn (LH) neurons in *Drosophila* are the equivalents of the mammalian amygdala and primary olfactory cortex, where most of the neural plasticity is believed to occur (Davis, 2004). *In vivo* recordings have shown that the spiking activity in MB Kenyon cells (KCs) is reduced compared with the high probability of response to odor stimulus in its input, the projection neurons (PNs) (Perez-Orive et al., 2002). By anatomical and physiological analysis, the study found that the sparse odor representation in KCs is caused by feed-forward inhibition from GABAergic neurons in the lateral horn in an odor-stimulated manner (Perez-Orive et al., 2002). The sparse response of MB neurons is also noted in a study based on calcium imaging, which shows only small sets of MB neurons are activated by different odor stimuli (Wang et al., 2004). It is proposed that the LH-imposed constraint on MB neurons contributes to the neural substrate for associative learning because conditioning experience may disinhibit the KCs and thus modify the odor representation in learned animals (Davis, 2004; Olshausen and Field, 2004). The relevance of this model to behavioral performance is recently tested. By optical imaging and thermogenic manipulation of neuronal activity, Lin et al. found a negative feedback circuit between Kenyon cells and the GABAergic anterior paired lateral (APL) neurons (Lin et al., 2014). KCs activate APL and APL neurons inhibit KC, resulting in the sparse odor presentation in the mushroom body. Disrupting the feedback circuit decreases sparseness in KC response and impairs animal's learning to discriminate similar odors, suggesting the inhibitory circuit helps maintain odor specificity of memory (Lin et al., 2014). Similar techniques are used to elucidate the role of dopaminergic modulation of cAMP signaling in establishing spatial patterns of plasticity in olfactory learning

(Boto et al., 2014). As new toolkits are developed for intravital microscopy and optogenetic manipulation (Sinha et al., 2013; Dipt et al., 2014; Inagaki et al., 2014; Wu et al., 2014), studies of the neuronal circuit will complement the classic findings in behavioral genetics and provide a holistic understanding of olfactory learning and memory in *Drosophila*.

Neural underpinnings of olfactory learning in *C. elegans*

The nematode *Caenorhabditis elegans* offers an opportunity for further characterizing the neural mechanisms of olfactory learning. Olfaction is one of the most highly developed sensory modalities in the tiny soil-dwelling creature (Bargmann, 2006b), and multiple forms of laboratory assays have been established to evaluate the behavioral plasticity in olfactory response (Ardiel and Rankin, 2010; Sasakura and Mori, 2013). More than half of the 20,000 genes in *C. elegans* have a human homolog (Kamath et al., 2003), and many have elucidated conserved pathways (Chalfie and Jorgensen, 1998). The neurotransmitters in *C. elegans* are laregly the same as those in mammals, such as acetylcholine, GABA, glutamate and the modulatory monoamines (Chalfie and Jorgensen, 1998).With a fully sequenced genome and a well characterized nervous system (Brenner, 1974; White et al., 1986; Consortium, 1998), *C. elegans* is highly accessible by genetic analysis, neurophysiological recording and transgenic manipulation. Therefore, it is desirable and feasible to use *C. elegans* as a model organism to study olfactory learning, especially to evaluate functions of genes and molecules in the context of neural circuits.

The olfactory system of C. elegans

C. elegans uses a highly developed chemosensory system to navigate in its living environment, detecting and responding to volatile and water-soluble chemicals that represent food, danger, mate, or other species (Bargmann, 2006b). Feeding on bacteria, *C. elegans* is attracted to many volatile organic molecules produced by bacterial metabolism, including alcohols, ketones, aldehydes, esters, aromatic and heterocyclic compounds, etc. (Bargmann et al., 1993). These volatile compounds can be detected at a broad range of concentrations, from undiluted to 10^{-6} diluted or even lower, suggesting *C. elegans* may chemotaxis to them at a longer range than the non-volatile salts (Bargmann et al., 1993). *C. elegans* has eleven pairs of chemosensory neurons in its compact nervous system, including the olfactory neurons AWA, AWB and AWC (Bargmann et al., 1993; Troemel et al., 1997; Bargmann, 2006b). All of the three pairs are amphid neurons with ciliated nerve endings in the sheath cell (Ward et al., 1975; Perkins et al., 1986; Bargmann et al., 1993). AWA and AWC are required for detecting attractive odorants, whereas AWB recognizes repellents. The chemicals detected by AWC include butanone, isoamyl alcohol, benzaldehyde, 2,3-pentanedione, and 2,4,5-trimethylthiazole; those detected by AWA include diacetyl, pyrazine, and 2,4,5-trimethylthiazole (Bargmann et al., 1993); the repellent 2-nonanone is detected in part by AWB (Troemel et al., 1997).

As in mammals and insects, olfaction is mediated by receptors belonging to the seven-transmembrane G-protein-coupled receptor class (GPCRs) in *C. elegans* (Robertson and Thomas, 2006). Based on the genome sequence, researchers have identified a number of gene families that comprise more than 1,000 predicted GPCR genes, most of which are predicted to encode chemoreceptors (Bargmann, 2006b; Robertson and Thomas, 2006). Unlike the ‘one neuron, one receptor’ rule in the mammalian olfactory system, a single neuron may express multiple different chemoreceptor genes in *C. elegans* (Bargmann, 2006a). The first olfactory

receptor in *C. elegans* that was linked to an identified odor ligand is ODR-10, encoded by the *odr-10* gene (Sengupta et al., 1996). *odr-10* mediates the animal's chemotaxis to diacetyl in the AWA neurons, and its expression in cultured human cells has shown ODR-10 indeed responds to diacetyl (Sengupta et al., 1996; Zhang et al., 1997). In addition, ectopic expression of *odr-10* in the repellent-detecting AWB neurons results in avoidance to diacetyl, suggesting the behavioral response to an odor in *C. elegans* is defined by the olfactory neuron in which its olfactory receptor is activated rather than the receptor itself (Troemel et al., 1997). Several other candidate olfactory receptors have been identified in mutant screens and behavioral analysis, but detailed understanding of ligand-receptor interaction remains unclear (Bargmann, 2006b).

In response to odorants, the olfactory neurons utilize a G-protein-coupled signaling pathway to transduce the sensory information. The *C. elegans* genome encodes more than 20 subunits of heterotrimeric G proteins, including Gs, Gq, Go and nematode-specific Gi-like proteins (Jansen et al., 1999). Many of the genes encoding G proteins have been identified in genetic screens and characterized in chemotaxis assays (Roayaie et al., 1998; Jansen et al., 1999; Bargmann, 2006b). For example, *odr-3* encodes a Gi-like protein in the AWA, AWB, AWC and ASH sensory neurons, and the *odr-3* mutant is defective in olfactory responses mediated by these neurons (Roayaie et al., 1998). Downstream of G protein signaling, the receptor-like guanylyl cyclase (RGC) DAF-11 and ODR-1 function in the AWB and AWC neurons to produce cGMP from GTP, and both *daf-11* and *odr-1* mutants show defects in chemosensation (Vowels and Thomas, 1994; Birnby et al., 2000; L'Etoile and Bargmann, 2000). The cGMP signal then opens the cGMP-gated channel TAX-4/TAX-2 in AWC to depolarize the neuron (Coburn and Bargmann, 1996). For AWA and possibly ASH neurons, the ODR-3 G protein regulates the synthesis or degradation of phospholipids containing polyunsaturated fatty acids (PUFA) and

transduces signal to activate the TRPV channels OSM-9/OCR-2 (Colbert et al., 1997; Tobin et al., 2002; Kahn-Kirby et al., 2004; Bargmann, 2006b). Opening of the TRP channels excites the neuron and elicits behavioral response via the coordinated function of the sensori-motor circuit.

Plasticity in C. elegans olfactory response

Like many other behaviors, the olfactory preference of *C. elegans* is not only determined by the chemical structure of the odorant, but also influenced by multiple factors such as the intensity of the stimuli, animal's feeding status and previous experience. For example, low concentration of benzaldehyde serves as a strong attractant to wild-type *C. elegans*, but the undiluted pure chemical induces avoidance (Bargmann et al., 1993). The switch between attraction and repulsion to the same odor can be mediated by the molecular machinery in one neuron, or the recruitment of different chemosensory neurons (Tsunozaki et al., 2008; Yoshida et al., 2012). One elegant example shows the receptor-like guanylyl cyclase GCY-28 interacts with components in the DAG/PKC signaling pathway to regulate behavioral response to AWC^{ON}-sensed odors (Tsunozaki et al., 2008). *gcy-28* mutants show aversive response to odorants that are attractive to wild type, although the calcium response in AWC^{ON} is largely normal (Tsunozaki et al., 2008). Genetic interaction and neurophysiology data show that the reversed preference is likely mediated by a presynaptic mechanism in AWC^{ON} (Tsunozaki et al., 2008). In another example, *C. elegans* is attracted to low concentration of isoamyl alcohol (IAA) and repelled by IAA at high concentration (Yoshida et al., 2012). The concentration-dependent olfactory preference is mediated by the involvement of different neurons. AWC neurons respond to lower concentration of IAA and mediate attraction, whereas ASH neurons are only responsive to higher concentration of IAA and thus initiate avoidance (Yoshida et al., 2012). Both mechanisms may contribute to versatile olfactory preferences in a dynamic environment.

Feeding status is another important factor in olfactory response. Starved or well-fed animals behave differently because of changed internal states such as the level of serotonin, which often signals the presence of food (Horvitz et al., 1982; Bargmann, 2006b). For example, starvation enhances olfactory discrimination and acuity in *C. elegans*, and increases olfactory adaptation caused by prolonged exposure to an odorant (Colbert and Bargmann, 1997). Starvation or changed serotonin signaling also alters the sensitivity to repulsive odors by recruiting different subsets of neurons of a chemosensory circuit (Chao et al., 2004). When animals are off-food, the ASH-sensed repellent octanol are detected by ADL, AWB in addition to ASH, and the decreased sensitivity can be reversed by serotonin via the G-protein signaling pathway (Chao et al., 2004). The ability to adjust olfactory response as per feeding status improves foraging efficiency and hence survival.

The olfactory preference of *C. elegans* can also be altered by events induced by previous experience, such as adaptation, sensitization and associative learning (Tsunozaki et al., 2008). Here I will primarily discuss the olfactory learning behavior. Although the structure of the nervous system of *C. elegans* was characterized four decades ago (White et al., 1986), it was not until the 1990s that the research community recognized that the seemingly simple organism is able to learn from its own experience (Rankin et al., 1990; Ardiel and Rankin, 2010). Many learning paradigms have been established since then. Among them, the associative learning assays often pair chemical cues, either volatile odorants or water-soluble salts, with the presence or absence of food and test the animal's chemotaxis behavior pre- and post-conditioning (Wen et al., 1997; Morrison et al., 1999; Saeki et al., 2001; Nuttley et al., 2002; Torayama et al., 2007). Much progress has been made in understanding the molecular and cellular circuitry underlying neural plasticity (Tomioka et al., 2006; Torayama et al., 2007; Ardiel and Rankin, 2010;

Sasakura and Mori, 2013), and some initial clues are provided regarding how the retrieval of olfactory memory is influenced by contextual cues during acquisition (Law et al., 2004).

One interesting form of olfactory plasticity is the food-enhanced butanone chemotaxis (Torayama et al., 2007). Between the two asymmetric AWC neurons in *C. elegans*, AWC^{ON} responds to the attractant butanone (Bargmann et al., 1993; Troemel et al., 1999; Sagasti et al., 2001). The butanone chemotaxis can be enhanced by pre-exposure to butanone on bacterial food, and this enhancement requires normal development and function of AWC^{ON} mediated by the NSY-1/ASK1 MAPKKK pathway as well as the DAF-11/ODR-1 guanylyl cyclases (Torayama et al., 2007). The learning occurs as fast as in one hour, suggesting new meaning is assigned acutely to the odorant to guide foraging. Analogous to the classical conditioning paradigm, learned butanone enhancement can be 'unlearned' by exposing trained animals to butanone in the absence of food (Torayama et al., 2007). However, the learning seems distinct from other food- or starvation-induced plasticity because exogenous serotonin cannot replace food in this setting, and the serotonin synthesis mutants show normal butanone enhancement (Nuttley et al., 2002; Chao et al., 2004; Zhang et al., 2005; Torayama et al., 2007). It is somewhat surprising that many key components involved in neurotransmission such as *cat-2*, *tdc-1*, *eat-4* and *egl-3* (Sulston et al., 1975; Rankin and Wicks, 2000; Kass et al., 2001; Alkema et al., 2005), or other forms of olfactory plasticity such as *egl-4* and *hen-1* (Ishihara et al., 2002; L'Etoile et al., 2002) all appear dispensable in this behavior (Torayama et al., 2007). It remains unclear which neurotransmitters or downstream interneurons are required for butanone enhancement. It is interesting, however, that the Bardet-Biedl syndrome genes are implied in the behavior based on mutant analysis (Blacque et al., 2004; Torayama et al., 2007). Bardet-Biedl syndrome is a ciliopathic genetic disorder causing multivisceral abnormalities, including obesity, retinopathy

and learning disabilities (Rooryck and Lacombe, 2008). Further investigation into the roles of sensory cilia and the molecular mechanisms of butanone enhancement may provide hints to the molecular underpinnings of Bardet-Biedl syndrome.

Pathogenic bacteria-induced learning in C. elegans

This dissertation studies an ecologically relevant form of olfactory plasticity in *C. elegans*, pathogenic bacteria-induced learning (Zhang et al., 2005). Feeding on microbes in its natural habitat, *C. elegans* has a well-developed chemosensory system, efficient foraging strategies as well as rather sophisticated regulation of its bacterial diet preference (Bargmann et al., 1993; Bargmann, 2006b; Shtonda and Avery, 2006; Iino and Yoshida, 2009; Harris et al., 2014). Wild-type *C. elegans* cultivated on the common food *E. coli* OP50 shows olfactory preference for the *P. aeruginosa* strain PA14 to OP50 (Ha et al., 2010). This innate food odor preference requires neuropeptidergic signaling from the AWB and AWC olfactory neurons, and is executed by a circuit comprising interneurons AIY, AIB, AIZ and downstream motor machinery (Ha et al., 2010; Harris et al., 2014).

The food odor preference in *C. elegans* can be altered by experience. The pathogenic bacteria *P. aeruginosa* strain PA14 causes intestinal infection and eventually death in *C. elegans* (Tan et al., 1999; Kurz and Ewbank, 2003; Nicholas and Hodgkin, 2004). In addition to innate immunity and lawn leaving behaviors (Pujol et al., 2001; Nicholas and Hodgkin, 2004; Chang et al., 2011), *C. elegans* protects itself from fetal infection by learning to avoid the odor of PA14 after feeding on PA14 for a few hours (Zhang et al., 2005; Ha et al., 2010). This aversive olfactory learning requires serotonin signaling from ADF to the AIY/AIZ neurons, and can be promoted by exogenous serotonin (Zhang et al., 2005).

Recent studies in the Zhang lab have revealed more mechanistic insights into the behavior (Fig. 1. 5): first, two distinct neuronal circuits have been identified that regulate the innate and learned olfactory preferences (Ha et al., 2010). The interneuron RIA is specifically required in learning, because animals lacking RIA fail to suppress their olfactory preference for PA14, even though their innate preference is unimpaired (Ha et al., 2010). Second, two molecular signaling pathways that are previously implied in innate immunity have been found to regulate olfactory learning (Nicholas and Hodgkin, 2004; Zhang and Zhang, 2012; Chen et al., 2013). In the Insulin/IGF-1 pathway, two insulin-like peptides (ILPs) INS-6 and INS-7 play antagonistic roles in learning: INS-7 from the URX neuron inhibits learned olfactory preference by antagonizing the DAF-2 receptor on RIA, whereas INS-6 from the ASI neuron enables learning by repressing *ins-7* transcription in URX (Chen et al., 2013). In the TGF-β pathway, the *C. elegans* TGF-β homolog DBL-1 generated by the AVA command interneuron is required for the aversive learning, and the receptor SMA-6 acts in hypodermis to allow the olfactory plasticity to occur (Zhang and Zhang, 2012). These findings have revealed key components in a network that senses the external and internal environment of the animal and signals to the central circuit responsible for olfactory plasticity. Additionally, calcium imaging of AWB and AWC neurons has shown similar response to OP50 and PA14 smells in naïve and trained animals (Ha et al., 2010), suggesting plasticity may occur at the level of interneuron and/or motor neuron instead.

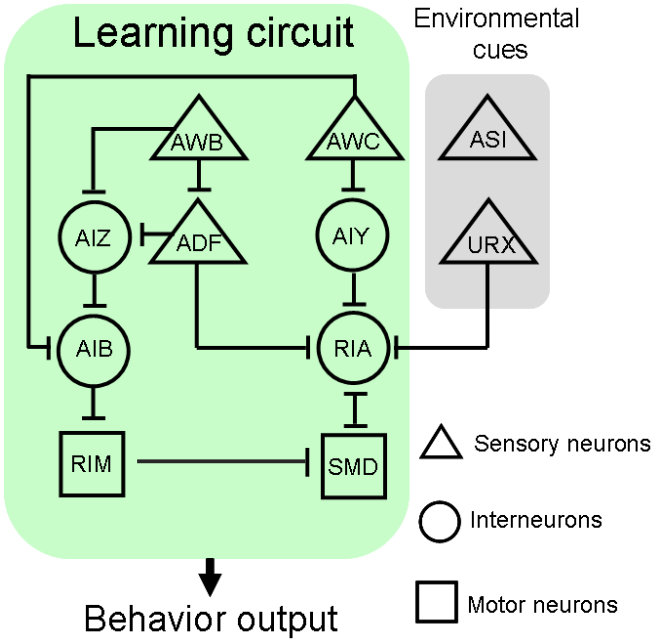

Figure 1. 5 Neural circuit underlying olfactory aversive learning in *C. elegans*. The sensory neurons AWB and AWC are responsible for detecting *E. coli* OP50 and *P. aeruginosa* PA14 odors, the interneurons AIY, AIZ, AIB are important for transducing signals. Interneuron RIA is required for olfactory learning. Motor neurons including SMD and RIM regulate turning frequency in response to different bacterial odors. The ASI and URX neurons may sense environmental cues and modulate the function of the learning circuit (Modified from Chen et al. 2013 and Ha et al. 2010).

The learned olfactory aversion to pathogenic bacteria in *C. elegans* shares some similarity with conditioned taste aversion, or 'Garcia effect', and related taste-potentiated odor aversion in mammals (Garcia et al., 1974; Palmerino et al., 1980; Chambers, 1990; Bernstein, 1999). While this phenomenon was originally identified four decades ago, the neural mechanism is still under investigation (Hatfield et al., 1992; Shema et al., 2007; Xin et al., 2014). Learning from its feeding experience to make correct dietary choice has adaptive values to *C. elegans* (Zhang et al., 2005), and genes with critical functions are often conserved. Therefore, studies on *C. elegans* olfactory aversive learning may provide mechanistic insights at the molecular and cellular level. In Chapter 3 of this dissertation, I characterize the role of an evolutionarily conserved molecule EOL-1, as well as its mammalian homolog Dom3Z, in *C. elegans* olfactory learning.

References

Alkema MJ, Hunter-Ensor M, Ringstad N, Horvitz HR (2005) Tyramine Functions independently of octopamine in the Caenorhabditis elegans nervous system. Neuron 46:247-260.

Altun ZF, Hall DH (2011) Nervous system, general description. WormAtlas.

Alvarez FJ, Jonas PC, Sapir T, Hartley R, Berrocal MC, Geiman EJ, Todd AJ, Goulding M (2005) Postnatal phenotype and localization of spinal cord V1 derived interneurons. The Journal of comparative neurology 493:177-192.

Andersson O, Forssberg H, Grillner S, Wallen P (1981) Peripheral feedback mechanisms acting on the central pattern generators for locomotion in fish and cat. Can J Physiol Pharmacol 59:713-726.

Ardiel EL, Rankin CH (2010) An elegant mind: learning and memory in Caenorhabditis elegans. Learn Mem 17:191-201.

Atanasova B, Graux J, El Hage W, Hommet C, Camus V, Belzung C (2008) Olfaction: a potential cognitive marker of psychiatric disorders. Neurosci Biobehav Rev 32:1315-1325.

Bannatyne BA, Edgley SA, Hammar I, Jankowska E, Maxwell DJ (2003) Networks of inhibitory and excitatory commissural interneurons mediating crossed reticulospinal actions. Eur J Neurosci 18:2273-2284.

Bargmann CI (2006a) Chemosensation in C. elegans. WormBook:1-29.

Bargmann CI (2006b) Comparative chemosensation from receptors to ecology. Nature 444:295-301.

Bargmann CI, Hartwieg E, Horvitz HR (1993) Odorant-selective genes and neurons mediate olfaction in C. elegans. Cell 74:515-527.

Beato M, Nistri A (1999) Interaction between disinhibited bursting and fictive locomotor patterns in the rat isolated spinal cord. J Neurophysiol 82:2029-2038.

Bernstein IL (1999) Taste aversion learning: a contemporary perspective. Nutrition 15:229-234.

Birnby DA, Link EM, Vowels JJ, Tian H, Colacurcio PL, Thomas JH (2000) A transmembrane guanylyl cyclase (DAF-11) and Hsp90 (DAF-21) regulate a common set of chemosensory behaviors in caenorhabditis elegans. Genetics 155:85-104.

Blacque OE, Reardon MJ, Li C, McCarthy J, Mahjoub MR, Ansley SJ, Badano JL, Mah AK, Beales PL, Davidson WS, Johnsen RC, Audeh M, Plasterk RH, Baillie DL, Katsanis N, Quarmby LM, Wicks SR, Leroux MR (2004) Loss of C. elegans BBS-7 and BBS-8 protein function results in cilia defects and compromised intraflagellar transport. Genes Dev 18:1630-1642.

Bodyak N, Slotnick B (1999) Performance of mice in an automated olfactometer: odor detection, discrimination and odor memory. Chem Senses 24:637-645.

Borgius L, Nishimaru H, Caldeira V, Kunugise Y, Low P, Reig R, Itohara S, Iwasato T, Kiehn O (2014) Spinal glutamatergic neurons defined by EphA4 signaling are essential components of normal locomotor circuits. J Neurosci 34:3841-3853.

Boto T, Louis T, Jindachomthong K, Jalink K, Tomchik SM (2014) Dopaminergic modulation of cAMP drives nonlinear plasticity across the Drosophila mushroom body lobes. Curr Biol 24:822-831.

Brenner S (1974) The genetics of Caenorhabditis elegans. Genetics 77:71-94.

Brocard F, Ryczko D, Fenelon K, Hatem R, Gonzales D, Auclair F, Dubuc R (2010) The transformation of a unilateral locomotor command into a symmetrical bilateral activation in the brainstem. J Neurosci 30:523-533.

Brown TG (1911) The Intrinsic Factors in the Act of Progression in the Mammal. Proceedings of the Royal Society of London Series B, Containing Papers of a Biological Character 84:308-319.

Brown TG (1914) On the nature of the fundamental activity of the nervous centres; together with an analysis of the conditioning of rhythmic activity in progression, and a theory of the evolution of function in the nervous system. J Physiol 48:18-46.

Buchanan JT (1982) Identification of interneurons with contralateral, caudal axons in the lamprey spinal cord: synaptic interactions and morphology. J Neurophysiol 47:961-975.

Buchanan JT, Grillner S (1987) Newly identified 'glutamate interneurons' and their role in locomotion in the lamprey spinal cord. Science 236:312-314.

Buchanan JT, Grillner S, Cullheim S, Risling M (1989) Identification of excitatory interneurons contributing to generation of locomotion in lamprey: structure, pharmacology, and function. J Neurophysiol 62:59-69.

Buchanan TW, Tranel D, Adolphs R (2003) A specific role for the human amygdala in olfactory memory. Learn Mem 10:319-325.

Cahill L, Babinsky R, Markowitsch HJ, McGaugh JL (1995) The amygdala and emotional memory. Nature 377:295-296.

Cangiano L, Grillner S (2002) Fast and slow locomotor burst generation in the hemi-spinal cord of the lamprey. In: Society for Neuroscience.

Carmichael ST, Clugnet MC, Price JL (1994) Central olfactory connections in the macaque monkey. The Journal of comparative neurology 346:403-434.

Cazalets JR, Bertrand S, Sqalli-Houssaini Y, Clarac F (1998) GABAergic control of spinal locomotor networks in the neonatal rat. Ann N Y Acad Sci 860:168-180.

Chalfie M, Jorgensen EM (1998) C. elegans neuroscience: genetics to genome. Trends Genet 14:506-512.

Chalfie M, Sulston JE, White JG, Southgate E, Thomson JN, Brenner S (1985) The neural circuit for touch sensitivity in Caenorhabditis elegans. J Neurosci 5:956-964.

Chambers KC (1990) A neural model for conditioned taste aversions. Annu Rev Neurosci 13:373-385.

Chang HC, Paek J, Kim DH (2011) Natural polymorphisms in C. elegans HECW-1 E3 ligase affect pathogen avoidance behaviour. Nature 480:525-529.

Chao MY, Komatsu H, Fukuto HS, Dionne HM, Hart AC (2004) Feeding status and serotonin rapidly and reversibly modulate a Caenorhabditis elegans chemosensory circuit. Proc Natl Acad Sci U S A 101:15512-15517.

Chen CN, Denome S, Davis RL (1986) Molecular analysis of cDNA clones and the corresponding genomic coding sequences of the Drosophila dunce+ gene, the structural gene for cAMP phosphodiesterase. Proc Natl Acad Sci U S A 83:9313-9317.

Chen Z, Hendricks M, Cornils A, Maier W, Alcedo J, Zhang Y (2013) Two insulin-like peptides antagonistically regulate aversive olfactory learning in C. elegans. Neuron 77:572-585.

Chess A, Simon I, Cedar H, Axel R (1994) Allelic inactivation regulates olfactory receptor gene expression. Cell 78:823-834.

Chu S, Downes JJ (2000) Odour-evoked autobiographical memories: psychological investigations of proustian phenomena. Chem Senses 25:111-116.

Chu S, Downes JJ (2002) Proust nose best: odors are better cues of autobiographical memory. Mem Cognit 30:511-518.

Coburn CM, Bargmann CI (1996) A putative cyclic nucleotide-gated channel is required for sensory development and function in C. elegans. Neuron 17:695-706.

Cohen AH, Wallen P (1980) The neuronal correlate of locomotion in fish. "Fictive swimming" induced in an in vitro preparation of the lamprey spinal cord. Exp Brain Res 41:11-18.

Colbert HA, Bargmann CI (1997) Environmental signals modulate olfactory acuity, discrimination, and memory in Caenorhabditis elegans. Learn Mem 4:179-191.

Colbert HA, Smith TL, Bargmann CI (1997) OSM-9, a novel protein with structural similarity to channels, is required for olfaction, mechanosensation, and olfactory adaptation in Caenorhabditis elegans. J Neurosci 17:8259-8269.

Consortium CeS (1998) Genome sequence of the nematode C. elegans: a platform for investigating biology. Science 282:2012-2018.

Conti MZ, Vicini-Chilovi B, Riva M, Zanetti M, Liberini P, Padovani A, Rozzini L (2013) Odor identification deficit predicts clinical conversion from mild cognitive impairment to dementia due to Alzheimer's disease. Arch Clin Neuropsychol 28:391-399.

Corfas G, Dudai Y (1989) Habituation and dishabituation of a cleaning reflex in normal and mutant Drosophila. J Neurosci 9:56-62.

Cowley KC, Schmidt BJ (1995) Effects of inhibitory amino acid antagonists on reciprocal inhibitory interactions during rhythmic motor activity in the in vitro neonatal rat spinal cord. J Neurophysiol 74:1109-1117.

Cowley KC, Schmidt BJ (1997) Regional distribution of the locomotor pattern-generating network in the neonatal rat spinal cord. J Neurophysiol 77:247-259.

Crone SA, Quinlan KA, Zagoraiou L, Droho S, Restrepo CE, Lundfald L, Endo T, Setlak J, Jessell TM, Kiehn O, Sharma K (2008) Genetic ablation of V2a ipsilateral interneurons disrupts left-right locomotor coordination in mammalian spinal cord. Neuron 60:70-83.

Dade LA, Zatorre RJ, Jones-Gotman M (2002) Olfactory learning: convergent findings from lesion and brain imaging studies in humans. Brain 125:86-101.

Davis RL (2004) Olfactory learning. Neuron 44:31-48.

Derjean D, Moussaddy A, Atallah E, St-Pierre M, Auclair F, Chang S, Ren X, Zielinski B, Dubuc R (2010) A novel neural substrate for the transformation of olfactory inputs into motor output. PLoS Biol 8:e1000567.

Di Prisco GV, Wallen P, Grillner S (1990) Synaptic effects of intraspinal stretch receptor neurons mediating movement-related feedback during locomotion. Brain Res 530:161-166.

Dipt S, Riemensperger T, Fiala A (2014) Optical calcium imaging using DNA-encoded fluorescence sensors in transgenic fruit flies, Drosophila melanogaster. Methods Mol Biol 1071:195-206.

Dottori M, Hartley L, Galea M, Paxinos G, Polizzotto M, Kilpatrick T, Bartlett PF, Murphy M, Kontgen F, Boyd AW (1998) EphA4 (Sek1) receptor tyrosine kinase is required for the development of the corticospinal tract. Proc Natl Acad Sci U S A 95:13248-13253.

Doucette W, Gire DH, Whitesell J, Carmean V, Lucero MT, Restrepo D (2011) Associative cortex features in the first olfactory brain relay station. Neuron 69:1176-1187.

Dougherty KJ, Kiehn O (2010) Functional organization of V2a-related locomotor circuits in the rodent spinal cord. Ann N Y Acad Sci 1198:85-93.

Dubuc R, Bongianni F, Ohta Y, Grillner S (1993a) Dorsal root and dorsal column mediated synaptic inputs to reticulospinal neurons in lampreys: involvement of glutamatergic, glycinergic, and GABAergic transmission. J Comp Neurol 327:251-259.

Dubuc R, Bongianni F, Ohta Y, Grillner S (1993b) Anatomical and physiological study of brainstem nuclei relaying dorsal column inputs in lampreys. J Comp Neurol 327:260-270.

Dudai Y (2002) Memory from A to Z : keywords, concepts, and beyond. Oxford ; New York: Oxford University Press.

Dudai Y, Jan YN, Byers D, Quinn WG, Benzer S (1976) dunce, a mutant of Drosophila deficient in learning. Proc Natl Acad Sci U S A 73:1684-1688.

El Manira A, Pombal MA, Grillner S (1997) Diencephalic projection to reticulospinal neurons involved in the initiation of locomotion in adult lampreys Lampetra fluviatilis. J Comp Neurol 389:603-616.

Feany MB, Quinn WG (1995) A neuropeptide gene defined by the Drosophila memory mutant amnesiac. Science 268:869-873.

Fletcher ML (2012) Olfactory aversive conditioning alters olfactory bulb mitral/tufted cell glomerular odor responses. Front Syst Neurosci 6:16.

Garcia J, Hankins WG, Rusiniak KW (1974) Behavioral regulation of the milieu interne in man and rat. Science 185:824-831.

Glusman G, Yanai I, Rubin I, Lancet D (2001) The complete human olfactory subgenome. Genome Res 11:685-702.

Gottfried JA, Smith AP, Rugg MD, Dolan RJ (2004) Remembrance of odors past: human olfactory cortex in cross-modal recognition memory. Neuron 42:687-695.

Goulding M (2009) Circuits controlling vertebrate locomotion: moving in a new direction. Nat Rev Neurosci 10:507-518.

Grillner S (1981) Control of Locomotion in Bipeds, Tetrapods, and Fish. In: Comprehensive Physiology: John Wiley & Sons, Inc.

Grillner S (2003) The motor infrastructure: from ion channels to neuronal networks. Nat Rev Neurosci 4:573-586.

Grillner S, Wallen P (2002) Cellular bases of a vertebrate locomotor system-steering, intersegmental and segmental co-ordination and sensory control. Brain Res Brain Res Rev 40:92-106.

Grillner S, Williams T, Lagerback PA (1984) The edge cell, a possible intraspinal mechanoreceptor. Science 223:500-503.

Grillner S, Wallen P, Brodin L, Lansner A (1991) Neuronal network generating locomotor behavior in lamprey: circuitry, transmitters, membrane properties, and simulation. Annu Rev Neurosci 14:169-199.

Guo ZV, Hart AC, Ramanathan S (2009) Optical interrogation of neural circuits in Caenorhabditis elegans. Nat Methods 6:891-896.

Ha HI, Hendricks M, Shen Y, Gabel CV, Fang-Yen C, Qin Y, Colon-Ramos D, Shen K, Samuel AD, Zhang Y (2010) Functional organization of a neural network for aversive olfactory learning in Caenorhabditis elegans. Neuron 68:1173-1186.

Haberly LB (2001) Parallel-distributed processing in olfactory cortex: new insights from morphological and physiological analysis of neuronal circuitry. Chem Senses 26:551-576.

Hagglund M, Borgius L, Dougherty KJ, Kiehn O (2010) Activation of groups of excitatory neurons in the mammalian spinal cord or hindbrain evokes locomotion. Nat Neurosci 13:246-252.

Harris G, Shen Y, Ha H, Donato A, Wallis S, Zhang X, Zhang Y (2014) Dissecting the signaling mechanisms underlying recognition and preference of food odors. J Neurosci 34:9389-9403.

Hatfield T, Graham PW, Gallagher M (1992) Taste-potentiated odor aversion learning: role of the amygdaloid basolateral complex and central nucleus. Behav Neurosci 106:286-293.

Herz RS, Cupchik GC (1995) The emotional distinctiveness of odor-evoked memories. Chem Senses 20:517-528.

Herz RS, Schooler JW (2002) A naturalistic study of autobiographical memories evoked by olfactory and visual cues: testing the Proustian hypothesis. Am J Psychol 115:21-32.

Herz RS, Eliassen J, Beland S, Souza T (2004) Neuroimaging evidence for the emotional potency of odor-evoked memory. Neuropsychologia 42:371-378.

Hinton DE, Pich V, Chhean D, Pollack MH, Barlow DH (2004) Olfactory-triggered panic attacks among Cambodian refugees attending a psychiatric clinic. Gen Hosp Psychiatry 26:390-397.

Horvitz HR, Chalfie M, Trent C, Sulston JE, Evans PD (1982) Serotonin and octopamine in the nematode Caenorhabditis elegans. Science 216:1012-1014.

Hudry J, Saoud M, D'Amato T, Dalery J, Royet JP (2002) Ratings of different olfactory judgements in schizophrenia. Chem Senses 27:407-416.

Hultborn H, Jankowska E, Lindstrom S (1971) Recurrent inhibition from motor axon collaterals of transmission in the Ia inhibitory pathway to motoneurones. J Physiol 215:591-612.

Iino Y, Yoshida K (2009) Parallel use of two behavioral mechanisms for chemotaxis in Caenorhabditis elegans. J Neurosci 29:5370-5380.

Inagaki HK, Jung Y, Hoopfer ED, Wong AM, Mishra N, Lin JY, Tsien RY, Anderson DJ (2014) Optogenetic control of Drosophila using a red-shifted channelrhodopsin reveals experience-dependent influences on courtship. Nature methods 11:325-332.

Ishihara T, Iino Y, Mohri A, Mori I, Gengyo-Ando K, Mitani S, Katsura I (2002) HEN-1, a secretory protein with an LDL receptor motif, regulates sensory integration and learning in Caenorhabditis elegans. Cell 109:639-649.

Jaeger SR, McRae JF, Bava CM, Beresford MK, Hunter D, Jia Y, Chheang SL, Jin D, Peng M, Gamble JC, Atkinson KR, Axten LG, Paisley AG, Tooman L, Pineau B, Rouse SA,

Newcomb RD (2013) A Mendelian trait for olfactory sensitivity affects odor experience and food selection. Current biology : CB 23:1601-1605.

Jansen G, Thijssen KL, Werner P, van der Horst M, Hazendonk E, Plasterk RH (1999) The complete family of genes encoding G proteins of Caenorhabditis elegans. Nat Genet 21:414-419.

Jones SV, Heldt SA, Davis M, Ressler KJ (2005) Olfactory-mediated fear conditioning in mice: simultaneous measurements of fear-potentiated startle and freezing. Behav Neurosci 119:329-335.

Jones SV, Choi DC, Davis M, Ressler KJ (2008) Learning-dependent structural plasticity in the adult olfactory pathway. J Neurosci 28:13106-13111.

Jones-Gotman M, Zatorre RJ (1993) Odor recognition memory in humans: role of right temporal and orbitofrontal regions. Brain Cogn 22:182-198.

Kadohisa M (2013) Effects of odor on emotion, with implications. Front Syst Neurosci 7:66.

Kahn-Kirby AH, Dantzker JL, Apicella AJ, Schafer WR, Browse J, Bargmann CI, Watts JL (2004) Specific polyunsaturated fatty acids drive TRPV-dependent sensory signaling in vivo. Cell 119:889-900.

Kamath RS, Fraser AG, Dong Y, Poulin G, Durbin R, Gotta M, Kanapin A, Le Bot N, Moreno S, Sohrmann M, Welchman DP, Zipperlen P, Ahringer J (2003) Systematic functional analysis of the Caenorhabditis elegans genome using RNAi. Nature 421:231-237.

Kandel ER (2001) The molecular biology of memory storage: a dialogue between genes and synapses. Science 294:1030-1038.

Kass J, Jacob TC, Kim P, Kaplan JM (2001) The EGL-3 proprotein convertase regulates mechanosensory responses of Caenorhabditis elegans. J Neurosci 21:9265-9272.

Kass MD, Rosenthal MC, Pottackal J, McGann JP (2013) Fear learning enhances neural responses to threat-predictive sensory stimuli. Science 342:1389-1392.

Kawano T, Po MD, Gao S, Leung G, Ryu WS, Zhen M (2011) An imbalancing act: gap junctions reduce the backward motor circuit activity to bias C. elegans for forward locomotion. Neuron 72:572-586.

Keller A, Zhuang H, Chi Q, Vosshall LB, Matsunami H (2007) Genetic variation in a human odorant receptor alters odour perception. Nature 449:468-472.

Kiehn O (2006) Locomotor circuits in the mammalian spinal cord. Annual review of neuroscience 29:279-306.

Kiehn O (2011) Development and functional organization of spinal locomotor circuits. Curr Opin Neurobiol 21:100-109.

Kjaerulff O, Kiehn O (1996) Distribution of networks generating and coordinating locomotor activity in the neonatal rat spinal cord in vitro: a lesion study. J Neurosci 16:5777-5794.

Kjaerulff O, Kiehn O (1997) Crossed rhythmic synaptic input to motoneurons during selective activation of the contralateral spinal locomotor network. J Neurosci 17:9433-9447.

Kline NA, Rausch JL (1985) Olfactory precipitants of flashbacks in posttraumatic stress disorder: case reports. J Clin Psychiatry 46:383-384.

Knaapila A, Zhu G, Medland SE, Wysocki CJ, Montgomery GW, Martin NG, Wright MJ, Reed DR (2012) A genome-wide study on the perception of the odorants androstenone and galaxolide. Chem Senses 37:541-552.

Kozlov AK, Kardamakis AA, Hellgren Kotaleski J, Grillner S (2014) Gating of steering signals through phasic modulation of reticulospinal neurons during locomotion. Proc Natl Acad Sci U S A 111:3591-3596.

Kullander K, Croll SD, Zimmer M, Pan L, McClain J, Hughes V, Zabski S, DeChiara TM, Klein R, Yancopoulos GD, Gale NW (2001) Ephrin-B3 is the midline barrier that prevents corticospinal tract axons from recrossing, allowing for unilateral motor control. Genes Dev 15:877-888.

Kurz CL, Ewbank JJ (2003) Caenorhabditis elegans: an emerging genetic model for the study of innate immunity. Nat Rev Genet 4:380-390.

Kwan AC, Dietz SB, Webb WW, Harris-Warrick RM (2009) Activity of Hb9 interneurons during fictive locomotion in mouse spinal cord. J Neurosci 29:11601-11613.

L'Etoile ND, Bargmann CI (2000) Olfaction and odor discrimination are mediated by the C. elegans guanylyl cyclase ODR-1. Neuron 25:575-586.

L'Etoile ND, Coburn CM, Eastham J, Kistler A, Gallegos G, Bargmann CI (2002) The cyclic GMP-dependent protein kinase EGL-4 regulates olfactory adaptation in C. elegans. Neuron 36:1079-1089.

Law E, Nuttley WM, van der Kooy D (2004) Contextual taste cues modulate olfactory learning in C. elegans by an occasion-setting mechanism. Curr Biol 14:1303-1308.

LeDoux JE (2000) Emotion circuits in the brain. Annu Rev Neurosci 23:155-184.

Leifer AM, Fang-Yen C, Gershow M, Alkema MJ, Samuel AD (2011) Optogenetic manipulation of neural activity in freely moving Caenorhabditis elegans. Nature methods 8:147-152.

Levin LR, Han PL, Hwang PM, Feinstein PG, Davis RL, Reed RR (1992) The Drosophila learning and memory gene rutabaga encodes a Ca2+/Calmodulin-responsive adenylyl cyclase. Cell 68:479-489.

Li W, Luxenberg E, Parrish T, Gottfried JA (2006) Learning to smell the roses: experience-dependent neural plasticity in human piriform and orbitofrontal cortices. Neuron 52:1097-1108.

Li W, Howard JD, Parrish TB, Gottfried JA (2008) Aversive learning enhances perceptual and cortical discrimination of indiscriminable odor cues. Science 319:1842-1845.

Lin AC, Bygrave AM, de Calignon A, Lee T, Miesenbock G (2014) Sparse, decorrelated odor coding in the mushroom body enhances learned odor discrimination. Nat Neurosci 17:559-568.

Liu L, Wolf R, Ernst R, Heisenberg M (1999) Context generalization in Drosophila visual learning requires the mushroom bodies. Nature 400:753-756.

Lombion-Pouthier S, Vandel P, Nezelof S, Haffen E, Millot JL (2006) Odor perception in patients with mood disorders. J Affect Disord 90:187-191.

MacLeod AR, Talbot K (1983) A processed gene defining a gene family encoding a human non-muscle tropomyosin. Journal of molecular biology 167:523-537.

MacLeod AR, Karn J, Brenner S (1981) Molecular analysis of the unc-54 myosin heavy-chain gene of Caenorhabditis elegans. Nature 291:386-390.

Marder E, Bucher D (2001) Central pattern generators and the control of rhythmic movements. Curr Biol 11:R986-996.

Maricq AV, Peckol E, Driscoll M, Bargmann CI (1995) Mechanosensory signalling in C. elegans mediated by the GLR-1 glutamate receptor. Nature 378:78-81.

Martzke JS, Kopala LC, Good KP (1997) Olfactory dysfunction in neuropsychiatric disorders: review and methodological considerations. Biol Psychiatry 42:721-732.

McClellan AD, Grillner S (1984) Activation of 'fictive swimming' by electrical microstimulation of brainstem locomotor regions in an in vitro preparation of the lamprey central nervous system. Brain Res 300:357-361.

McCrea DA, Pratt CA, Jordan LM (1980) Renshaw cell activity and recurrent effects on motoneurons during fictive locomotion. J Neurophysiol 44:475-488.

McRae JF, Jaeger SR, Bava CM, Beresford MK, Hunter D, Jia Y, Chheang SL, Jin D, Peng M, Gamble JC, Atkinson KR, Axten LG, Paisley AG, Williams L, Tooman L, Pineau B, Rouse SA, Newcomb RD (2013) Identification of regions associated with variation in sensitivity to food-related odors in the human genome. Current biology : CB 23:1596-1600.

Menard A, Grillner S (2008) Diencephalic locomotor region in the lamprey--afferents and efferent control. J Neurophysiol 100:1343-1353.

Menard A, Auclair F, Bourcier-Lucas C, Grillner S, Dubuc R (2007) Descending GABAergic projections to the mesencephalic locomotor region in the lamprey Petromyzon marinus. J Comp Neurol 501:260-273.

Mesholam RI, Moberg PJ, Mahr RN, Doty RL (1998) Olfaction in neurodegenerative disease: a meta-analysis of olfactory functioning in Alzheimer's and Parkinson's diseases. Arch Neurol 55:84-90.

Mihalick SM, Langlois JC, Krienke JD, Dube WV (2000) An olfactory discrimination procedure for mice. J Exp Anal Behav 73:305-318.

Moberg PJ, Agrin R, Gur RE, Gur RC, Turetsky BI, Doty RL (1999) Olfactory dysfunction in schizophrenia: a qualitative and quantitative review. Neuropsychopharmacology 21:325-340.

Moberg PJ, Arnold SE, Doty RL, Kohler C, Kanes S, Seigel S, Gur RE, Turetsky BI (2003) Impairment of odor hedonics in men with schizophrenia. Am J Psychiatry 160:1784-1789.

Moran DT, Rowley JC, 3rd, Jafek BW, Lovell MA (1982) The fine structure of the olfactory mucosa in man. J Neurocytol 11:721-746.

Morrison GE, Wen JY, Runciman S, van der Kooy D (1999) Olfactory associative learning in Caenorhabditis elegans is impaired in lrn-1 and lrn-2 mutants. Behav Neurosci 113:358-367.

Nicholas HR, Hodgkin J (2004) Responses to infection and possible recognition strategies in the innate immune system of Caenorhabditis elegans. Mol Immunol 41:479-493.

Northcutt RG (1979) Experimental determination of the primary trigeminal projections in lampreys. Brain Res 163:323-327.

Nuttley WM, Atkinson-Leadbeater KP, Van Der Kooy D (2002) Serotonin mediates food-odor associative learning in the nematode Caenorhabditiselegans. Proc Natl Acad Sci U S A 99:12449-12454.

Olshausen BA, Field DJ (2004) Sparse coding of sensory inputs. Curr Opin Neurobiol 14:481-487.

Otto T, Cousens G, Herzog C (2000) Behavioral and neuropsychological foundations of olfactory fear conditioning. Behav Brain Res 110:119-128.

Palmerino CC, Rusiniak KW, Garcia J (1980) Flavor-illness aversions: the peculiar roles of odor and taste in memory for poison. Science 208:753-755.

Paschall GY, Davis M (2002) Olfactory-mediated fear-potentiated startle. Behav Neurosci 116:4-12.

Pause BM, Raack N, Sojka B, Goder R, Aldenhoff JB, Ferstl R (2003) Convergent and divergent effects of odors and emotions in depression. Psychophysiology 40:209-225.

Pavesi E, Heldt SA, Fletcher ML (2013) Neuronal nitric-oxide synthase deficiency impairs the long-term memory of olfactory fear learning and increases odor generalization. Learn Mem 20:482-490.

Perez-Orive J, Mazor O, Turner GC, Cassenaer S, Wilson RI, Laurent G (2002) Oscillations and sparsening of odor representations in the mushroom body. Science 297:359-365.

Perkins LA, Hedgecock EM, Thomson JN, Culotti JG (1986) Mutant sensory cilia in the nematode Caenorhabditis elegans. Dev Biol 117:456-487.

Pratt CA, Jordan LM (1987) Ia inhibitory interneurons and Renshaw cells as contributors to the spinal mechanisms of fictive locomotion. J Neurophysiol 57:56-71.

Proust M (1932) Remembrance of things past. New York: Random House.

Pujol N, Link EM, Liu LX, Kurz CL, Alloing G, Tan MW, Ray KP, Solari R, Johnson CD, Ewbank JJ (2001) A reverse genetic analysis of components of the Toll signaling pathway in Caenorhabditis elegans. Curr Biol 11:809-821.

Quinn WG, Harris WA, Benzer S (1974) Conditioned behavior in Drosophila melanogaster. Proc Natl Acad Sci U S A 71:708-712.

Quinn WG, Sziber PP, Booker R (1979) The Drosophila memory mutant amnesiac. Nature 277:212-214.

Rankin CH, Wicks SR (2000) Mutations of the caenorhabditis elegans brain-specific inorganic phosphate transporter eat-4 affect habituation of the tap-withdrawal response without affecting the response itself. J Neurosci 20:4337-4344.

Rankin CH, Beck CD, Chiba CM (1990) Caenorhabditis elegans: a new model system for the study of learning and memory. Behavioural brain research 37:89-92.

Rebollo E, Karkali K, Mangione F, Martin-Blanco E (2014) Live imaging in Drosophila: The optical and genetic toolkits. Methods 68:48-59.

Roayaie K, Crump JG, Sagasti A, Bargmann CI (1998) The G alpha protein ODR-3 mediates olfactory and nociceptive function and controls cilium morphogenesis in C. elegans olfactory neurons. Neuron 20:55-67.

Robertson HM, Thomas JH (2006) The putative chemoreceptor families of C. elegans. WormBook:1-12.

Rooryck C, Lacombe D (2008) [Bardet-Biedl syndrome]. Ann Endocrinol (Paris) 69:463-471.

Rovainen CM (1974) Synaptic interactions of identified nerve cells in the spinal cord of the sea lamprey. J Comp Neurol 154:189-206.

Ryczko D, Gratsch S, Auclair F, Dube C, Bergeron S, Alpert MH, Cone JJ, Roitman MF, Alford S, Dubuc R (2013) Forebrain dopamine neurons project down to a brainstem region controlling locomotion. Proc Natl Acad Sci U S A 110:E3235-3242.

Saeki S, Yamamoto M, Iino Y (2001) Plasticity of chemotaxis revealed by paired presentation of a chemoattractant and starvation in the nematode Caenorhabditis elegans. J Exp Biol 204:1757-1764.

Sagasti A, Hisamoto N, Hyodo J, Tanaka-Hino M, Matsumoto K, Bargmann CI (2001) The CaMKII UNC-43 activates the MAPKKK NSY-1 to execute a lateral signaling decision required for asymmetric olfactory neuron fates. Cell 105:221-232.

Sasakura H, Mori I (2013) Behavioral plasticity, learning, and memory in C. elegans. Curr Opin Neurobiol 23:92-99.

Schellinck HM, Forestell CA, LoLordo VM (2001) A simple and reliable test of olfactory learning and memory in mice. Chem Senses 26:663-672.

Schrodel T, Prevedel R, Aumayr K, Zimmer M, Vaziri A (2013) Brain-wide 3D imaging of neuronal activity in Caenorhabditis elegans with sculpted light. Nature methods 10:1013-1020.

Sengupta P, Chou JH, Bargmann CI (1996) odr-10 encodes a seven transmembrane domain olfactory receptor required for responses to the odorant diacetyl. Cell 84:899-909.

Shema R, Sacktor TC, Dudai Y (2007) Rapid erasure of long-term memory associations in the cortex by an inhibitor of PKM zeta. Science 317:951-953.

Shtonda BB, Avery L (2006) Dietary choice behavior in Caenorhabditis elegans. J Exp Biol 209:89-102.

Sinha S, Liang L, Ho ET, Urbanek KE, Luo L, Baer TM, Schnitzer MJ (2013) High-speed laser microsurgery of alert fruit flies for fluorescence imaging of neural activity. Proc Natl Acad Sci U S A 110:18374-18379.

Sirota MG, Di Prisco GV, Dubuc R (2000) Stimulation of the mesencephalic locomotor region elicits controlled swimming in semi-intact lampreys. Eur J Neurosci 12:4081-4092.

Small DM, Prescott J (2005) Odor/taste integration and the perception of flavor. Exp Brain Res 166:345-357.

Stepien AE, Arber S (2008) Probing the locomotor conundrum: descending the 'V' interneuron ladder. Neuron 60:1-4.

Sulston J, Dew M, Brenner S (1975) Dopaminergic neurons in the nematode Caenorhabditis elegans. The Journal of comparative neurology 163:215-226.

Talpalar AE, Kiehn O (2010) Glutamatergic mechanisms for speed control and network operation in the rodent locomotor CpG. Front Neural Circuits 4.

Tan MW, Mahajan-Miklos S, Ausubel FM (1999) Killing of Caenorhabditis elegans by Pseudomonas aeruginosa used to model mammalian bacterial pathogenesis. Proc Natl Acad Sci U S A 96:715-720.

Tempel BL, Bonini N, Dawson DR, Quinn WG (1983) Reward learning in normal and mutant Drosophila. Proc Natl Acad Sci U S A 80:1482-1486.

Tobin D, Madsen D, Kahn-Kirby A, Peckol E, Moulder G, Barstead R, Maricq A, Bargmann C (2002) Combinatorial expression of TRPV channel proteins defines their sensory functions and subcellular localization in C. elegans neurons. Neuron 35:307-318.

Tokunaga T, Hirose O, Kawaguchi S, Toyoshima Y, Teramoto T, Ikebata H, Kuge S, Ishihara T, Iino Y, Yoshida R (2014) Automated detection and tracking of many cells by using 4D live-cell imaging data. Bioinformatics 30:i43-51.

Tomioka M, Adachi T, Suzuki H, Kunitomo H, Schafer WR, Iino Y (2006) The insulin/PI 3-kinase pathway regulates salt chemotaxis learning in Caenorhabditis elegans. Neuron 51:613-625.

Tong MT, Peace ST, Cleland TA (2014) Properties and mechanisms of olfactory learning and memory. Front Behav Neurosci 8:238.

Torayama I, Ishihara T, Katsura I (2007) Caenorhabditis elegans integrates the signals of butanone and food to enhance chemotaxis to butanone. J Neurosci 27:741-750.

Troemel ER, Kimmel BE, Bargmann CI (1997) Reprogramming chemotaxis responses: sensory neurons define olfactory preferences in C. elegans. Cell 91:161-169.

Troemel ER, Sagasti A, Bargmann CI (1999) Lateral signaling mediated by axon contact and calcium entry regulates asymmetric odorant receptor expression in C. elegans. Cell 99:387-398.

Tsunozaki M, Chalasani SH, Bargmann CI (2008) A behavioral switch: cGMP and PKC signaling in olfactory neurons reverses odor preference in C. elegans. Neuron 59:959-971.

Tully T, Quinn WG (1985) Classical conditioning and retention in normal and mutant Drosophila melanogaster. J Comp Physiol A 157:263-277.

Vassar R, Ngai J, Axel R (1993) Spatial segregation of odorant receptor expression in the mammalian olfactory epithelium. Cell 74:309-318.

Vermetten E, Bremner JD (2003) Olfaction as a traumatic reminder in posttraumatic stress disorder: case reports and review. J Clin Psychiatry 64:202-207.

Vermetten E, Schmahl C, Southwick SM, Bremner JD (2007) Positron tomographic emission study of olfactory induced emotional recall in veterans with and without combat-related posttraumatic stress disorder. Psychopharmacol Bull 40:8-30.

Viana Di Prisco G, Boutin T, Petropoulos D, Brocard F, Dubuc R (2005) The trigeminal sensory relay to reticulospinal neurons in lampreys. Neuroscience 131:535-546.

Vowels JJ, Thomas JH (1994) Multiple chemosensory defects in daf-11 and daf-21 mutants of Caenorhabditis elegans. Genetics 138:303-316.

Waddell S, Quinn WG (2001) Flies, genes, and learning. Annual review of neuroscience 24:1283-1309.

Wang Y, Guo HF, Pologruto TA, Hannan F, Hakker I, Svoboda K, Zhong Y (2004) Stereotyped odor-evoked activity in the mushroom body of Drosophila revealed by green fluorescent protein-based Ca2+ imaging. The Journal of neuroscience : the official journal of the Society for Neuroscience 24:6507-6514.

Ward S, Thomson N, White JG, Brenner S (1975) Electron microscopical reconstruction of the anterior sensory anatomy of the nematode Caenorhabditis elegans.?2UU. The Journal of comparative neurology 160:313-337.

Wen JY, Kumar N, Morrison G, Rambaldini G, Runciman S, Rousseau J, van der Kooy D (1997) Mutations that prevent associative learning in C. elegans. Behav Neurosci 111:354-368.

White JG, Southgate E, Thomson JN (1992) Mutations in the Caenorhabditis elegans unc-4 gene alter the synaptic input to ventral cord motor neurons. Nature 355:838-841.

White JG, Southgate E, Thomson JN, Brenner S (1986) The structure of the nervous system of the nematode Caenorhabditis elegans. Philos Trans R Soc Lond B Biol Sci 314:1-340.

Wicks SR, Rankin CH (1995) Integration of mechanosensory stimuli in Caenorhabditis elegans. J Neurosci 15:2434-2444.

Willander J, Larsson M (2006) Smell your way back to childhood: autobiographical odor memory. Psychon Bull Rev 13:240-244.

Wilson DA, Best AR, Sullivan RM (2004) Plasticity in the olfactory system: lessons for the neurobiology of memory. The Neuroscientist : a review journal bringing neurobiology, neurology and psychiatry 10:513-524.

Wu MC, Chu LA, Hsiao PY, Lin YY, Chi CC, Liu TH, Fu CC, Chiang AS (2014) Optogenetic control of selective neural activity in multiple freely moving Drosophila adults. Proc Natl Acad Sci U S A 111:5367-5372.

Xin J, Ma L, Zhang TY, Yu H, Wang Y, Kong L, Chen ZY (2014) Involvement of BDNF signaling transmission from basolateral amygdala to infralimbic prefrontal cortex in conditioned taste aversion extinction. J Neurosci 34:7302-7313.

Yeshurun Y, Sobel N (2010) An odor is not worth a thousand words: from multidimensional odors to unidimensional odor objects. Annu Rev Psychol 61:219-241, C211-215.

Yin JC, Wallach JS, Del Vecchio M, Wilder EL, Zhou H, Quinn WG, Tully T (1994) Induction of a dominant negative CREB transgene specifically blocks long-term memory in Drosophila. Cell 79:49-58.

Yokoyama N, Romero MI, Cowan CA, Galvan P, Helmbacher F, Charnay P, Parada LF, Henkemeyer M (2001) Forward signaling mediated by ephrin-B3 prevents contralateral corticospinal axons from recrossing the spinal cord midline. Neuron 29:85-97.

Yoshida K, Hirotsu T, Tagawa T, Oda S, Wakabayashi T, Iino Y, Ishihara T (2012) Odour concentration-dependent olfactory preference change in C. elegans. Nat Commun 3:739.

Zhang X, Zhang Y (2012) DBL-1, a TGF-beta, is essential for Caenorhabditis elegans aversive olfactory learning. Proc Natl Acad Sci U S A 109:17081-17086.

Zhang Y, Lu H, Bargmann CI (2005) Pathogenic bacteria induce aversive olfactory learning in Caenorhabditis elegans. Nature 438:179-184.

Zhang Y, Chou JH, Bradley J, Bargmann CI, Zinn K (1997) The Caenorhabditis elegans seven-transmembrane protein ODR-10 functions as an odorant receptor in mammalian cells. Proc Natl Acad Sci U S A 94:12162-12167.

Ziskind-Conhaim L, Mentis GZ, Wiesner EP, Titus DJ (2010) Synaptic integration of rhythmogenic neurons in the locomotor circuitry: the case of Hb9 interneurons. Ann N Y Acad Sci 1198:72-84.

Chapter 2. Oscillatory motor circuit regulates the gait of head deflection in *C. elegans*

Introduction

C. elegans moves forward by generating sinusoidal waves that propagate from head to tail in the dorsal-ventral plane. As part of the wave, the animal's head moves from side to side at 1 Hz with more flexibility at the nose tip (McIntire et al., 1993b; Karbowski et al., 2006; Shingai et al., 2013). The locomotory gait in *C. elegans* is controlled by motor neurons. Among the 95 rhomboid-shaped somatic muscle cells, the anteriormost four head muscles in each quadrant receive inputs from motor neurons in the nerve ring, including SMD, RME, RMD and SMB; the next four neck muscles in each quadrant are innervated by motor neurons of the nerve ring and the ventral nerve cord, including SMD, RME, RMD, SMB, RIV and RIM (White et al., 1986; Gray et al., 2005; Altun and Hall, 2009) (Fig. 2. 1A). During one head swing, the head and neck muscles on one side contract while those on the other side relax, driving animal's head away from the centerline of its body. The amplitude and frequency of the dorsal-ventral waves are modulated both genetically and environmentally in *C. elegans* (McIntire et al., 1993b; Gray et al., 2005; Li et al., 2006a; Fang-Yen et al., 2010; Vidal-Gadea et al., 2011; Hendricks et al., 2012; Shingai et al., 2013). However, few studies examined the head movement quantitatively, and the neural mechanisms underlying its gait regulation remain unclear.

Many of the head motor neurons are cholinergic based on the expression of the choline acetyltransferase CHA-1 (Rand and Russell, 1984; Alfonso et al., 1994; Duerr et al., 2008). Among them are the four-fold SMB and SMD neurons, and the six-fold RMD neurons (Duerr et al., 2008), all of which form neuromuscular junctions (NMJs) with head and neck muscles at the nerve ring (White et al., 1986; Altun and Hall, 2009). Previous studies have reported that the RMD neurons receive synaptic inputs from the mechanosensory OLQ and IL1, mediating the head-withdrawal reflex when animals were touched on the nose during forward movement

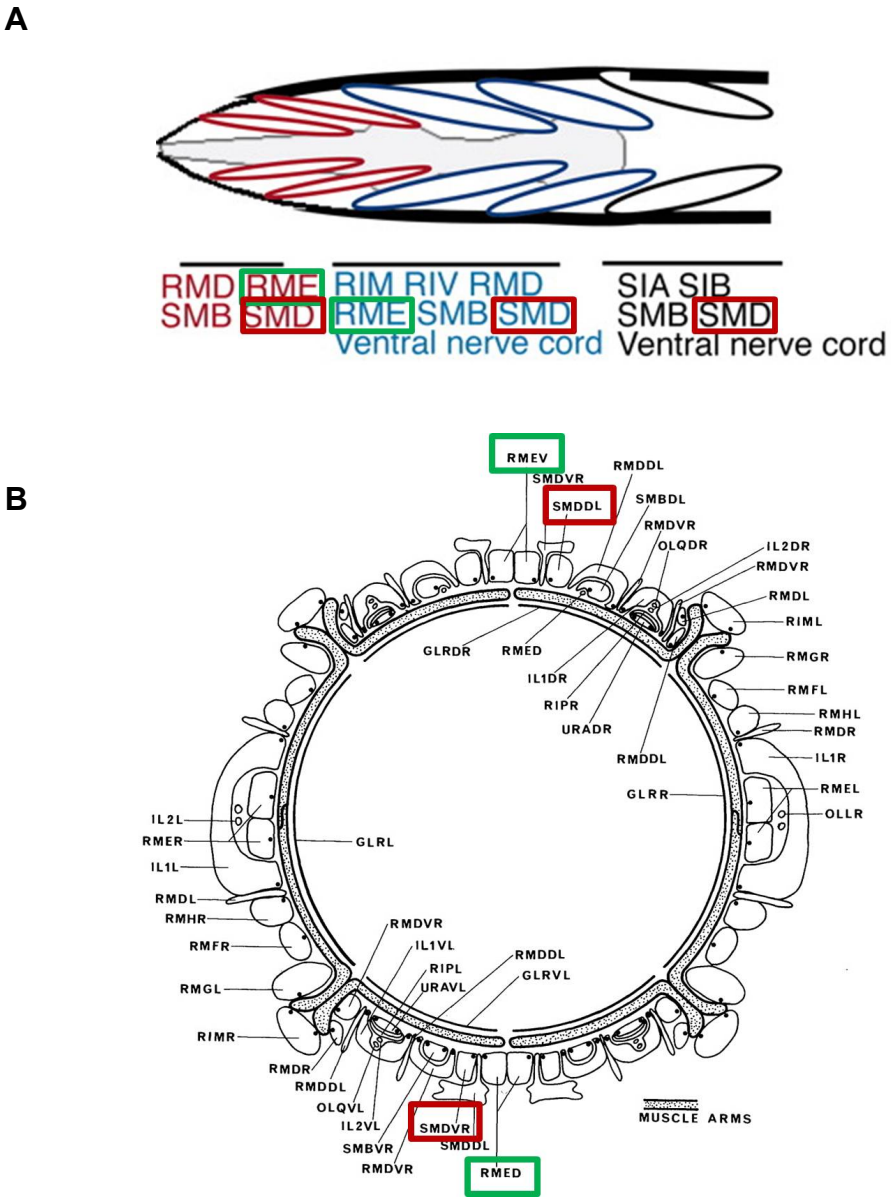

Figure 2. 1 Anatomy of head and neck muscles and motor neurons in *C. elegans*. A, Muscle groups (colored ellipse) and motor neurons that innervate the muscles, including SMD and RME. Only left-side muscles and some of the motor neurons are shown (Modified from Gray et al. 2005). B, Neuromuscular junctions (NMJs) in the nerve ring. Dots in the processes show presynaptic specializations. SMDD/V and RMED/V form NMJ at adjacent locations (Modified from White et al. 1986).

(Driscoll and Kaplan, 1997; Kindt et al., 2007). The SMB neurons regulate the undulatory locomotion of *C. elegans*, because killing SMB results in deeply flexed, loopy sinusoidal waves along the body (Gray et al., 2005). Asymmetric excitation of SMB in moving animals modulates the bending angle of animal's head, steering the direction of forward movement (Kocabas et al., 2012). The SMD neurons are also implied in regulating head bending: neurophysiological studies show that the calcium dynamics in SMD is correlated with head deflection in semi-constrained animals; interestingly, SMD has oscillatory calcium activity independent of physical displacement of the head, and its interaction with the interneuron RIA modulates animal's posture during forward movement (Hendricks et al., 2012). In a pilot project, I found that the rhythmic calcium activity of SMD remains in *unc-13* or *unc-31* mutants, which are defective in synaptic neurotransmitter release or neuropeptidergic signaling (Brenner, 1974; Avery et al., 1993; Miller et al., 1996; Kohn et al., 2000; Richmond and Broadie, 2002). It suggests that SMD may generate spontaneous activities, and it remains an intriguing question how SMD interacts with the other neurons to modulate the gait of head deflection.

The body wall muscles of *C. elegans* also receive inhibitory inputs from motor neurons. During one body bend, acetylcholine (ACh) depolarizes muscles on one side and GABA hyperpolarizes the antagonist muscle on the opposite side (Schuske et al., 2004; Jorgensen, 2005). Located at the nerve ring, the RME neurons are the only class of GABAergic motor neurons that innervate head and neck muscles (McIntire et al., 1993b). Among the four RMEs, the mid-dorsal RMED and the mid-ventral RMEV form NMJs onto the ventral and dorsal muscle quandrants, respectively; the left-lateral RMEL and the right-lateral RMER form NMJs onto the lateral quandrants (White et al., 1986). Previously, McIntire et al. reported that removing RME neurons by laser surgery caused 'loopy' head deflection during forward movement, mimicking

the exaggerated head swing observed in *unc-25* mutants (McIntire et al., 1993b). Because RME is post-synaptic to SMB, IL2 and other neurons with hypothetical stretch receptors, it was proposed that RME neurons respond to stretch-induced signals from SMB, SAA or other partners and inhibit the contralateral muscle to restrain head deflection (McIntire et al., 1993b; Jorgensen, 2005).

While the mechanisms by which RME neurons regulate head movement remain largely hypothetical, previous work on the GABAergic D-type motor neurons has provided insights (McIntire et al., 1993b; Dittman and Kaplan, 2008; Schultheis et al., 2011). In the ventral nerve cord (VNC), GABAergic VD and DD neurons receive exclusive excitatory inputs from cholinergic motor neurons; therefore, enhancement of acetylcholine release often results in a parallel increase in GABA release (Dittman and Kaplan, 2008). The acetylcholinesterase inhibitor aldicarb and the ionotropic cholinergic agonist levamisole are often used to measure animal's sensitivity to acetylcholine-mediated excitation (Miller et al., 1996; Dittman and Kaplan, 2008). Using pharmacological assays, Dittman et al. found that the B-type GABA receptor mutants *gbb-1/2* were hypersensitive to acetylcholine accumulation and normal in levamisole sensitivity (Bettler et al., 2004; Dittman and Kaplan, 2008). Because *gbb-1* expression was identified in VNC cholinergic but not GABAergic motor neurons or body wall muscles (Dittman and Kaplan, 2008), the results suggest that GBB-1/2 may detect GABA signals from neighboring D-type neurons and reduce neuronal activity when ACh is elevated. By photoactivating the VNC GABAergic neurons, Schultheis et al. found the GBB-1/2 receptor was involved in acute body relaxation and locomotion (Schultheis et al., 2011). These findings suggest the communication between cholinergic and GABAergic systems may not be one-way, and the motor gait is likely regulated by a balanced act of both systems.

This chapter of my dissertation is focused on characterizing a small motor neuron circuit that modulates the gait of head deflection in *C. elegans*. I started with quantitative analysis of the animal's locomotory behavior during forward movement. By analyzing local head curvature, I found the cholinergic neuron SMD facilitates head bending, whereas the GABAergic neuron RME restrains head bending. I then examined the calcium dynamics in RMED/V and found its activity is correlated with, but not dependent on, dorsal-ventral head movement. The oscillatory calcium activity in RME requires cholinergic synaptic transmission from the SMD neurons. In return, RME signals to the $GABA_B$ receptor GBB-1/2 in SMD and negatively regulates head deflection. Using a combination of neurophysiological, behavioral and optogenetic approaches, I have dissected a local circuit with oscillatory calcium dynamics that fine tunes the amplitude of head movement. My collaborator Dr. Quan Wen contributed to the head curvature data analysis and proposed a mathematical model demonstrating that regulated head curvature and bending angle optimize the animal's phase velocity in forward movement. Together, our findings propose a parsimonious model for a balancing act of motor neurons to regulate the locomotory gait.

Results

The amplitude of head deflection is regulated by motor neurons

To understand the neural circuits that regulate the head bending amplitude, I used an automated tracking system to videotape freely moving animals on an agar plate and quantified locomotion by a Matlab algorithm [(Fig. 2. 2) (Wen et al., 2012)]. Using a customized script written by Dr. Quan Wen (Wen et al., 2012), I was able to analyze the local head curvature at single-worm resolution. As previously reported, the cholinergic SMD neurons show oscillatory calcium activities in correlation with animal's head movement (Hendricks et al., 2012). However, it remains unclear how SMDs interact with the other neurons and together modulate the amplitude of head deflection.

To evaluate the role of SMD in regulating head movement, I first analyzed the behavior of transgenic animals expressing Tetanus toxin under the *glr-1* promoter. The expression of *glr-1::TeTx* blocks synaptic vesicle release from a group of neurons, including SMD and RMD (Schiavo et al., 1992; Brockie et al., 2001; Hendricks et al., 2012). Compared with non-transgenic controls, the head curvature of transgenic animals was dramatically decreased (Fig. 2. 3A). To examine whether the effect was caused by blocking neurotransmission from SMD, I ablated the four SMD neurons using a laser micro-beam and found that the SMD-ablated animals showed similar decrease in head curvature in comparison with mock controls (Fig. 2. 3B). The 'stiff' head movement in animals lacking SMD suggests that the SMD neurons, by contracting contralateral head muscles, positively regulate animal's head curvature during forward movement.

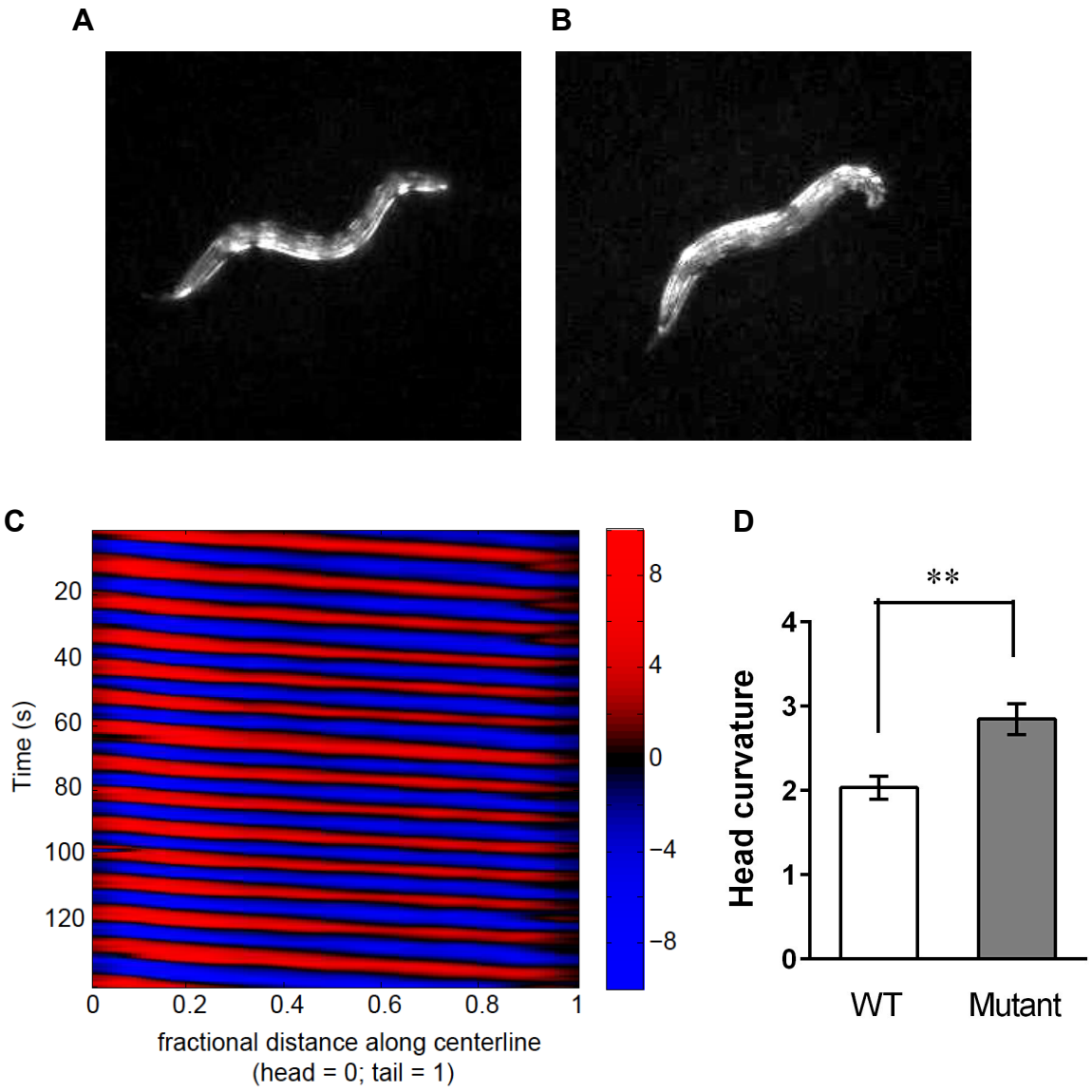

Figure 2. 2 Quantitative analysis of local curvature in *C. elegans*. A and B, Snapshot of a wild-type animal (A) and a mutant (B) during forward movement. C, Kymogram of time-varying curvature illustrating wave propagation along animal's body (Courtesy of Q. Wen). D, Head curvature of wild-type and mutant animals during forward movement over a 90-second period. Student's t-test, **p< 0.01. n≥ 10 animals. Mean ± SEM.

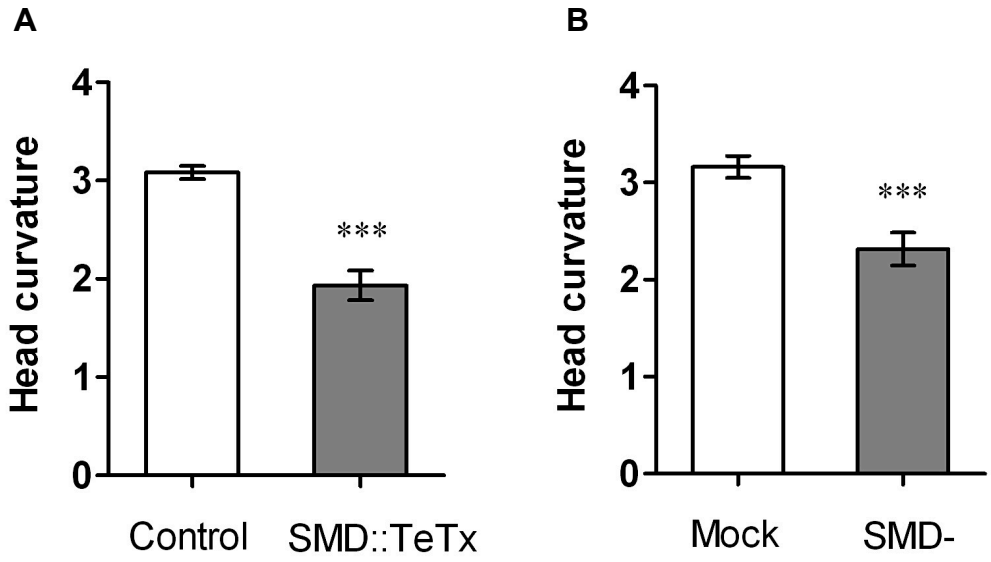

Figure 2. 3 SMD neurons facilitate head deflection during forward movement. A, Transgenic animals expressing *Pglr-1::TeTx* in neurons including SMD show decreased head curvature. B, SMD-ablated animals show decreased head curvature. Transgenic animals are compared with non-transgenic siblings; neuron-ablated animals are compared with mock controls. Student's t-test, ***$p < 0.001$. $n \geq 8$ animals. Mean ± SEM.

The cholinergic SMD neurons innervate the same group of head muscles as another class of motor neurons, the GABAergic RMEs (White et al., 1986) (Fig. 2. 1B). Previously, McIntire et al. described that RME-ablated animals make 'loopy' head swing during foraging (McIntire et al., 1993b). To characterize the phenotype quantitatively, I ablated the four RME neurons by laser surgery and analyzed head curvature. Consistent with previous observation (McIntire et al., 1993b), RME-ablated animals showed exaggerated head deflection during forward movement (Fig. 2. 4A). Because the RME group consists of the RMED/V pair and the RMEL/R pair, I ablated the two subsets respectively and found that ablating only RMED/V caused similarly exaggerated head movement along the dorsal-ventral axis, whereas ablating only RMEL/R did not alter dorsal-ventral head bending (Fig. 2. 4B). These results suggest that RMED/V neurons limit the amplitude of head deflection when animals move forward. Henceforth, RME refers to the RMED/V neurons.

To validate the relevance of GABA, I evaluated the effect of removing several key components in the GABA signaling pathway, including UNC-25, the GABA biosynthetic enzyme glutamic acid decarboxylase (GAD) and UNC-47, the transmembrane vesicular GABA transporter (McIntire et al., 1993a; Eastman et al., 1999; Jin et al., 1999). Consistently, *unc-25(e156)* and *unc-47(e307)* mutants show increased head bending amplitude during forward movement (Fig. 2. 5). Together, these results demonstrate that the gait of head movement is regulated by multiple motor neurons: cholinergic SMDs facilitate head bending, and GABAergic RMEs restrain head bending.

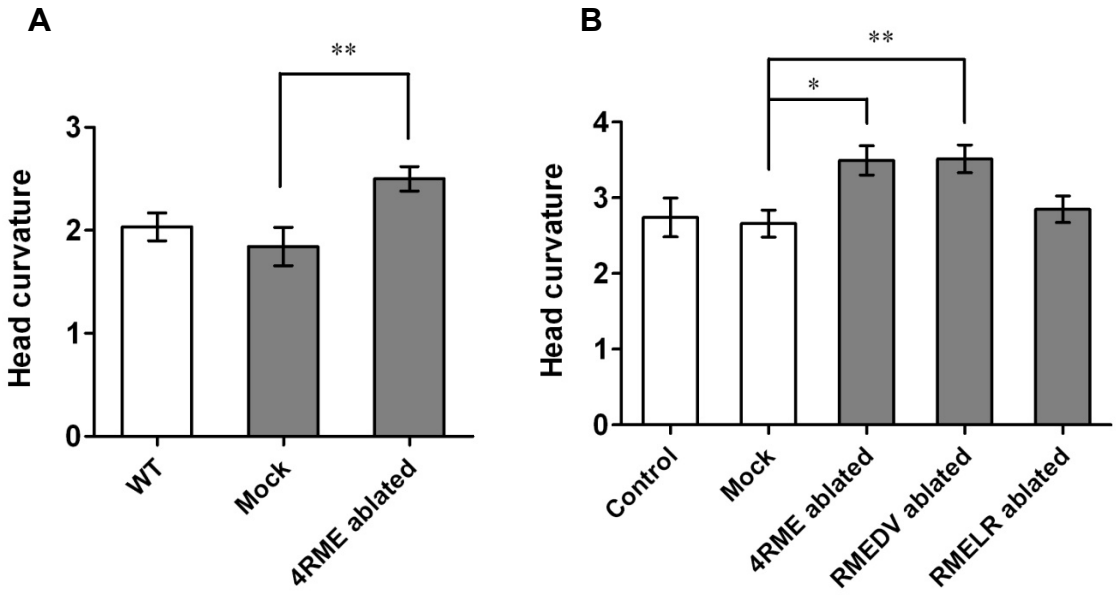

Figure 2. 4 RME neurons restrain head deflection during forward movement. A, Animals with all four RME neurons ablated show increased head curvature. B, RMEDV-ablated animals show increased head curvature, but RMELR-ablated animals are normal. Strain ZM6665 is used for neuron ablation in (A) and CZ1200 is used in (B) with baseline variation. Neuron-ablated animals are compared with mock controls. One-way ANOVA with Dunnett post test. *$p< 0.05$, **$p< 0.01$. $n\geq 9$ animals. Mean ± SEM.

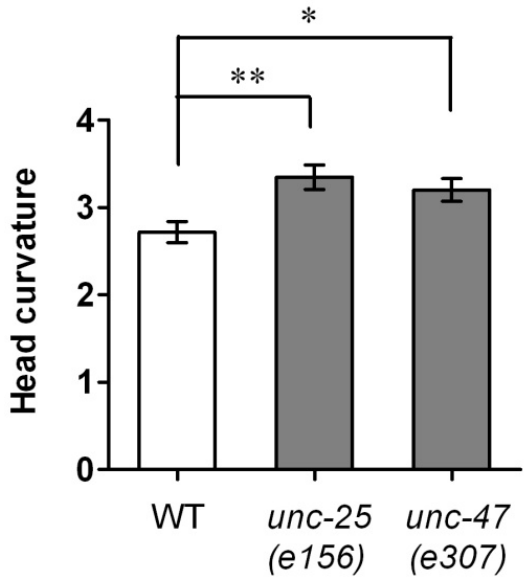

Figure 2. 5 Mutants that are defective in GABA synthesis or release show exaggerated head deflection. *unc-25* encodes glutamic acid decarboxylase (GAD), *unc-47* encodes vesicular GABA transporter (VGAT). Mutants are compared with wild-type controls. One-way ANOVA with Dunnett post test. *$p < 0.05$, **$p < 0.01$. $n \geq 9$ animals. Mean ± SEM.

Calcium dynamics in RME is correlated with head movement

The oscillatory calcium dynamics in SMD neurons underlies their role in facilitating head movement (Hendricks et al., 2012). To characterize the activity of RME neurons, I used the genetically encoded calcium indicator GCaMP3 driven by the GABAergic neuron-specific *unc-25* promoter to perform calcium imaging in a microfluidic device, in which semi-restrained transgenic animals wiggle their heads in the dorsal-ventral plane (Chronis et al., 2007; Hendricks et al., 2012). I found that RME neurons displayed rhythmic calcium activity during head bending: The calcium signal increased in RMEV and decreased in RMED during ventral head deflection, and it changed oppositely during dorsal head deflection (Fig. 2. 6A). When ventral bends were defined as positive and dorsal as negative, a cross-correlation analysis between head movement and calcium signals showed positive correlation between RMEV calcium activity and head movement, whereas RMED calcium activity was negatively correlated with head movement (Fig. 2. 6B). The calcium dynamics in RMEV and RMED was negatively correlated when animals make dorsal-ventral head movement (Fig. 2. 6C).

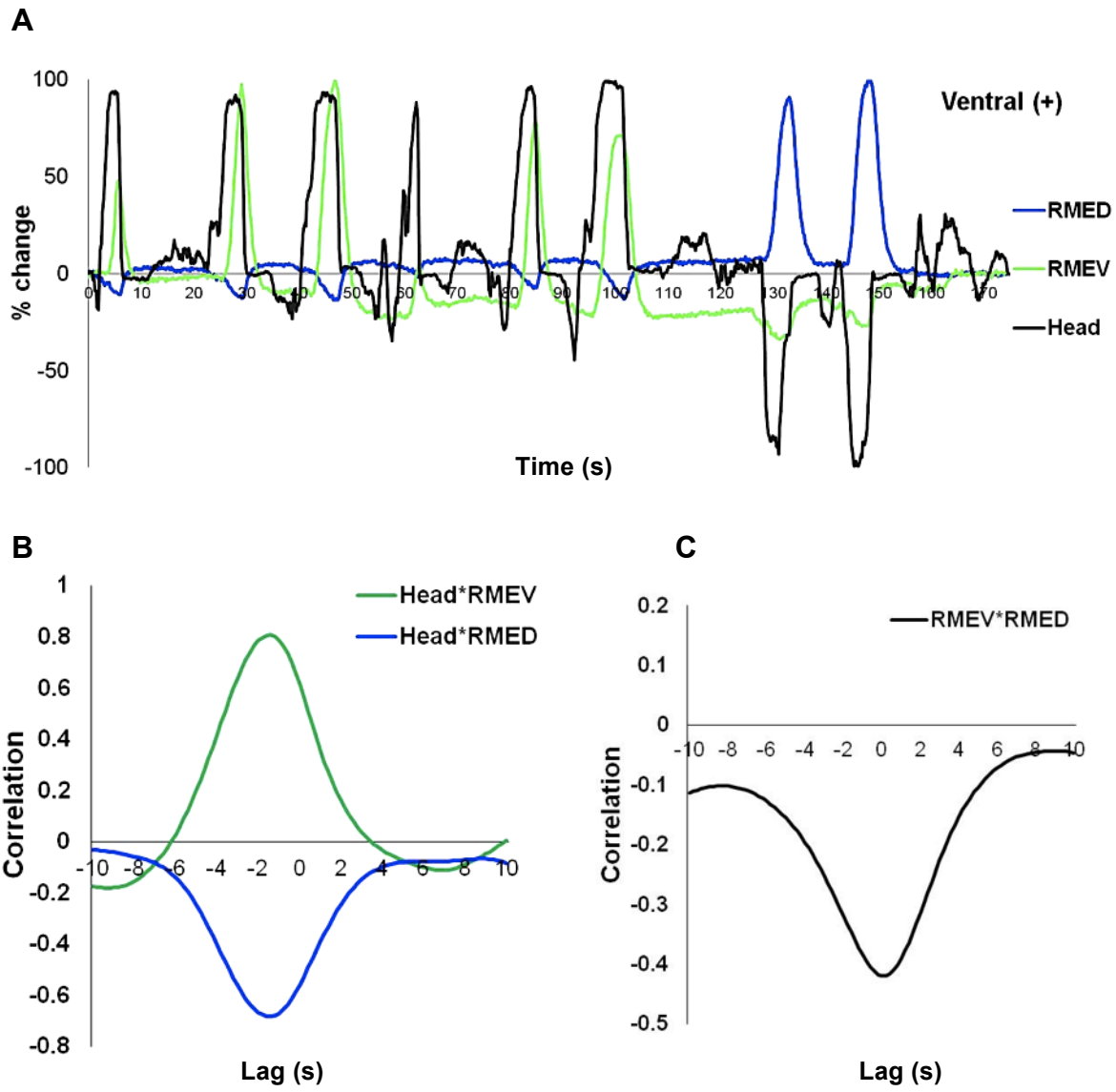

Figure 2. 6 Calcium dynamics in RMED/V during head movement. A, Representative trace of normalized calcium activity in RMED, RMEV and head movement (ventral bends as positive). B, Cross-correlation between head movement and RME calcium activity. C, Cross-correlation between calcium activity in RMEV and RMED.

Because both SMDD/V and RMED/V show bending-associated calcium activities, I generated animals that express *glr-1::GCaMP3* and *unc-25::GCaMP3* transgenes so that SMD and RME neurons can be imaged simultaneously (Fig. 2. 7A). In semi-restrained animals on agar pads, SMDV and RMEV were both excited during ventral head deflection, while SMDD and RMED were activated during dorsal head deflection (Fig. 2. 7B). Cross-correlation analysis showed that the activities of SMDV and RMEV, or SMDD and RMED, were positively correlated during forwarding-associated head swings, and SMD activity was slightly ahead of RME activity (Fig. 2. 7C). The correlation between SMD and RME calcium activities suggests that SMD activates one side of head muscle while RME relaxes the contralateral side. It remains unclear why the removal of RME neurons results in exaggerated head deflection.

Figure 2. 7 Simultaneous calcium imaging of SMD and RME neurons.

A, Volume view of a 3-D image stack from an animal expressing *Pglr-1::GCaMP3* and *Punc-25::GCaMP3*. B, Representative traces of calcium dynamics in SMDD and RMED during head movement. C, Cross-correlation between calcium activity in SMDD and RMED. n= 6 animals, Mean ± SEM.

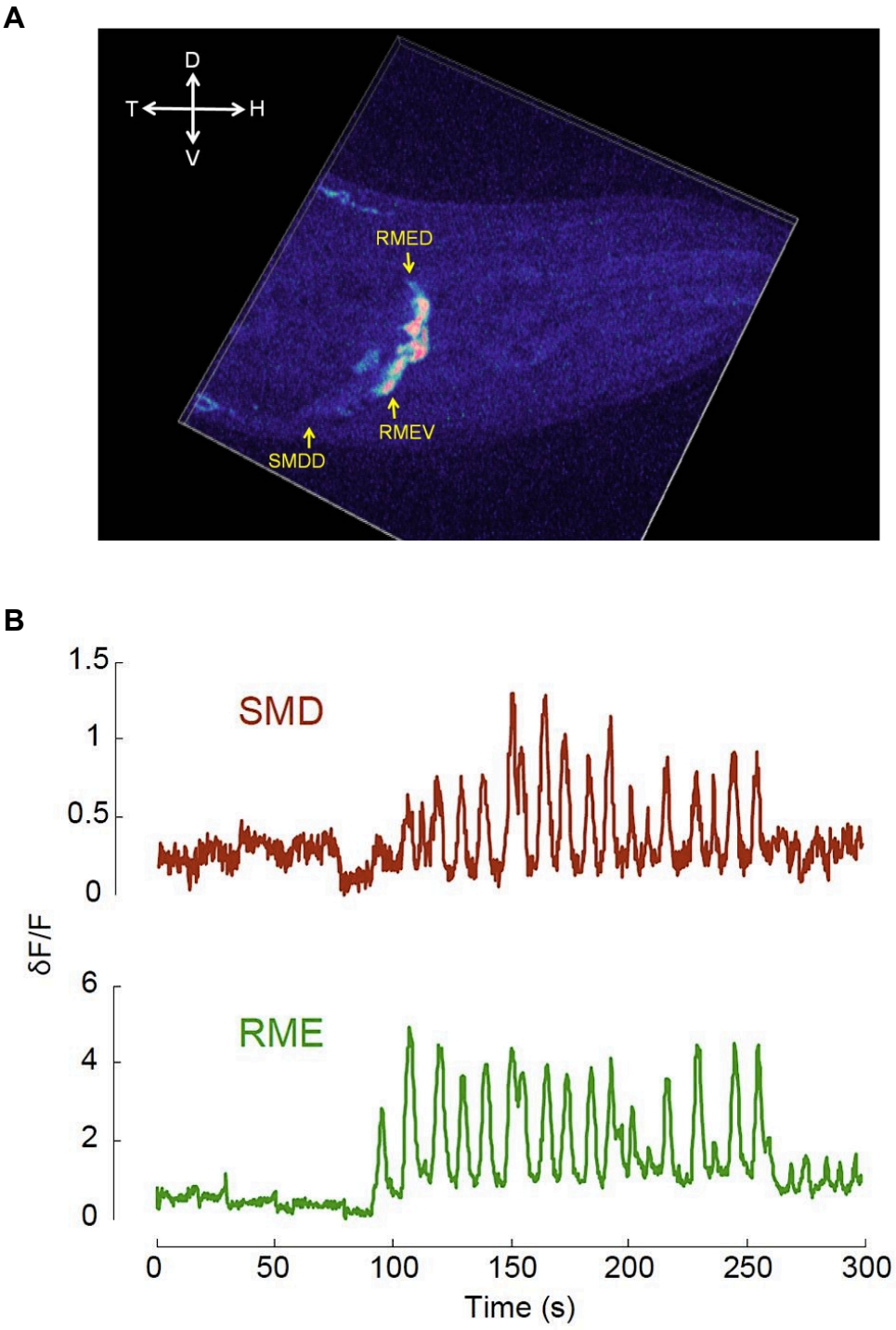

Figure 2. 7 (Continued)

C

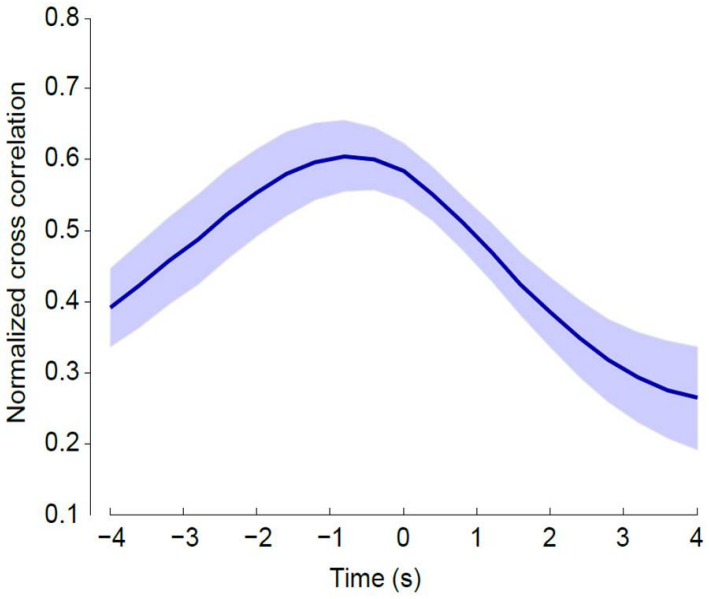

Figure 2. 7 (Continued)

Calcium activity of RME does not depend on physical displacement of head

The correlation between RME calcium signals and head movement could result from the response of RME to the stretch of head muscles (McIntire et al., 1993b; Jorgensen, 2005). To examine whether the calcium activity of RME depends on head movement, I used microbeads to restrain animals on agar pads and performed calcium imaging on RME (Fang-Yen et al., 2009). To monitor muscle activity in the immobilized animals, I expressed the RFP-based calcium indicator RCaMP in body-wall muscles using the *myo-3* promoter (Miller et al., 1986; Akerboom et al., 2013). When oscillatory RCaMP signal was observed in head muscles, the two RME neurons showed calcium activity in correlation with the ipsilateral muscle activity, even though no actual head movement was observed (Fig. 2. 8). Therefore, the rhythmic activity of RME is independent of physical displacement of animal's head.

Figure 2. 8 Calcium dynamics in RME neurons and head muscles in immobilized animals. A, Snapshot of a wild-type animal expressing *Punc-25::GCaMP3* (left, green channel) and *Pmyo-3::RCaMP* (right, red channel). B, Calcium activity in RMED and RMEV neurons (upper panel) and in head muscles (lower panel). Activities in RMED and dorsal muscle are correlated, and activities in RMEV and ventral muscle are correlated. C, Cross-correlation between calcium activities in ventral muscle and RMEV (green trace), and cross-correlation between calcium activities in dorsal muscle and RMED (blue trace).

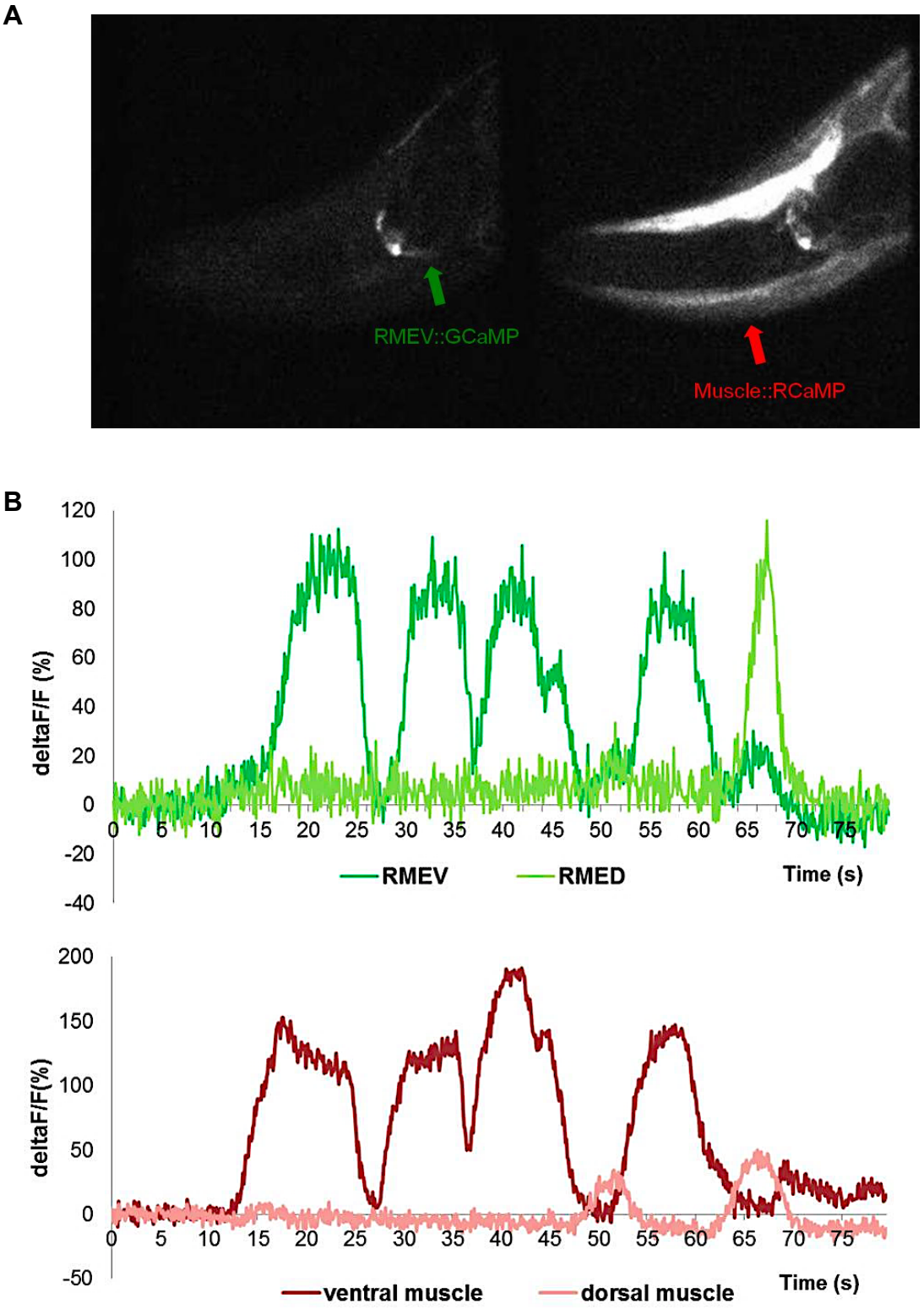

Figure 2. 8 (Continued)

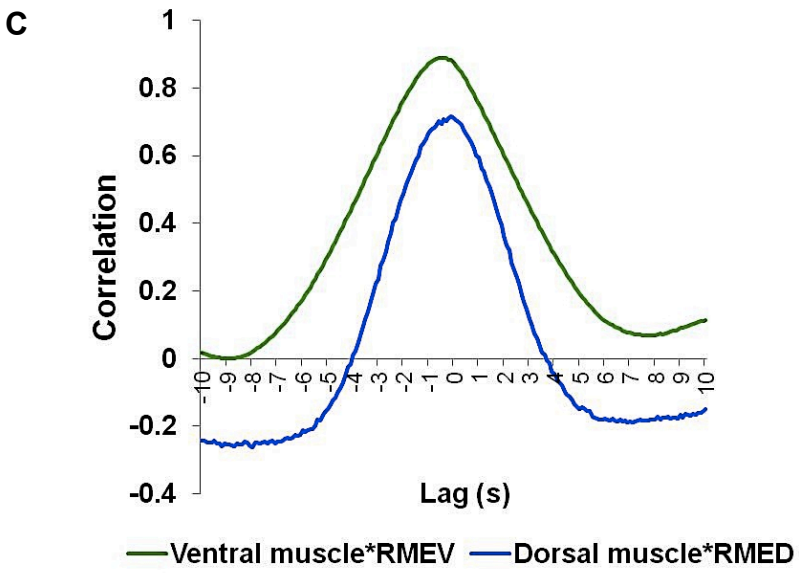

Figure 2. 8 (Continued)

Considering possible unnoticed muscle contraction in the immobilized animals, I examined RME and muscle calcium activity in the *unc-54* mutants, which lack a major myosin heavy chain protein and are thus defective in body-wall muscle contraction (MacLeod et al., 1977a; MacLeod et al., 1977b; Dibb et al., 1985). Interestingly, the calcium dynamics of RME largely remains when alternating calcium activity is detected in dorsal and ventral muscle cells (Fig. 2. 9), even with severely defective muscle contraction in *unc-54* null mutants (Dibb et al., 1985). These results show that head movement or normal head muscle contraction is not required for the oscillatory calcium activity in RME neurons.

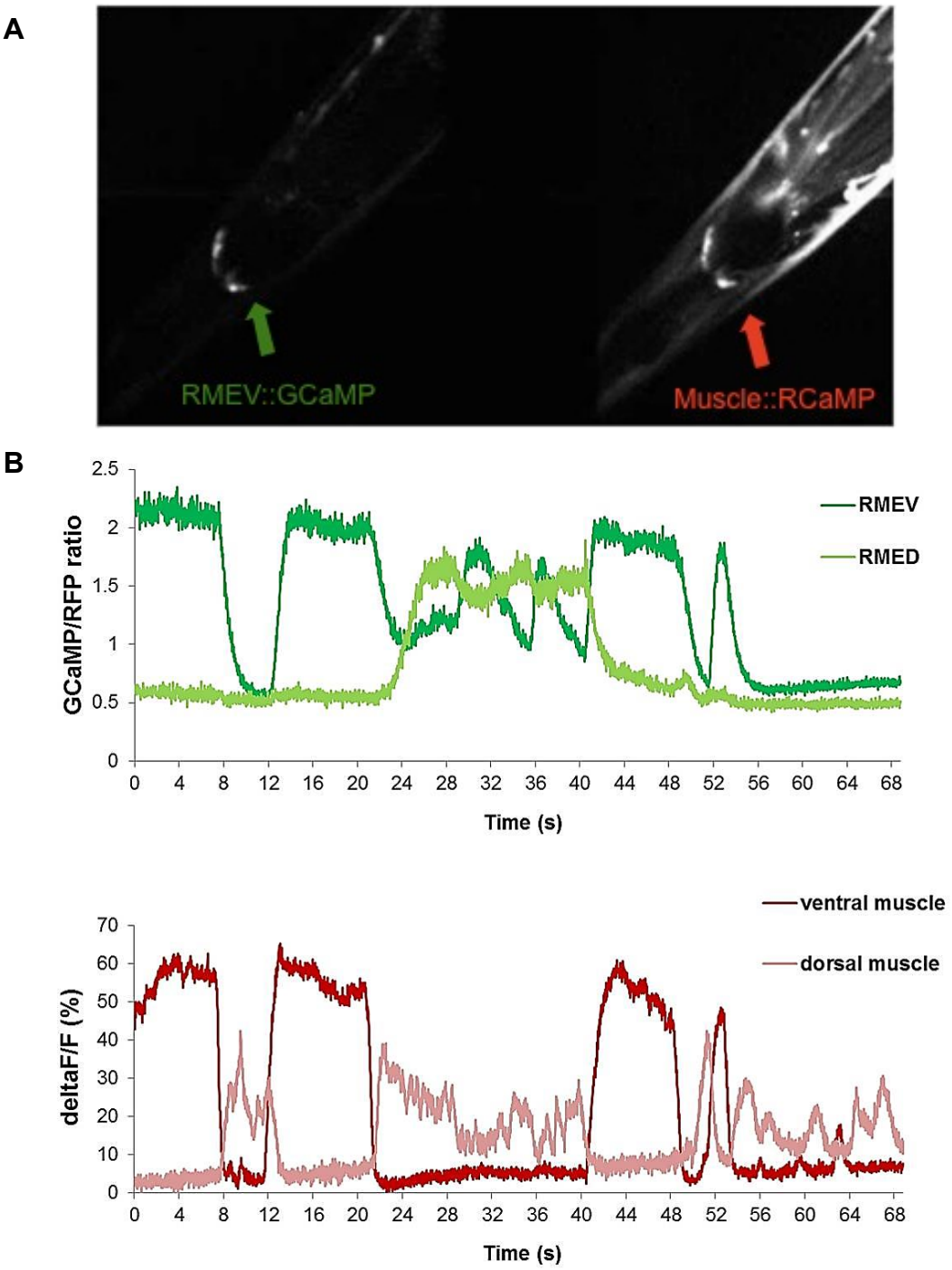

Figure 2. 9 Calcium dynamics in RME neurons and head muscles in *unc-54(e1092)* mutant. A, Snapshot of an *unc-54* animal expressing *Punc-25::GCaMP3::rfp* (left, green channel) and *Pmyo-3::RCaMP* (right, red channel). B, Calcium activities in RME and muscle. GCaMP3/RFP ratio is taken for RME imaging.

Correlation between RME activity and head movement depends on cholinergic synaptic transmission

To characterize the nature of RME calcium activity, I examined its dependence on classic neurotransmission and neuropeptide signaling. I performed RME calcium imaging in *unc-13* and *unc-31* mutants, which are defective in the release of classic neurotransmitters and dense-core vesicles, respectively (Brenner, 1974; Avery et al., 1993; Miller et al., 1996; Kohn et al., 2000; Richmond and Broadie, 2002). The correlation between RME somatic calcium activity and head movement was impaired in *unc-13 (e51)* (Fig. 2. 10). In contrast, *unc-31(e928)* animals displayed wild-type like calcium dynamics in RME (data not shown). These results show that the calcium activity of RME neurons, unlike that of SMDs, requires neurotransmission (Hendricks et al., 2012; data not shown).

Because RMED/V are post-synaptic to several cholinergic neurons (White et al., 1986; Duerr et al., 2008), I performed calcium imaging in mutants that lack the choline acetyltransferase CHA-1, which is required for the biosynthesis of acetylcholine (ACh) and is expressed in all cholinergic motor neurons (Rand and Russell, 1984; Alfonso et al., 1994; Hendricks et al., 2012). The hypomorphic allele *cha-1(p1152)* (Rand and Russell, 1984) showed defects in RME calcium response during head movement (Fig. 2. 10). This defect was rescued by a cosmid, ZC416, containing the genomic locus of *cha-1* (Hendricks et al., 2012). Together, these results indicate that the oscillatory calcium activity of RME neurons and its correlation with head deflection require cholinergic synaptic transmission.

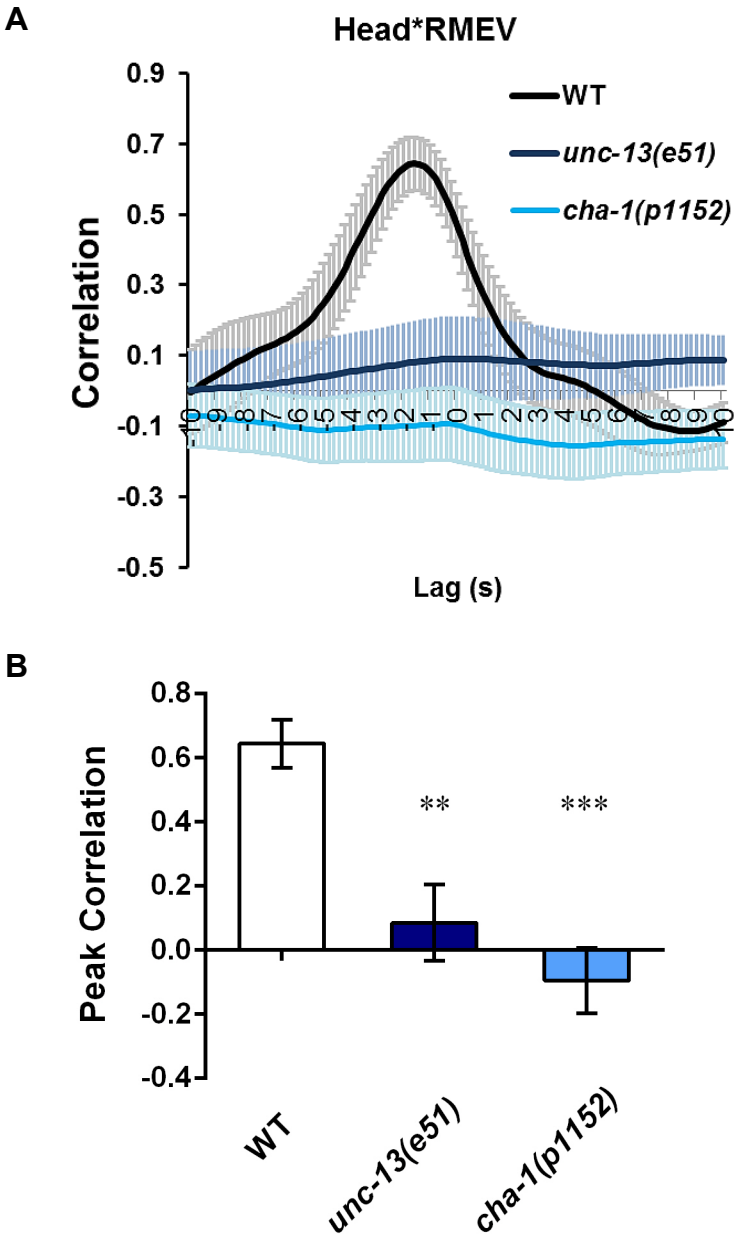

Figure 2. 10 Correlation between head movement and RME activity is impaired in *unc-13* and *cha-1* mutants. A, Cross-correlation between head movement and RMEV calcium activity. WT: wild type. n= 10 animals for WT, n= 13 animals for mutants, error bars denote SEM. B, Peak correlation in WT and mutants. One-way ANOVA with Dunnett post test, **p< 0.01, ***p< 0.001. Mean ± SEM.

Synaptic transmission from SMD is sufficient and necessary to drive RME calcium activity

To examine which presynaptic partner of RME drives its calcium dynamics, I expressed the full-length *cha-1* cDNA under neuron-specific promoters and performed calcium imaging in the transgenic animals. The major synaptic inputs to RMED/V are from the cholinergic neurons SMB and IL2 (White et al., 1986). Restoring *cha-1* expression in SMB by the *odr-2(18)* promoter, or in IL2 by the *klp-6* promoter (Chou et al., 2001; Peden and Barr, 2005; Lee et al., 2012), did not rescue the RME calcium defects in *cha-1* mutants (Fig. 2. 11). Because a recently updated connectome of the *C. elegans* nervous system reported a small number of synaptic inputs from SMD to RME (Emmons et al.; Fig. 2. 12), I tested animals expressing *cha-1* cDNA under the *glr-1* and the *lad-2* promoters. Both the *glr-1* and *lad-2* promoters drive expression in multiple cells, but the only neuron pair where the expression overlaps is SMD (Brockie et al., 2001; Wang et al., 2008; Hendricks et al., 2012). Strikingly, both *glr-1::cha-1* cDNA and *lad-2::cha-1* cDNA transgenes fully rescued the oscillatory calcium dynamics in RME and its correlation with head movement along the dorsal-ventral axis (Fig. 2. 11). These results suggest that *cha-1* expression in SMD was sufficient to restore normal calcium activity in the RME neurons. It prompted me to hypothesize that SMDs drive calcium oscillations in RME.

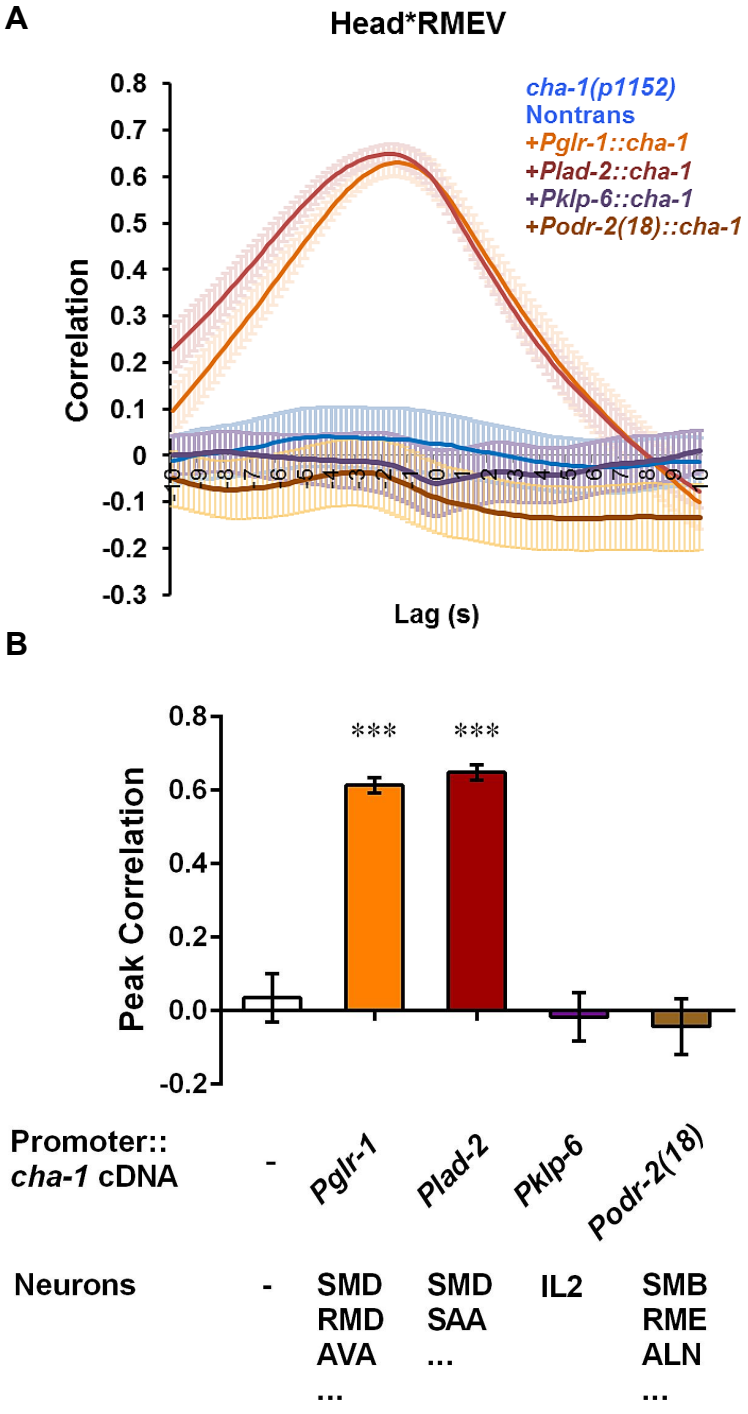

Figure 2. 11 Cell-specific rescue in *cha-1* mutants. A, Cross-correlation between head movement and RME calcium activity in controls and animals expressing *cha-1* cDNA under cell-specific promoters. B, Peak correlation in controls and transgenic animals

(continue on next page).

Figure 2. 11 (Continued) Neurons that express *cha-1* under different promoters are listed. One-way ANOVA with Dunnett post test, ***p< 0.001. n≥ 10 animals, Mean ± SEM.

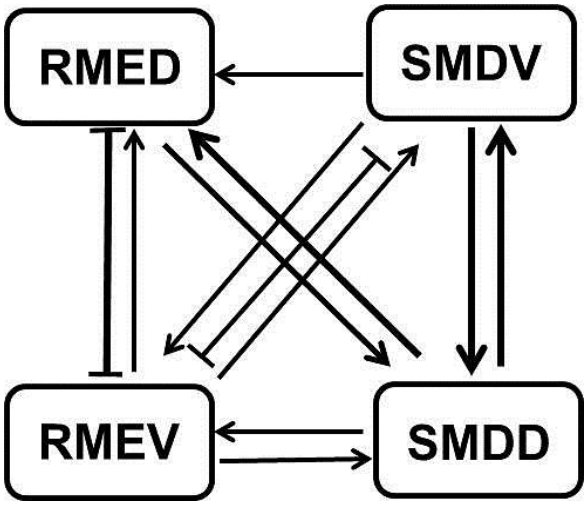

Figure 2. 12 Synaptic connection between SMD and RME neurons. A small number of synapses exist between SMD and RME based on the updated connectome database http://wormwiring.org (Emmons et al.). Arrows denote chemical synapses and bar-ended lines denote gap junctions.

To test this hypothesis, I first blocked neurotransmission from the SMD neurons by expressing Tetanus toxin (TeTx) under either the *glr-1* or *lad-2* promoter and examined the calcium dynamics in RME (Schiavo et al., 1992). Transgenic animals expressing *glr-1::TeTx* or *lad-2::TeTx* lost the RME calcium activities in correlation with head bending (Fig. 2. 13). Few calcium signals were detected in RME during head movement (data not shown). In contrast, animals expressing *odr-2(18)::TeTx* in SMB, or *klp-6::TeTx* in IL2, or both *odr-2(18)::TeTx* and *klp-6::TeTx*, seemed to be indistinguishable from non-transgenic siblings in their RME calcium activity (Fig. 2. 14). Because the expression of TeTx under *glr-1* and *lad-2* promoters only overlaps in SMD (Brockie et al., 2001; Wang et al., 2008; Hendricks et al., 2012), these results suggest that neurotransmitter release from SMD, but not SMB or IL2, is required for the calcium oscillation in RME. To confirm that, I used a laser micro-beam to kill all the four SMD neurons in L1-L2 larvae and performed RME calcium imaging when the recovered animals reached adulthood. Consistently, compared with mock controls, SMD-ablated animals were defective in head-bending correlated-RME calcium dynamics (Fig. 2. 15), whereas ablation of all the six IL2 neurons did not cause the defect (data not shown). Together, these results show that synaptic transmission from SMD drives the oscillatory calcium activities in RME in correlation with head bending.

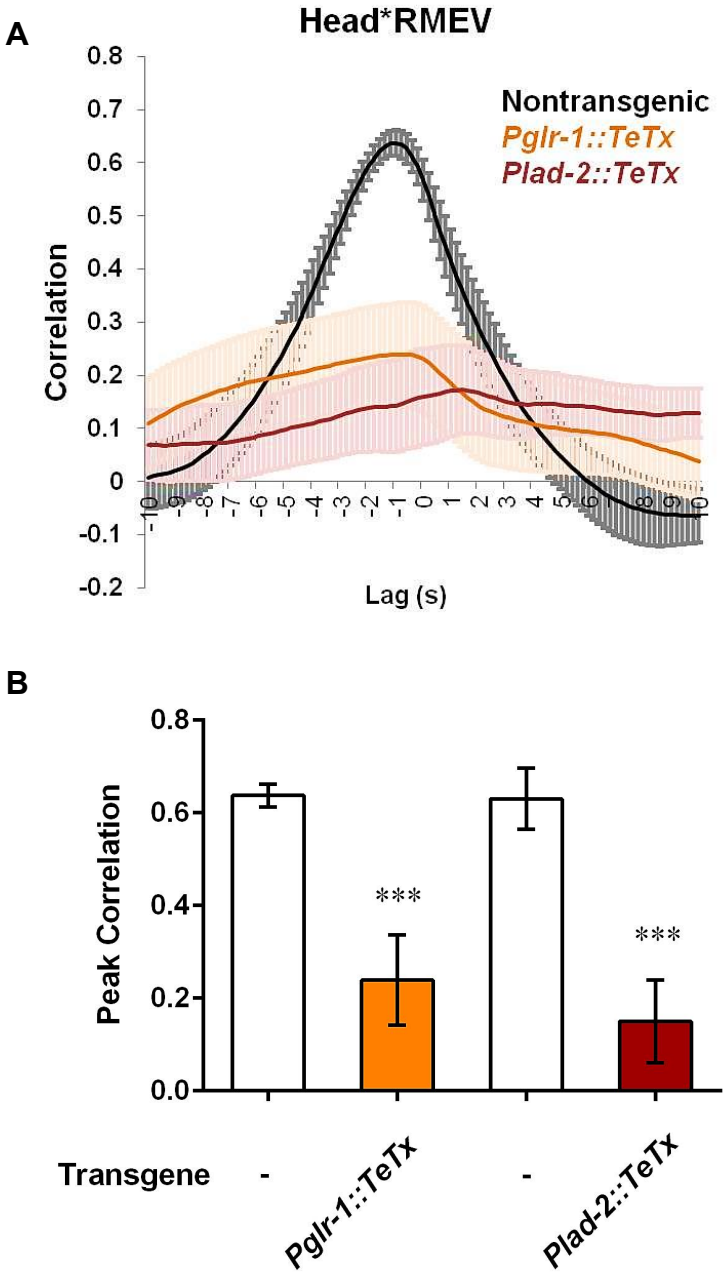

Figure 2. 13 Blockade of synaptic transmission from SMD impairs the correlation between head movement and RME calcium activity. A, Cross-correlation between head movement and RME activity in animals expressing *Pglr-1::TeTx* or *Plad-2::TeTx* and nontransgenic controls. B, Peak correlation data in nontansgenic and transgenic animals are compared. Student's t-test, ***p< 0.001. n≥ 9 animals, Mean ± SEM.

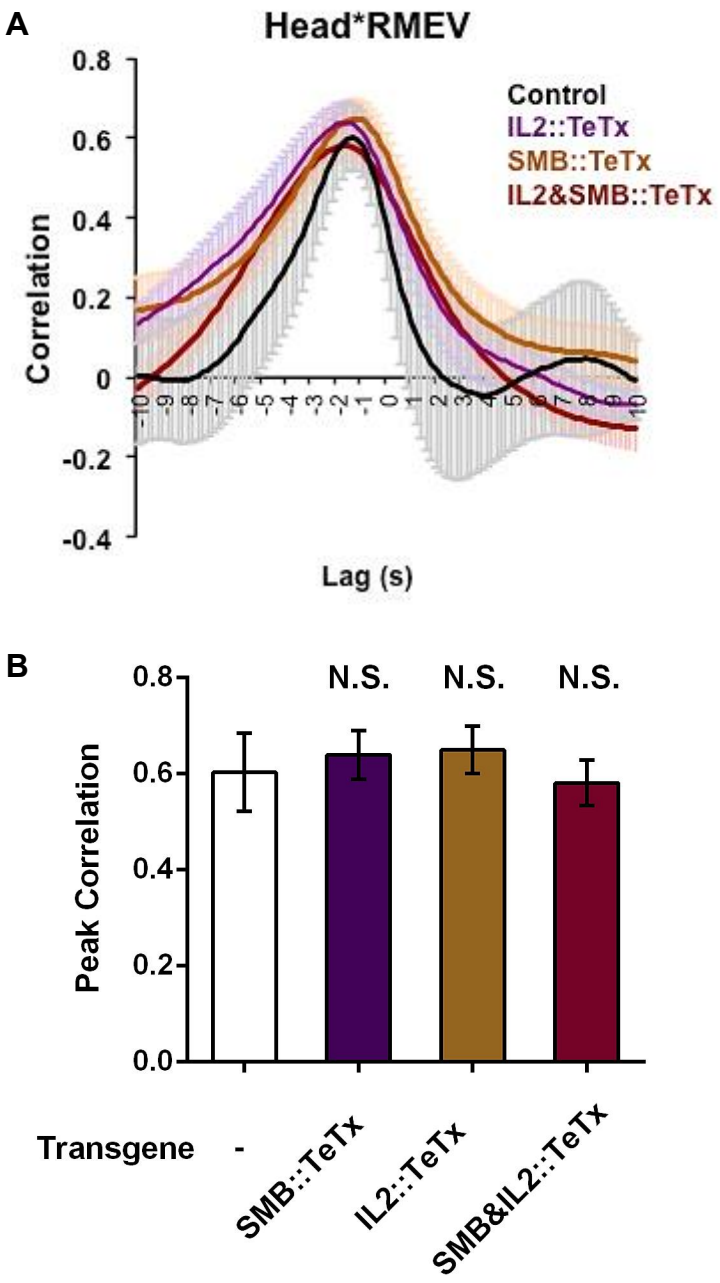

Figure 2. 14 Blockade of synaptic transmission from IL2 or SMB does not impair the correlation between head movement and RME calcium activity. A, Cross-correlation between head movement and RME activity in animals expressing *Pklp-6::TeTx* in IL2 or *Podr-2(18)::TeTx* in SMB and nontransgenic controls. B, Peak correlation data in nontansgenic and transgenic animals are compared. One-way AVONA with Dunnett post test. N.S., not significant. n≥ 8 animals, Mean ± SEM.

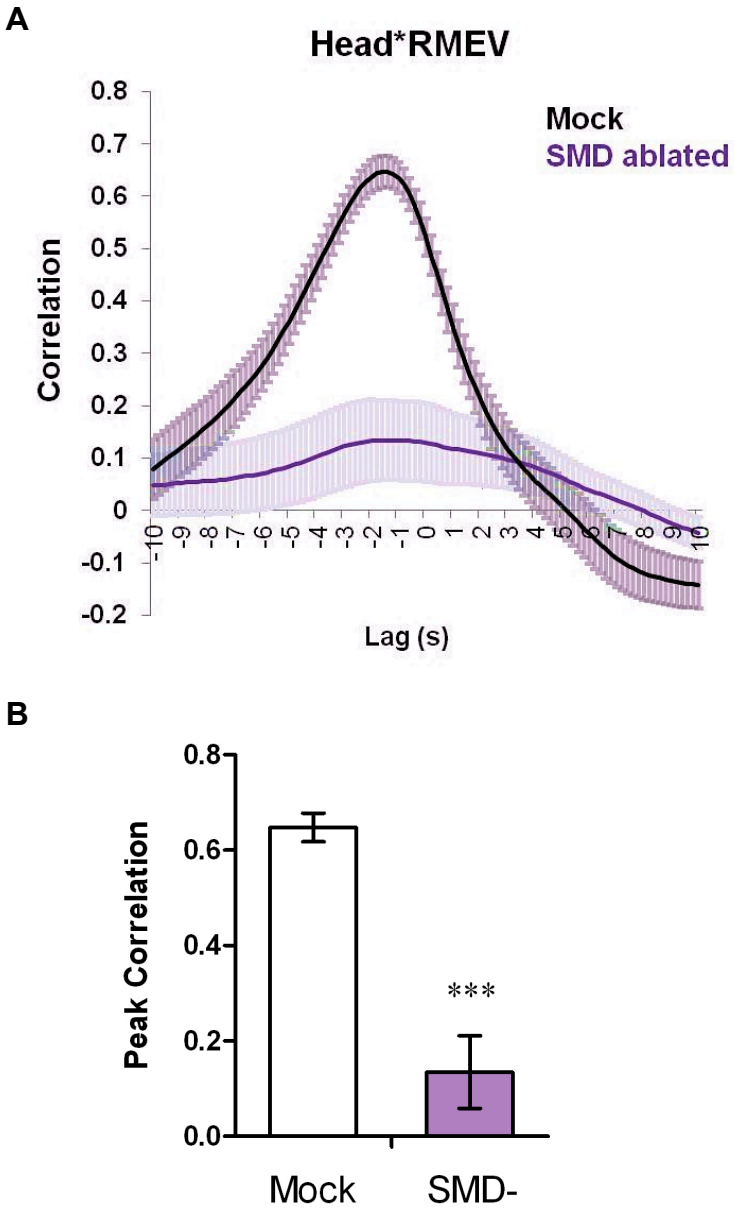

Figure 2. 15 SMD ablation abolishes the correlation between head movement and RME calcium activity. A, Cross-correlation between head movement and RME activity in SMD-ablated animals and mock controls. B, Peak correlation data in ablated animals and mock controls are compared. Student's t-test, ***$p < 0.001$. $n \geq 9$ animals, Mean ± SEM.

$GABA_B$ receptor GBB-1/2 functions in SMD to limit head bending amplitude

RME neurons form neuromuscular junctions (NMJ) on the contralateral head and neck muscles (White et al., 1986; McIntire et al., 1993b). Upon activation, elevated GABA binds the inotropic $GABA_A$ receptor UNC-49, which conducts Cl^- to hyperpolarize the muscle cell (McIntire et al., 1993a; Bamber et al., 1999; Richmond and Jorgensen, 1999; Bamber et al., 2005). It is possible that graded release of GABA also tunes down muscle activity (Liu et al., 2009). However, the temporal dynamics of RME activity suggests that its role in restraining head deflection is not mainly mediated by the muscle-expressed UNC-49.

C. elegans has another type of GABA receptor that is homologous to the $GABA_B$ receptor in mammals (Bettler et al., 2004; Dittman and Kaplan, 2008; Vashlishan et al., 2008). An RNA interference screen for aldicarb hypersensitivity has identified two genes, *gbb-1* (Y41G9A.4) and *gbb-2* (zk180.1/2), encoding the $GABA_B$R1 and $GABA_B$R2 subunits that function as obligate heterodimers (Dittman and Kaplan, 2008; Vashlishan et al., 2008). To determine whether the $GABA_B$ receptor GBB-1/2 is involved in regulating the gait of head deflection, I analyzed the behavior of the deletion allele *gbb-1(tm1406)* and the double mutant *gbb-1(tm1406);gbb-2(tm1165)*, both of which are predicted to eliminate $GABA_B$ receptor function (Dittman and Kaplan, 2008). Using the automated tracking system (Materials and Methods) to quantify head curvature, I found that both strains made bigger head swing during forward movement (Fig. 2. 16); the head curvature of the *gbb-1;gbb-2* double mutants was indistinguishable from that of the *gbb-1* single mutant, consistent with the prediction that GBB-1 and GBB-2 function as heterodimer (Bettler et al., 2004; Dittman and Kaplan, 2008). The exaggerated head deflection in *gbb-1* was rescued by expressing the *gbb-1* cDNA under the *gbb-*

1 endogenous promoter (Fig. 2. 17). Together, these results demonstrate that $GABA_B$ receptor is required to limit head deflection.

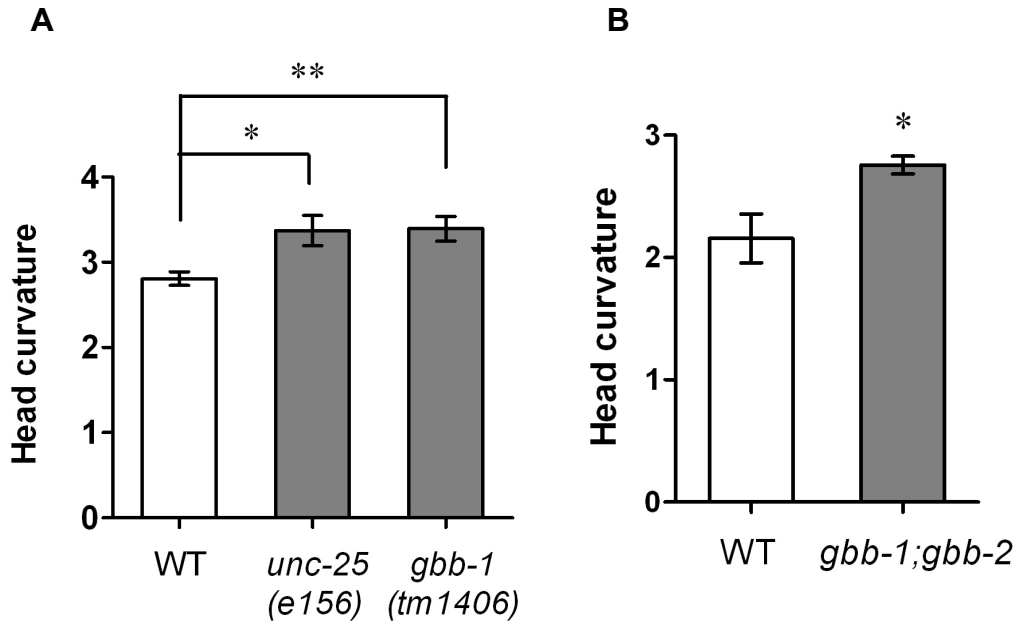

Figure 2. 16 $GABA_B$ receptor mutants show exaggerated head deflection. A, *gbb-1 (tm1406)* mutants show increased head curvature as *unc-25(e156)* mutants. One-way ANOVA with Dunnett post test, *p< 0.05, **p< 0.01. n≥ 10 animals, Mean ± SEM. B, *gbb-1(tm1406);gbb-2(tm1165)* double mutants show increased head curvature. Student's t-test, *p< 0.05. n≥ 10 animals, Mean ± SEM.

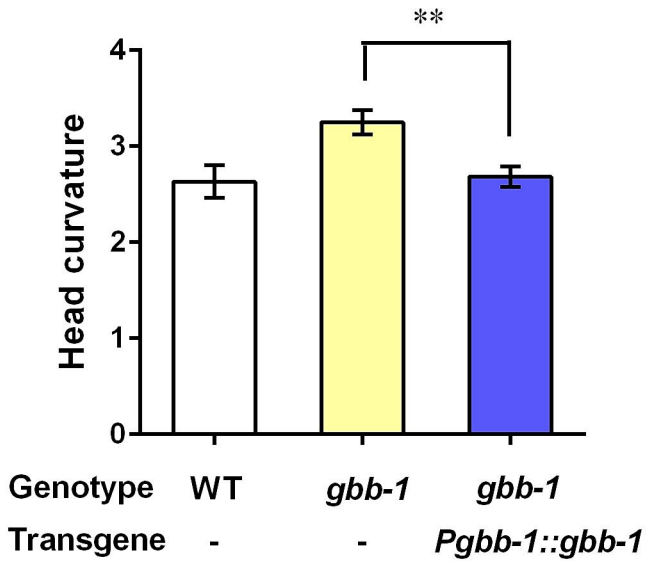

Figure 2. 17 The exaggerated head deflection in *gbb-1(tm1406)* mutants is rescued by expressing *gbb-1* cDNA under the endogenous promoter of *gbb-1*. Transgenic animals are compared with non-transgenic siblings. One-way ANOVA with Boferroni correction, **p< 0.01. n≥ 10 animals, Mean ± SEM.

To characterize how the GBB-1/2 receptor modulates head movement, I examined the expression pattern of *gbb-1*. The expression of a GFP reporter driven by the *gbb-1* promoter was observed in the nervous system, including the cholinergic neurons along the ventral nerve cord, but not GABAergic neurons or muscle (Dittman and Kaplan, 2008). Using the same transcriptional reporter, I identified *gbb-1::gfp* expression in a number of head neurons, including SMD and possibly SAA (Fig. 2. 18 and data not shown). To address whether GBB-1/2 acts in SMD to regulate head deflection, I used cell-specific promoters to drive the expression of the wild-type *gbb-1* cDNA in *gbb-1* mutants. Compared with non-transgenic siblings, expressing *gbb-1* cDNA under the *glr-1* promoter or the *lad-2* promoter restored the normal head curvature in the *gbb-1* mutant animals (Fig. 2. 19). Among the neurons that endogenously express *gbb-1*, the expression of *glr-1::gbb-1* and *lad-2::gbb-1* only overlaps in the SMD neurons (Brockie et al., 2001; Wang et al., 2008; Hendricks et al., 2012). Therefore, the GBB-1/2 $GABA_B$ receptor functions in SMD to negatively regulate the amplitude of head deflection in *C. elegans*.

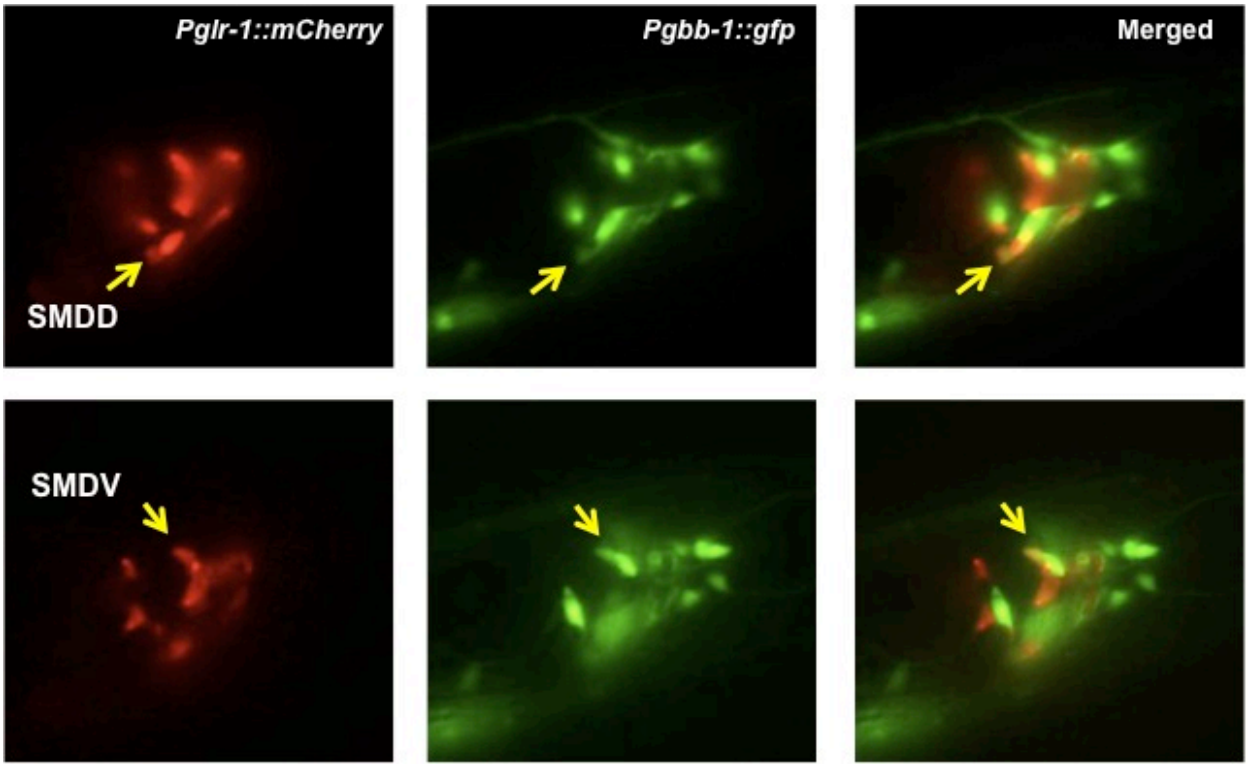

Figure 2. 18 *gbb-1* is expressed in head neurons. *Pglr-1::mCherry* is expressed in SMD, RMD, AVA and additional cells (Brockie et al., 2001). *Pgbb-1::gfp* and *Pglr-1::mCherry* overlap in SMD. Arrows denote SMDD and SMDV neurons.

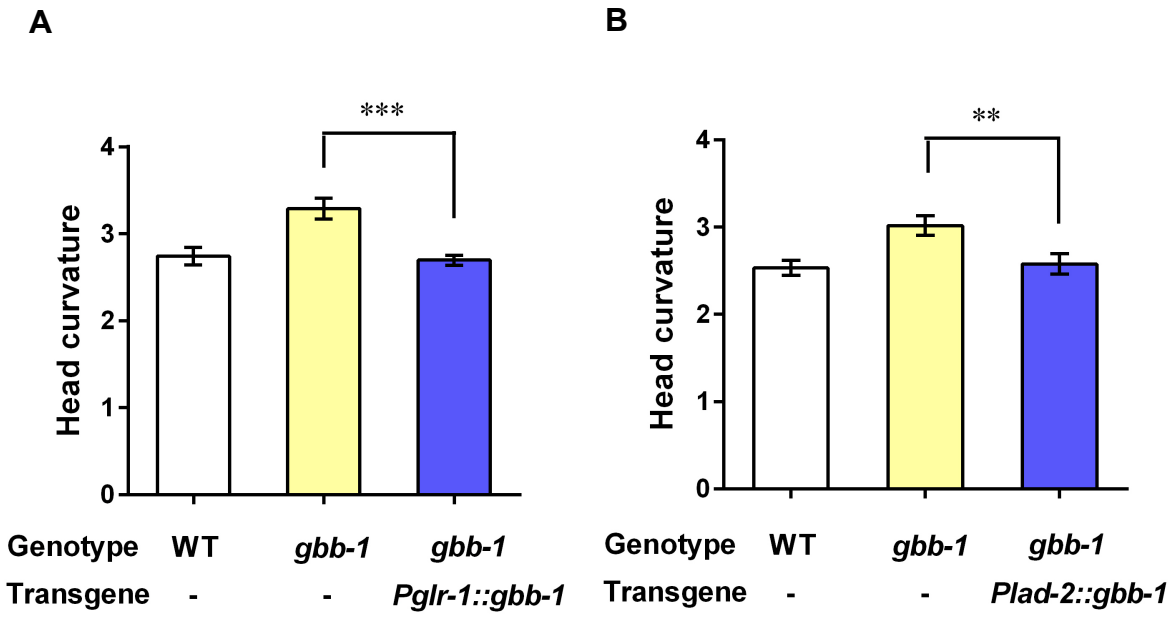

Figure 2. 19 The exaggerated head deflection in *gbb-1(tm1406)* mutants is rescued by expressing *gbb-1* cDNA under the *glr-1* promoter and the *lad-2* promoter. Transgenic animals are compared with non-transgenic siblings. One-way ANOVA with Boferroni correction, **p< 0.01, ***p< 0.001. n≥ 13 animals, Mean ± SEM.

Optogenetic analysis of SMD and RME circuit

So far, I have characterized the function of the RME neurons in regulating head movement by neuronal physiology and quantitative behavioral analysis. I propose that the RME neurons, while receiving cholinergic inputs from SMD, send negative feedback to SMD via $GABA_B$ receptors to down-regulate SMD activity and thus restrain head deflection. To test this hypothesis, I took an optogenetic approach to manipulate the activity of RME and monitor the behavioral consequence.

First, I evaluated the effect of RME inhibition using transgenic animals that express the photon-sensitive proton pump archaerhodopsin (ArCh) in all the GABAergic neurons (Chow et al., 2010; Okazaki et al., 2012). I used the CoLBeRT system developed in the Samuel lab to track free-moving animals and illuminate the RME neurons selectively (Leifer et al., 2011). During forward movement, laser illumination at ~550 nm activated ArCh expressed in the RME neurons and produced exaggerated head deflection, mimicking the effect of RME ablation (Fig. 2. 20). The normal head curvature resumed immediately upon the removal of laser illumination (Fig. 2. 20). Quantitative analysis of multiple trials shows that inhibiting RME by ArCh increases head curvature during forward movement (Fig. 2. 20B).

Next, I examined the effect of activating RME in transgenic animals expressing the light-gated ion channel channelrhodopsin (ChR2) in the GABAergic neurons (Nagel et al., 2003; Liu et al., 2009). The experiments were performed on the CoLBeRT system using blue laser, which opens the cation channel and depolarizes the target neuron (Nagel et al., 2003). Because RME neurons are adjacent to the process of the interneuron RIS, blue light illumination of the head region induced RIS-dependent sleep-like quiescence (Turek et al., 2013; data not shown). Ablation of RIS itself does not have a significant impact on head curvature (McIntire et al.,

1993b; data not shown). Therefore, in the following experiments on ChR2-expressing animals, I ablated the RIS neuron in each animal at L1-L2 stage and analyzed the behavior response in recovered adults. In animals moving forward, over activating RME neurons by blue laser caused 'stiff' head, mimicking the effect of SMD ablation (Fig. 2. 21). Removal of blue light relieved the constraint and restored normal amplitude of head deflection (Fig. 2. 21). Data from multiple trials show that RME activation by ChR2 reduces head curvature (Fig. 2. 21B). Together, the optogenetic analysis indicates that RME inhibits SMD and restrains head deflection during forward movement.

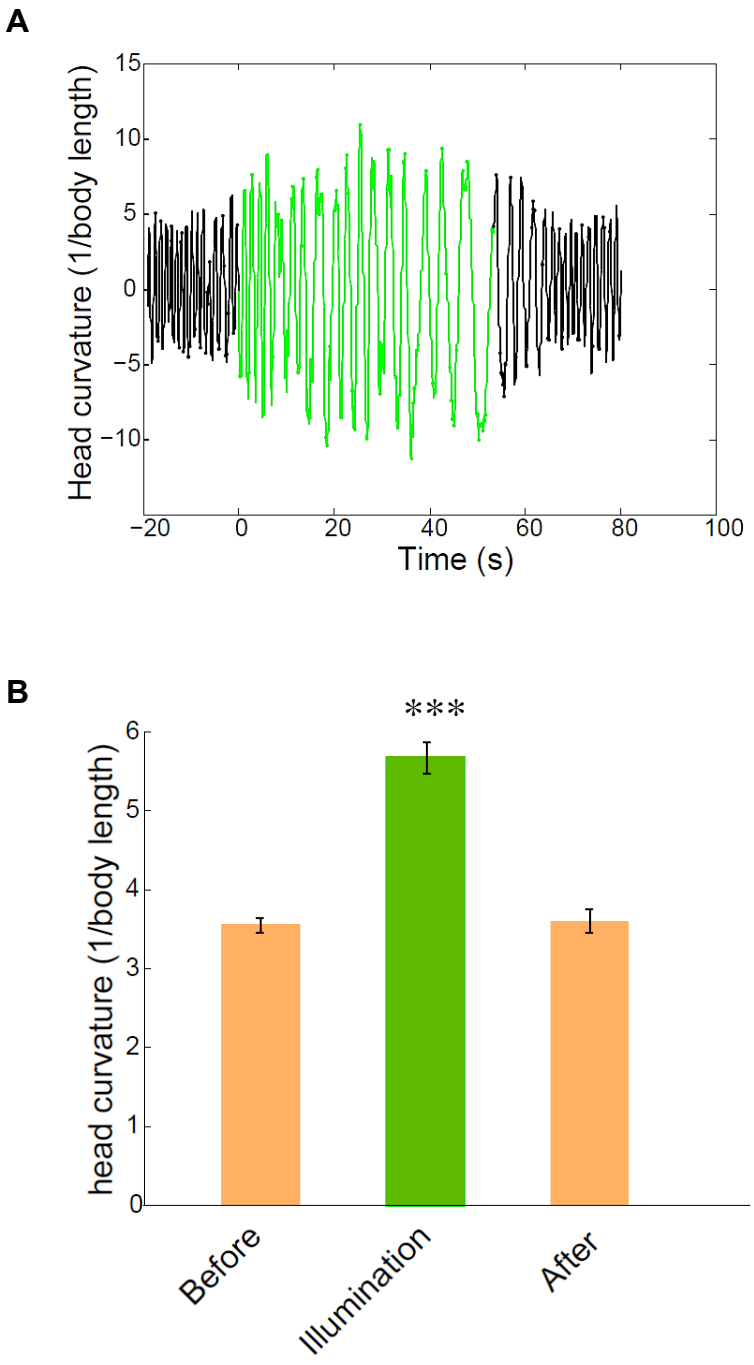

Figure 2. 20 Light-inhibition of RME by ArCh increases head curvature during forward movement. A, Representative trace of head curvature before (black), during (green), and after (black) green laser illumination. B, Quantified head curvature before (orange bar), during (green bar) and after (orange bar) illumination. One-way ANOVA with Boferroni correction, ***$p<0.001$. $n\geq 13$ trials, Mean ± SEM.

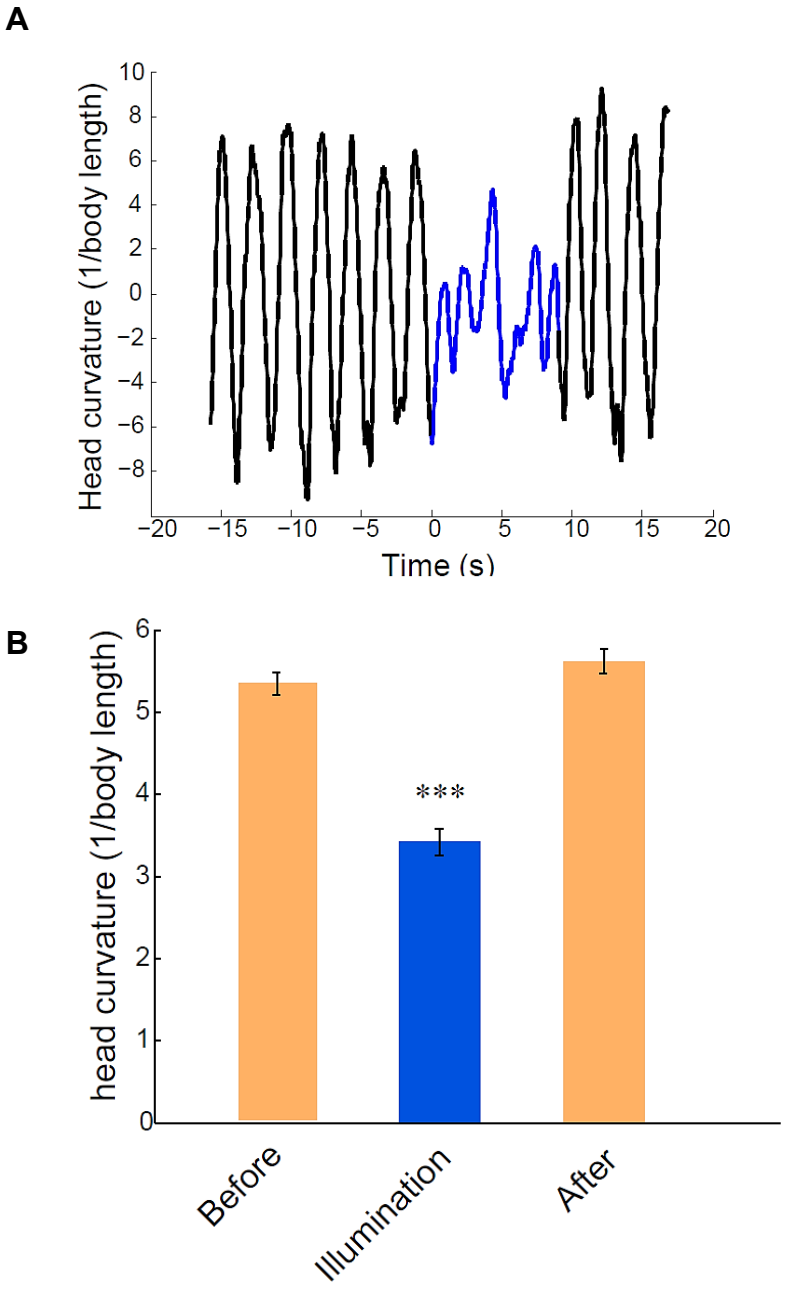

Figure 2. 21 Light-excitation of RME by ChR2 decreases head curvature during forward movement. A, Representative trace of head curvature before (black), during (blue), and after (black) blue laser illumination. B, Quantified head curvature before (orange bar), during (blue bar) and after (orange bar) illumination. One-way ANOVA with Boferroni correction, ***$p<0.001$. $n\geq 12$ trials, Mean ± SEM.

To understand the underlying mechanisms, I crossed the ChR2 transgene into several key mutants in the GABA signaling pathway and optogenetically manipulated RME activity in the mutant background. First, I stimulated RME in the *unc-25* mutants to test whether the behavioral response indeed depends on GABA. As expected, activating RME in *unc-25(e156)* did not change head curvature (Fig. 2. 22), indicating that RME restrains head deflection via GABA signaling. Next, I analyzed the GABA receptor mutant *unc-49.* Interestingly, RME activation in the *unc-49(e407)* mutants also decreased head curvature (Fig. 2. 22), suggesting that GABA released by RME acts on targets other than the A-type receptors on muscles. I then activated RME in the *unc-49(e407); gbb-1(tm1406)* double mutants. After removing *gbb-1* from the *unc-49* background, RME activation by ChR2 no longer had any effect on head curvature during forward movement (Fig. 2. 22). Together, these results suggest that the neuronal receptor GBB-1/2 responds to the activation of GABAergic RME to restrain head deflection.

To identify the functional sites of GBB-1/2 in this context, I generated transgenic lines that express *gbb-1* cDNA in selected group of cells in the *unc-49; gbb-1* background. Non-transgenic animals, like the *unc-49; gbb-1* mutants, did not show any change in head curvature upon blue light-excitation of RME (data not shown). In contrast, transgenic animals expressing *gbb-1* under the *glr-1* promoter or the *lad-2* promoter showed decreased head curvature during illumination (Fig. 2. 22), suggesting both *glr-1::gbb-1* and *lad-2::gbb-1* were able to restore normal function of GBB-1/2 required for the RME-mediated inhibition of head movement. Expression driven by the *glr-1* and *lad-2* promoters only overlaps in SMD (Brockie et al., 2001; Wang et al., 2008; Hendricks et al., 2012). Therefore, these data are consistent with previous results, demonstrating that RME restrains head deflection in forward movement via the $GABA_B$ receptor GBB-1/2 in the SMD neurons.

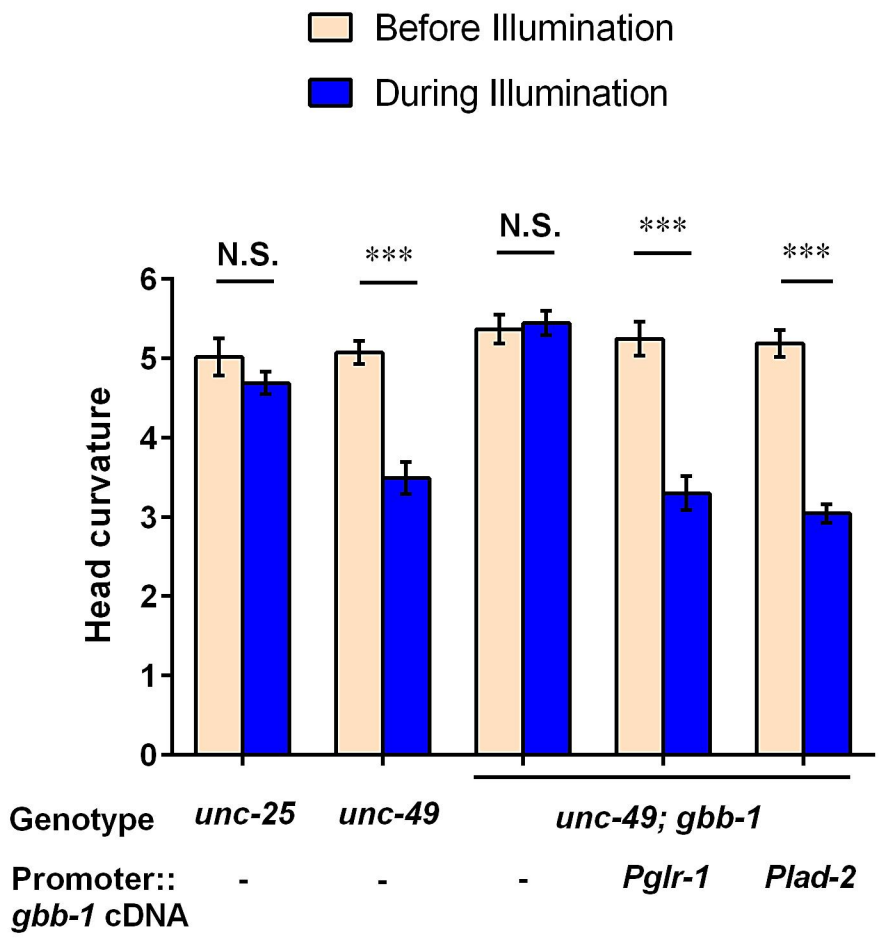

Figure 2. 22 Light-excitation of RME by ChR2 in mutants and transgenic animals expressing *gbb-1* under the *glr-1* or *lad-2* promoters in *unc-49;gbb-1* background. Head curvature before and during light illumination is compared within each genotype. Student's t-test, ***p<0.001. n≥ 20 trials from multiple animals. Mean ± SEM.

A mathematical model for the optimal angle of head deflection

In collaboration with Dr. Quan Wen, we propose a mathematical model for the optimal angle of head deflection in *C. elegans* that maximizes the speed of forward locomotion. The following model is by courtesy of Dr. Quan Wen. When undulatory animals such as *C. elegans* are swimming in water or Newtonian viscous fluids, the behavior of the fluid in the surrounding environment can be characterized by low Reynolds number hydrodynamics (Re ≤ 0.1). In this regime, by using slender body and small undulation amplitude approximation, we can obtain analytical solution that determines how the actual velocity of a worm depends upon the external mechanical load and the locomotory gait.

The viscous force transverse or tangent to a body segment experienced by a moving worm is proportional to its velocity along the corresponding directions:

$$F_{//} = c_{//} v_{//};$$

$$F_{\perp} = c_{\perp} v_{\perp};$$

Here $c_{//}$ and $c_{\perp}$ are the coefficients of viscous drags. When integrated along the whole body, the total force projected along the direction of motion, should be zero. If the actual velocity of a worm along the its motion direction is v, and the propagation velocity of undulatory waves measured along the reference frame of the worm body is v_w, we found that

$$\frac{v}{v_w} \approx \frac{c_{\perp} - c_{//}}{c_{\perp} + c_{//}/\langle sin^2\theta \rangle}$$

where $\langle ... \rangle$ denotes an average along the worm body, and θ is the angle of attack. The actual velocity of a worm v approaches the wave velocity v_w if $c_\perp \gg c_{//}$. However, for slender organisms swimming in Newtonian fluid, $\frac{c_\perp}{c_{//}} \approx 2$, suggesting that motion slippage is significant.

We note that increasing the angle of attack θ would reduce slippage. However, there comes a trade-off: the undulation period *T* increases as a function of angle of attack in wild type animals, and higher angle of attack may reduce wave velocity ($v_w = \lambda/T$), and thus reduce the actual velocity of motion. In the absence of a detailed mechanistic understanding of the head neuromuscular circuit, it is hard to derive an analytical relationship between angle of attack and wave velocity. Here, to be consistent with all observed data, we make simple assumptions that $T \sim \theta, v_w \sim \frac{1}{\theta}$. To maximize the actual speed of motion, and by taking into account small amplitude approximation $\sin\theta \approx \theta$, we find the optimal angle of attack is given by,

$$\theta \approx \sqrt{\frac{c_\perp}{2c_{//}}}$$

which is close to 45 degree and independent of the viscosity of the medium. This angle matches the average we observe in wild-type animals, whereas the SMD-ablated or RME-ablated animals show either smaller or larger angle of attack. The significance of the deflection angle in navigation and foraging awaits further investigation.

Discussion

A parsimonious model for gait regulation in *C. elegans*

The neural networks that regulate the locomotory gait are of different levels of complexity in different organisms, but many share common circuit properties (Grillner, 2003; Kiehn, 2006). Here, using *C. elegans* head deflection as a behavior model, I characterize a small neuronal circuit that fine-tunes the amplitude of head bending. The circuit consists of the cholinergic SMD and GABAergic RME motor neurons. With spontaneous calcium activity, SMD releases acetylcholine to contract muscle and drive the calcium activity in RME, which releases GABA to relax the contralateral muscle and facilitate head deflection; meanwhile, the elevated GABA tunes down SMD activity by acting on the $GABA_B$ receptor, posting a constraint on the bending amplitude (Figure 2. 23). The interaction between SMD and RME contributes to an excitation-inhibition balance at the NMJ and generates a bending angle that maximizes the phase velocity during forward movement. The oscillatory circuit presented here updates a previous model for the role of RME in regulating head deflection (McIntire et al., 1993b; Jorgensen, 2005).

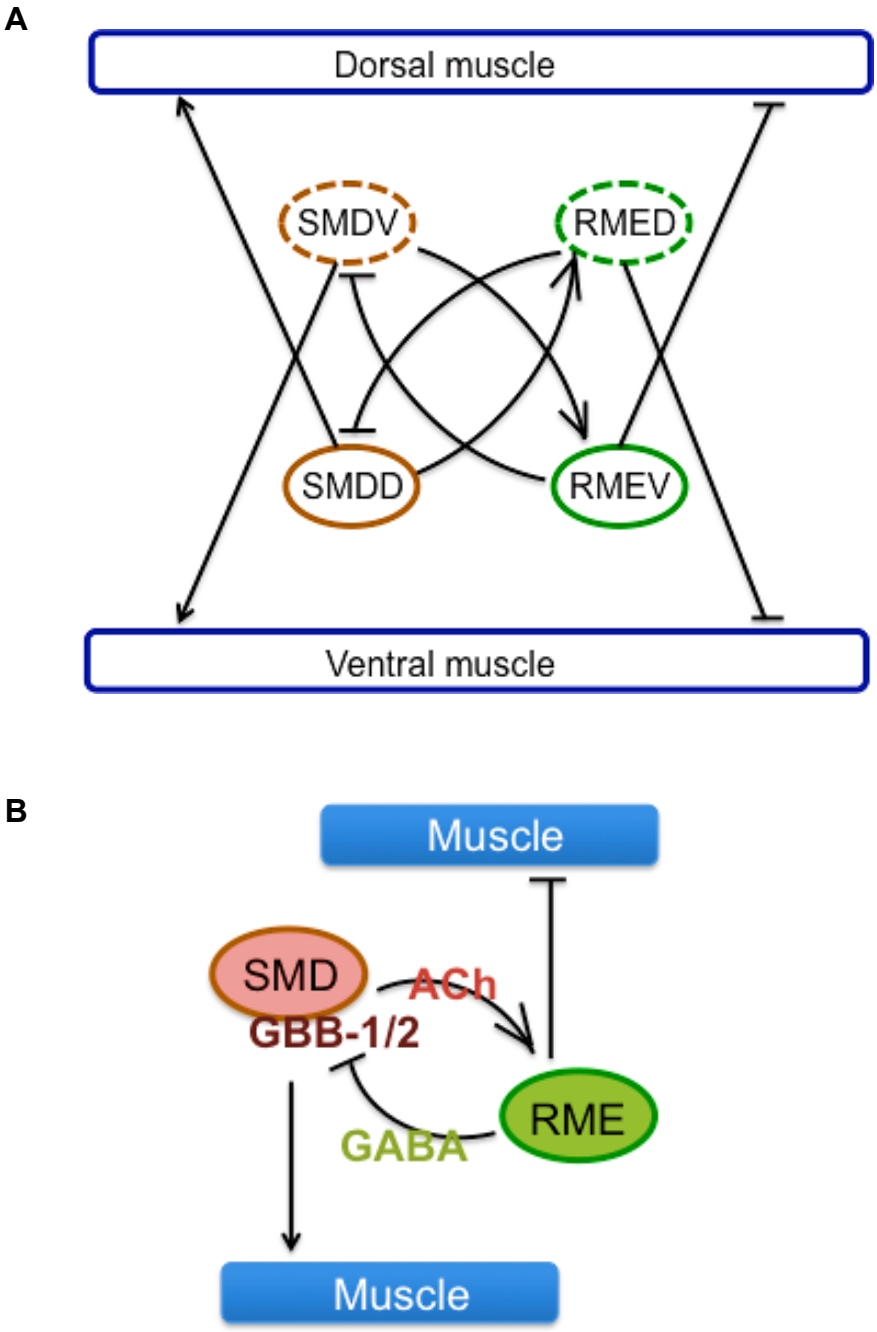

Figure 2. 23 Model of SMD-RME circuit. A, SMDD/V and RMED/V neurons innervate head and neck muscles and interact with each other. B, Simplified SMD-RME circuit with neurotransmitters denoted. Arrows denote activation, bar-headed lines denote inhibition.

In most vertebrates, cholinergic motor neuron is the sole player in the peripheral motor system, and GABA or glycine is present primarily in the interneurons (Grillner, 2003; Kiehn, 2006). In contrast, GABA acts mainly at neuromuscular synapses in nematodes (Jorgensen, 2005). The GABAergic motor neurons in *C. elegans* such as RME and D-type motor neurons (VD and DD) form synapses predominantly onto the contralateral body wall muscle, relaxing muscle cell via the GABA-gated chloride channel (White et al., 1986; Jorgensen, 2005). Here, we show that RME also sends negative feedback to SMD, suggesting it functions partially as an interneuron. The dual role of RME provides a parsimonious design to achieve two important properties of a circuit, contralateral inhibition and negative feedback. In the motor circuit underlying swimming in lamprey, contralateral commissural interneurons (CINs) on the left and right sides inhibit each other, and an additional inhibitory stretch-receptor neuron (SRI) provides negative feedback to the excitatory motor neurons (Grillner, 2003). In the microcircuit for flexor-extensor coordination in the spinal motor circuits underlying walking in mammals, reciprocal Ia interneurons (Ia-INs) related to flexor and extensor inhibit each other, and the glycinergic/ GABAergic ipsilaterally projecting inhibitory interneuron Renshaw cells (RCs) provide negative feedback to the motor neurons (Kiehn, 2006). Here, the role of RME in the oscillatory circuit essentially combines both. In the small nervous system of *C. elegans*, sensory neurons are often polymodal and interneurons multitask in a variety of behaviors (de Bono and Maricq, 2005; Komuniecki et al., 2014). The bi-directional communication between SMD and RME allows a small circuit to regulate head deflection.

Molecular underpinnings of SMD-RME communication

In the present model, SMD neurons drive calcium activity in RMEs, which send negative feedback to SMD to prevent exaggerated head deflection. Although the major neurotransmitters of SMD and RME have been identified to be acetylcholine and GABA, respectively (McIntire et al., 1993b; Duerr et al., 2008), it remains unknown whether the two sets of neurons communicate before their synaptic outputs converge at the head muscle arm (White et al., 1986).

In this study, I have found that cholinergic synaptic transmission from SMD is required for the oscillatory calcium dynamics in RME during head movement, whereas the inputs from the predominant presynaptic partners of RME, cholinergic SMB and IL2 neurons, are not required for such activity. Synaptic projection from SMD to RME is not described in the classic *C. elegans* connectome (White et al., 1986), but recent reconstruction of the EM data provides evidence for a small number of synapses from SMD to RME (Emmons et al.). It suggests that SMD may release acetylcholine to excite RME directly, although the possibility that SMD activates RME indirectly via other unidentified synaptic partners is not completely excluded. In either case, it remains unclear which receptor on RME receives the acetylcholine signal. Among the variety of acetylcholine receptors (AChR) in *C. elegans*, many of the receptor subunits are expressed in neurons (Jones and Sattelle, 2004; Jospin et al., 2009). In the ventral nerve cord, GABAergic D-type motor neurons express the nicotinic AChR subunit LEV-8 and receive synaptic inputs from the A- and B-type motor neurons (Towers et al., 2005). My preliminary data suggest that the AChR on RME may be sensitive to levamisole, because levamisole-treated animals lose oscillatory calcium activity in RME but not SMD neurons (data not shown). So far, the levamisole-sensitive and neuron-expressed AChR subunits I have tested include ACR-8, ACR-12, LEV-8, UNC-63, UNC-29 and UNC-38, but none of the single mutants that lack one of

the AChR subunits shows defective calcium dynamics in RME as *cha-1* or SMD-ablated animals (data not shown). It is possible that multiple AChR types function redundantly in RME, and a neuronal RNA profiling or exhaustive screen is desired to identify the receptor(s). Meanwhile, it is of interest to examine whether reciprocal inhibition exists between the SMDD and SMDV neurons via inhibitory AChR such as GAR-2 (Dittman and Kaplan, 2008).

The negative feedback from RME to SMD is mediated by GABA and the GBB-1/2 receptors expressed on SMD and possibly additional neurons. Although the GABAergic interneuron RIS forms synapses onto SMD, it does not play an essential role in regulating head deflection (McIntire et al., 1993b), and optogenetic stimulation of RME in RIS-ablated animals effectively manipulates head bending. The $GABA_B$ receptor GBB-1/2 is a neurotransmitter-gated GPCR with intrinsically slow kinetics (on timescales from ten to hundreds of milliseconds to seconds or more) (Dittman and Regehr, 1997), offering a delay in the GABA-mediated inhibition in this oscillatory circuit. The major synaptic output from RME is projected to muscles, and it forms a small number of synapses onto SMD based on the newly updated connectome. It is not impossible, however, the $GABA_B$ receptors detect elevated GABA extrasynaptically. In mammals, extrasynaptic GABA acts on metabotropic $GABA_B$ receptors to inhibit neuronal activity (Isaacson et al., 1993; Dittman and Regehr, 1997). In the ventral nerve cord of *C. elegans*, cholinergic motor neurons also express GBB-1/2 that may respond to extrasynaptic GABA released from neighboring D-type motor neurons (Dittman and Kaplan, 2008). The negative feedback signal in lampreys or the mammalian spinal cord is mediated by the inhibitory glycine or GABA released by interneurons (Grillner, 2003; Kiehn, 2006).

Head deflection and undulatory locomotion in *C. elegans*

As part of the sinusoidal wave along the body, the head of *C. elegans* moves from side to side rhythmically in the dorsal-ventral plane. This behavior is referred to as "foraging movements" in literature, and RME ablation causes "loopy" foraging (McIntire et al., 1993b; Jorgensen, 2005). Other studies on the locomotory behavior in *C. elegans* have also identified mutants or neuron-ablated animals with abnormal posture, some described as "loopy", during forward movement (Gray et al., 2005; Li et al., 2006a). Interestingly, the local curvature of the head and the posture of the whole body can be decoupled, as revealed by detailed analysis. In an earlier joint project (Qin, 2013), we found that the *gar-3* mutants display both increased head curvature and decreased posture aspect ratio (Hendricks et al., 2012), which represents loopy head and body bends; the SMB-ablated animals show deeply flexed body bends (Gray et al., 2005), but negligible increase in head curvature (Qin, 2013); in contrast, the *unc-25* mutants display exaggerated head deflection (McIntire et al., 1993b), i.e. increased head curvature, but the posture aspect ratio of the whole body-length is largely wild-type (Qin, 2013). It suggests that the locomotory gait is differentially modulated by different subsets of the motor machinery, and quantitative analysis of local body curvature uncovers rich detail. A similar notion is discussed by Shingai et al. in a recent study (Shingai et al., 2013). The study proposes two methods for evaluating the periodicity and irregularity of head movement, and shows the head movement becomes more irregular in aged animals (Shingai et al., 2013).

There is no doubt that the movement of the head and the rest of the body is well coordinated by the nervous system to generate locomotion. In vertebrate and invertebrate systems, central pattern generators (CPGs) distributed along the body can be coupled and evoked sequentially to generate local rhythmic behaviors (Grillner, 2003; Kiehn, 2006). In *C. elegans*,

proprioception within the motor circuit is found to play a key role in the undulatory wave propagation (Wen et al., 2012). The B-type cholinergic motor neurons transduce proprioceptive signal to transmit the rhythmic movement initiated near the head to the following body regions during forward movement (Wen et al., 2012). Although I found the cholinergic neurotransmission from SMB or IL2 is not required for the calcium dynamics in RME in correlation with head movement, it is possible that these neurons provide additional inputs to the SMD-RME circuit to coordinate locomotory gait in response to environmental changes (Kocabas et al., 2012; Lee et al., 2012).

In addition, the head and body posture of *C. elegans* is regulated by environmental condition as well as the animal's behavioral status. For example, the undulatory gait varies with changes in external mechanical resistance when *C. elegans* moves in Newtonian fluids (Fang-Yen et al., 2010). Both wavelength and frequency of undulation decrease in response to increasing viscosity (Fang-Yen et al., 2010). The head oscillation is suppressed by a tyramine-dependent mechanism during backward movement, facilitating touch-responsive escape from predacious fungi (Alkema et al., 2005; Maguire et al., 2011). Because SMD is postsynaptic to sensory neurons OLL, ALN and multiple interneurons, including the RIA neuron implicated in signal integration (White et al., 1986; Ha et al., 2010; Chang et al., 2011; Hendricks et al., 2012), the SMD-RME circuit is likely also modulated by sensory inputs or feedback signals. Previous behavioral and computational studies have proposed theoretical models for a neural network that generates head swing (Sakata and Shingai, 2004; Karbowski et al., 2008). With oscillatory calcium dynamics and potential sensory modulation, SMD and RME may function as part of a CPG in the head to initiate rhythmic movement.

Excitation-inhibition balance in the nervous system

The negative feedback circuit of SMD and RME generates a balanced output onto head and neck muscles. Similar to the ventral nerve cord (VNC) motor circuit, conditions that elevate acetylcholine release will cause an increase in GABA release in parallel (Dittman and Kaplan, 2008). Here, $GABA_B$ receptors in SMD receive inhibitory signal from RME, preventing exaggerated head deflection due to over-excitation. Animals with a broken SMD-RME circuit because of genetic mutation or defective neurotransmission show either exaggerated or insufficient head deflection.

The imbalance between excitation and inhibition can be deleterious. In the locomotory circuit in *C. elegans*, the excitability of cholinergic motor neurons is modulated by a variety of G-protein coupled receptors such as GBB-1/2 and GAR-2, and ionotropic receptor with distinct pharmacology such as ACR-2 (Dittman and Kaplan, 2008; Jospin et al., 2009). Mutants that lack balanced neuronal activity often show convulsion or uncoordinated movement, likely caused by disproportional excitation or inhibition of muscle cells (Jospin et al., 2009). In the mammalian brain, GABAergic inhibition plays a critical role to overcome excessive synaptic excitation (Isaacson et al., 1993; Mann and Mody, 2008). Failure in the excitation-inhibition balance underlies multiple neurological diseases, including epilepsy, autism spectrum disorders (ASD) and Rett syndrome (Dani et al., 2005; Oblak et al., 2009; Baroncelli et al., 2011; Sgado et al., 2011). Studies in model organisms may provide insights into how such imbalance changes the properties of a neural circuit and its behavioral output.

Materials and Methods

Strains

C. elegans strains were raised under standard conditions at 20 ºC (Brenner, 1974). Strains used in this study include: N2 Bristol, CB156 *unc-25(e156)*III, CB307 *unc-47(e307)*III, CB407 *unc-49(e407)*III, MT7929 *unc-13(e51)*I, CB928 *unc-31(e928)*IV, PR1152 *cha-1(p1152)*IV, PR1158 *cha-1(b401)*IV, RB1195 *acr-8(ok1240)*X, VC188 *acr-12(ok367)*X, ZZ15 *lev-8(x15)*X, VC1041 *lev-8(ok1519)*X, ZZ13 *unc-63(x13)*I, CB193 *unc-29(e193)*I, CB403 *unc-29(e403)*I, CB904 *unc-38(e264)*I, EG5025 *oxIs351*[*Punc-47::ChR2::mCherry::unc-54 3'UTR*; *lin-15(+)*; LITMUS 38i]X, FX01165 *gbb-2(tm1165)*IV, FX01406 *gbb-1(tm1406)*X, KP3447 *nuEx1066*[*Pgbb-1::gfp*; *Pttx-3::dsRed2*], KP6566 *gbb-1(tm1406)*X; *gbb-2(tm1165)*IV, ST2351 *ncEx2351*[*Punc-47::Arch::eGFP*; *Pmyo-2::mCherry*], VC1669 *aptf-1(gk794)*III, ZC1148 *yxIs1*[*Pglr-1::GCaMP3.3*; *Punc-122::gfp*]V, ZC361 *lin-15B(n765)*X; *kyIs30*[*Pglr-1::gfp*; *lin-15(+)*]X (CX2610 crossed with N2), ZM6665 *hpIs268*[*Punc-25::GCaMP3::UrSL::wCherry*], ZC1553 *yxEx750*[*Pglr-1::TeTx::mCherry*; *Punc-122::gfp*], ZC1615 *kyIs30*; *yxEx791*[*Plad-2::mCherry*; *Punc-122::gfp*], ZC2138 *unc-13(e51)*I; *yxIs1*, ZC2141 *unc-31(e928)*IV; *yxIs1*, ZC2161 *yxEx1154*[*Pglr-1::mCherry*; *Punc-122::gfp*], ZC2181 *unc-13(e51)*I; *hpIs268*, ZC2276 *unc-13(s69)*I; *hpIs268*, ZC2186 *unc-31(e928)*IV; *hpIs268*, ZC2204 *cha-1(p1152)*IV; *hpIs268*, ZC2271 *cha-1(b401)*IV; *hpIs268*, ZC2211 *cha-1(p1152)*IV; *hpIs268*; *yxEx809*[cosmid ZC416, *Punc-122:gfp*], ZC2219 *yxEx1173*[*Podr-2(18)::gfp*; *Punc-122::dsRed*], ZC2222 *yxEx1176*[*Podr-2(18)::TeTx::mCherry*; *Punc-122::dsRed*], ZC2234 *hpIs268*; *yxEx1176*, ZC2251 *yxEx1190*[*Pklp-6::gfp*; *Punc-122::dsRed*], ZC2256 *yxEx1195*[*Pmyo-3::RCaMP*; *Punc-122::dsRed*], ZC2258 *yxEx1197*[*Pklp-6::TeTx::mCherry*; *Punc-122::dsRed*], ZC2264 *hpIs268*; *yxEx1190*, ZC2273 *hpIs268*; *yxEx1197*, ZC2298 *nuEx1066*; *yxEx1154*, ZC2299 *hpIs268*;

yxEx1176; *yxEx1197*, ZC2300 *nuEx1066*; *yxEx1176*, ZC2309 *nuEx1066*; *yxEx791*, ZC2316 *unc-49(e407)*III; *ljIs131*, ZC2324 *unc-54(e190)*I; *hpIs268*; *yxEx1195*, ZC2325 *unc-54(e1092)*I; *hpIs268*; *yxEx1195*, ZC2327 *cha-1(p1152)*IV; *hpIs268*; *yxEx1211*[*Podr-2(18)::cha-1::mCherry*; *Punc-122::dsRed*], ZC2329 *cha-1(p1152)*IV; *hpIs268*; *yxEx1213*[*Pklp-6::cha-1::mCherry*; *Punc-122::dsRed*], ZC2330 *cha-1(p1152)*IV; *hpIs268*; *yxEx1214*[*Pglr-1::cha-1::mCherry*; *Punc-122::dsRed*], ZC2332 *yxIs1/hpIs268*; *yxEx1195*, ZC2336 *hpIs268*; *yxEx750*, ZC2339 *unc-25(e156)*III; *yxIs1*, ZC2340 *gbb-1(tm1406)*X; *yxIs1*, ZC2342 *hpIs268*; *yxEx1154*, ZC2343 *juIs76*[*Punc-25::gfp*; *lin-15(+)*]II; *lin-15B(n765)*X (CZ1200 4× crossed with N2), ZC2363 *hpIs268*; *yxEx778*[*Plad-2::TeTx::mCherry*; *Punc-122::gfp*], ZC2365 *acr-8(ok1240)*X; *hpIs268*, ZC2366 *acr-12(ok367)*X; *hpIs268*, ZC2367 *lev-8(x15)*X; *hpIs268*, ZC2368 *lev-8(ok1519)*X; *hpIs268*, ZC2374 *gbb-1(tm1406)*X; *yxEx1234*[*Pglr-1::gbb-1*; *Punc-122::dsRed*], ZC2375 *cha-1(p1152)*IV; *hpIs268*; *yxEx1235*[*Plad-2::cha-1::mCherry*; *Punc-122::dsRed*], ZC2383 *gbb-1(tm1406)*X; *yxEx1243*[*Pgbb-1::gbb-1*; *Punc-122::dsRed*], ZC2404 *gbb-1(tm1406)*X; *yxEx1254*[*Plad-2::gbb-1*; *Punc-122::dsRed*], ZC2414 *unc-63(x13)*I; *hpIs268*, ZC2415 *unc-29(e193)*I; *hpIs268*, ZC2416 *unc-29(e403)*I; *hpIs268*, ZC2417 *unc-38(e264)*I; *hpIs268*, ZC2422 *unc-49(e407)*III; *oxIs351*, ZC2423 *gbb-1(tm1406)*X; *oxIs351*, ZC2430 *yxIs30*[*Punc-47::Arch::eGFP*; *Pmyo-2::mCherry*], ZC2432 *unc-49(e407)*III; *gbb-1(tm1406)*X; *oxIs351*, ZC2433 *unc-25(e156)*III; *oxIs351*, ZC2446 *unc-49(e407)*III; *gbb-1(tm1406)*X; *oxIs351*; *yxEx1234*, ZC2447 *unc-49(e407)*III; *gbb-1(tm1406)*X; *oxIs351*; *yxEx1254*, ZC2449 *aptf-1(gk794)*III; *oxIs351*. For behavioral analysis, *unc-25(e156)*III, *unc-49(e407)*III, *gbb-1 (tm1406)*X and *gbb-2(tm1165)*IV are at least 2× outcrossed with the wild-type strain N2. The extrachromosomal array *ncEx2351* was integrated by a UV cross-linker (Stratalinker 2400, energy setting 300) and 6× outcrossed with N2.

Molecular biology

Molecular cloning in this study was performed using the Gateway system (Invitrogen) unless otherwise specified. The 1.9 kb *cha-1* cDNA was cut by NotI and AgeI enzyme sites from *Podr-2::cha-1::gfp* (a gift from J. Lee) and ligated upstream of *mCherry* to produce *pPD95.77-cha-1::mCherry*, and a Gateway recombination cassette (rfB) was ligated upstream of the *cha-1* cDNA to produce *pPD95.77-rfB-cha-1::mCherry*. The 2565 bp *gbb-1* cDNA was cut by NheI and KpnI sites from a pBlueScript vector (KP#1026, a gift from J. Dittman) and cloned into the *pPD49.26* vector to produce *pPD49.26-rfB-gbb-1*. The genetically encoded calcium indicator *RCaMP* was cut by SmaI and XhoI sites from *pCAG-RCaMP181* (a gift from L. Looger) and cloned into the *pPD95.77* vector to produce *pPD95.77-rfB-RCaMP*. The destination vectors *pPD95.77-rfB-gfp*, *pPD95.77-rfB-mCherry* and *pSM-rfB-TeTx::mCherry* were generated previously in the lab (Hendricks et al. 2012). A 2.4-kb genomic fragment upstream of the *odr-2* gene (forward primer 5' AGT TCA CCA AGC TCT TCT CGT TTA TTC, reverse primer 5' CCA TCA GCC AAA TGT AGG CTC GGT TC), 1.5-kb upstream of the *klp-6* gene (forward primer 5’ CAC CAA AAA ATT CAT TAA, reverse primer 5’ TAT TCT GAA AAG TTC AAC TAA TA), 2-kb upstream of the *myo-3* gene (forward primer 5' TGT GTG TGA TTG CTT TTT CAC AAT C, reverse primer 5' TTC TAG ATG GAT CTA GTG GTC GTG), and 3-kb upstream of the *gbb-1* gene (forward primer 5' CGT CGT TCT CAT TGT ATG CCG TTT AAC, reverse primer 5' CGG AAA CGT GCC ACC GAT GTG AAG) were amplified by polymerase chain reaction (PCR) and ligated to the *pCR8* backbone to produce the Gateway entry vectors. The *pCR8-Pglr-1* and *pCR8-Plad-2* entry clones were generated previously in the lab (Hendricks et al. 2012). LR recombination reactions were performed using Gateway® LR Clonase® enzyme kits according to the protocol provided (Invitrogen), generating the expression clones *Podr-*

2(18)::cha-1::mCherry, *Pklp-6::cha-1::mCherry*, *Pglr-1::cha-1::mCherry*, *Plad-2::cha-1::mCherry*, *Podr-2(18)::TeTx::mCherry*, *Pklp-6::TeTx::mCherry*, *Pklp-6::gfp*, *Podr-2(18)::gfp*, *Pglr-1::mCherry*, *Pgbb-1::gbb-1*, *Pglr-1::gbb-1*, *Plad-2::gbb-1*, and *Pmyo-3::RCaMP*. For rescue experiments, *Pgbb-1::gbb-1* was injected at 1 ng/µl. *Pglr-1::gbb-1* and *Plad-2::gbb-1* were injected at 10 ng/µl and the other plasmids were injected at 25 ng/µl. Microinjection was performed as described (Mello et al., 1991) with either *Punc-122::gfp* or *Punc-122::dsRed* as a co-injection marker for all the transgenic lines.

Laser ablation

Laser ablation was performed based on a previously described protocol with slight modifications (Bargmann and Avery, 1995; Fang-Yen et al., 2012). Femtosecond laser pulses at 1kHz were focused onto neurons of interest through a 60× Nikon water immersion objective on a custom-built Nikon Confocal spinning disk microscope. Target neurons were labeled by expressing fluorescent proteins with cell-specific promoters and identified by fluorescence signals combined with morphological and positional characteristics. Laser surgery was performed on L1-L2 larvae. Animals that underwent laser ablation or mock procedures were recovered and raised at 20°C under standard conditions for 2 days till they reached adulthood. After behavioral assays, each ablated animal was recovered and the fluorescence signal was examined under a 40× objective on a Nikon TE2000-U microscope. Animals with fluorescent signals remaining in target neurons were excluded from analysis.

Calcium imaging

Calcium imaging was performed in a microfluidic device as previously described (Chronis et al., 2007; Hendricks et al., 2012) with modifications. An SU-8 master (Harvard Center for Nanoscale Systems) was applied to cast Polydimethylsiloxane (PDMS) (Dow Corning

Sylgard 184, Ellsworth Adhesives, Germantown, WI). Chips with inlet holes were bonded to glass coverslips with a handheld corona treater (Haubert et al., 2006) and connected to an Automate Scientific Valvebank perfusion system (Berkeley, CA) as previously described (Ha et al., 2010). Fluorescence time-lapse imaging (100-200ms exposure, 5Hz) was performed on a Nikon Eclipse TE2000-U inverted microscope with a 40× oil immersion objective and a Photometrics CoolSnap EZ camera. To image neurons on different focal planes, a Piezo was used to scan an image stack on a confocal spinning disk microscope. Animals were washed by NGM buffer (1mM $CaCl_2$, 1mM $MgSO_4$, 25mM KPO_4 pH6.0) briefly before being loaded in the worm channel, and were presented with slow streams of NGM buffer throughout the recording of up to 3 minutes. For RME imaging, the strain ZM6665 was crossed with mutants or transgenic lines, and F2 progeny were cloned to select for homozygotes of the integrated *hpIs268* transgene and the mutation or transgene of interest. For simultaneous imaging of SMD and RME, the strain ZM6665 was crossed with ZC1148, and F1 or F2 heterozygote progeny were selected because the integration sites of *hpIs268* and *yxIs1* were closely located on Chromosome V.

All image analysis was performed with ImageJ (NIH, MD) unless otherwise specified. Frames were aligned using the StackReg plugin where necessary. For RME imaging, total fluorescence intensity was measured by subtracting background from the region of interest (ROI) corresponding to the cell body of RMED or RMEV neurons during the animal's head deflection. The fluorescence intensity data were normalized across individuals to a linear scale by the formula $(F - F_{min})/(F_{max} - F_{min})$ (Hendricks et al., 2012). For simultaneous imaging of SMD and RME, image stacks were composed and processed by a customized program written in Matlab (Mathworks, Natick). Imaging on immobilized animals were performed on a 10F% agarose pad with 0.3- 0.5 µl of 0.1 µm diameter polystyrene microspheres (Polysciences 00876-15, 2.5% w/v

suspension) (Fang-Yen et al., 2009). Where noted, animals were soaked in 2 mM levamisole-M9 solution (Tetramisole HCl; Sigma L9756) or 1 mM musimol-M9 solution (Sigma M1523) immediately before and during imaging.

Head movement analysis

Head deflection of the animals in the microfluidic chip was quantified with ImageJ (NIH, MD) essentially as described (Hendricks et al., 2012). Images were binarized with all background pixels converted to 0 and all pixels representing the animal converted to 1. An ROI comprising the moving part of the head was selected and fit into an ellipse in ImageJ, where the angle of the ellipse was measured for each frame. The difference in angle between individual frames and the reference frame (minimum head deflection) was calculated, generating either positive or negative values that represent head deflection along the ventral-dorsal axis. The head displacement was then normalized to the maximum deflection, generating an index between -1 and 1. Ventral bending was defined as positive.

Cross-correlation analysis

Cross-correlation between calcium signals and head deflection was analyzed in JMP10 software (SAS) as described (Hendricks et al., 2012) with modifications. Time series data of fluorescence intensity and head position were normalized across individuals and taken for cross-correlation with a time lag of 20s (100 frames). Head position was used as input. Comparison between peak correlations of different genotypes was performed as described (Hendricks et al., 2012). In brief, the peak of the mean control correlation was identified at time T_p and the maximum correlation, positive or negative, was taken from strains of interest in a 1-s time window centered on T_p (Hendricks et al. 2012). Unless otherwise specified, mutants were

compared with wild-type controls and transgenic animals were compared with non-transgenic siblings by Student's t-test or Analysis of variance (ANOVA).

Tracking and head curvature analysis

Tracking of freely moving animals were performed on a custom-built single-worm tracker. Well-fed adult hermaphrodites were washed briefly in NGM buffer and loaded to a 9-cm NGM agar plate without food. Animals were allowed to move freely on the plate for 2 minutes before being recorded for at least 1 minute. The plate was placed on a moving stage under a DMK 21AU04 monochrome scan camera (IMAGESOURCE, 30 Hz) and was illuminated by infrared light from a LED ring. Images were captured with a customized program written in LabVIEW8.5 (National Instrument) and saved every 6 frames.

The video recorded was processed by a customized script written in Matlab (Mathworks, Natick) (Fang-Yen et al., 2010; Wen et al., 2012). Frames in which animals were making reversals or turns were excluded and at least 150 frames per trial (30 seconds) were used for analysis. In brief, the head and tail of an animal were identified as the points of maximum convex curvature along the animal's boundary and confirmed manually (Wen et al., 2012). The centerline of the animal's body was extracted and smoothened, and the local body curvature (positive or negative) was calculated as the magnitude of the derivative of the unit vector tangent to the centerline with reference to the body coordinate along it (Wen et al., 2012). The first 18% of the whole body-length from the nose tip was counted as the head region, and the standard deviation of the curvature data series was used as the output for further analysis.

Fluorescence Microscopy

Fluorescent images were collected with a Nikon Eclipse TE2000-U microscope with a 40× oil immersion objective. Images were processed with Image J (NIH).

Optogenetics

Optogenetic stimulation of RME neurons in a freely moving animal was performed on the custom-built Colbert system (Leifer et al., 2011), which consists of an Nikon TE2000 inverted microscope, a high speed CCD camera, blue and green solid state lasers, and a digital micromirror device all controlled by the MindControl software (Wen et al., 2012). Animals used in all the optogenetics experiments were raised in the dark at 20°C on NGM plates with OP50 and all-*trans* retinal. The OP50-retinal plates were prepared 1-2 days in advance by seeding a 6-cm NGM-agar plate with 250 µl of OP50 culture and 1 µl of 100 mM retinal in ethanol [(Wen et al., 2012), Supplemental Materials]. Adult animals were washed briefly in NGM buffer and transferred into a layer of 25% dextran solution (w/v) sandwiched between two glass slides separated by 75-µm spacers. The animal was slightly compressed to reduce head movement in the z direction. During the assay, an individual animal was imaged under infrared light with dark field illumination, and the first 10% of the body-length from nose tip was targeted by a laser beam reflected by the digital micromirror device. For RME inhibition by ArCh, the green laser (~550 nm) was switched on for 10-15 seconds in each trial. For RME activation by ChR2, the blue laser (~470 nm) was switched on for 3-4 seconds in each trial, and the RIS interneuron was removed by laser surgery in larvae at L1-L2 stage.

Acknowledgements

I thank the *Caenorhabditis* Genetics Center (funded by NIH Office of Research Infrastructure Programs P40 OD010440) and the *C. elegans* Gene Knockout Consortium for strains, the Wellcome Trust Sanger Institute for cosmids, Drs. M. Zhen, J. Lee, J. Kaplan, J. Dittman, L. Looger, A. Leifer and N. Ji for sharing reagents and protocols, Drs. E.R. Soucy and J. Greenwood for building the tracking system and programs. I thank Dr. Q. Wen for sharing the Matlab code, analyzing the data generated from optogenetics experiments and 3-D scanning imaging, developing the mathematical model, and for discussing the project. The strain ZM6665 is generated by Dr. T. Kawano in Dr. M. Zhen's lab. The optogenetics experiments are performed using the CoLBeRT system in Dr. A. Samuel's lab. I also thank Harvard college student C. Zhong for assistance in behavioral assays, Dr. Y. Qin for the *cha-1* cDNA cloning and microinjection, Dr. M. Hendricks for the strains ZC1148 and ZC1553, and the Zhang lab members for discussion.

References

Akerboom J et al. (2013) Genetically encoded calcium indicators for multi-color neural activity imaging and combination with optogenetics. Frontiers in molecular neuroscience 6:2.

Alfonso A, Grundahl K, McManus JR, Rand JB (1994) Cloning and characterization of the choline acetyltransferase structural gene (cha-1) from C. elegans. The Journal of neuroscience : the official journal of the Society for Neuroscience 14:2290-2300.

Alkema MJ, Hunter-Ensor M, Ringstad N, Horvitz HR (2005) Tyramine Functions independently of octopamine in the Caenorhabditis elegans nervous system. Neuron 46:247-260.

Altun ZF, Hall DH (2009) Muscle system, somatic muscle. In: WormAtlas.

Avery L, Bargmann CI, Horvitz HR (1993) The Caenorhabditis elegans unc-31 gene affects multiple nervous system-controlled functions. Genetics 134:455-464.

Bamber BA, Beg AA, Twyman RE, Jorgensen EM (1999) The Caenorhabditis elegans unc-49 locus encodes multiple subunits of a heteromultimeric GABA receptor. The Journal of neuroscience : the official journal of the Society for Neuroscience 19:5348-5359.

Bamber BA, Richmond JE, Otto JF, Jorgensen EM (2005) The composition of the GABA receptor at the Caenorhabditis elegans neuromuscular junction. British journal of pharmacology 144:502-509.

Bargmann CI, Avery L (1995) Laser killing of cells in Caenorhabditis elegans. Methods in cell biology 48:225-250.

Baroncelli L, Braschi C, Spolidoro M, Begenisic T, Maffei L, Sale A (2011) Brain plasticity and disease: a matter of inhibition. Neural plasticity 2011:286073.

Bettler B, Kaupmann K, Mosbacher J, Gassmann M (2004) Molecular structure and physiological functions of GABA(B) receptors. Physiological reviews 84:835-867.

Brenner S (1974) The genetics of Caenorhabditis elegans. Genetics 77:71-94.

Brockie PJ, Madsen DM, Zheng Y, Mellem J, Maricq AV (2001) Differential expression of glutamate receptor subunits in the nervous system of Caenorhabditis elegans and their regulation by the homeodomain protein UNC-42. The Journal of neuroscience : the official journal of the Society for Neuroscience 21:1510-1522.

Chang HC, Paek J, Kim DH (2011) Natural polymorphisms in C. elegans HECW-1 E3 ligase affect pathogen avoidance behaviour. Nature 480:525-529.

Chou JH, Bargmann CI, Sengupta P (2001) The Caenorhabditis elegans odr-2 gene encodes a novel Ly-6-related protein required for olfaction. Genetics 157:211-224.

Chow BY, Han X, Dobry AS, Qian X, Chuong AS, Li M, Henninger MA, Belfort GM, Lin Y, Monahan PE, Boyden ES (2010) High-performance genetically targetable optical neural silencing by light-driven proton pumps. Nature 463:98-102.

Chronis N, Zimmer M, Bargmann CI (2007) Microfluidics for in vivo imaging of neuronal and behavioral activity in Caenorhabditis elegans. Nature methods 4:727-731.

Dani VS, Chang Q, Maffei A, Turrigiano GG, Jaenisch R, Nelson SB (2005) Reduced cortical activity due to a shift in the balance between excitation and inhibition in a mouse model of Rett syndrome. Proceedings of the National Academy of Sciences of the United States of America 102:12560-12565.

de Bono M, Maricq AV (2005) Neuronal substrates of complex behaviors in C. elegans. Annual review of neuroscience 28:451-501.

Dibb NJ, Brown DM, Karn J, Moerman DG, Bolten SL, Waterston RH (1985) Sequence analysis of mutations that affect the synthesis, assembly and enzymatic activity of the unc-54 myosin heavy chain of Caenorhabditis elegans. Journal of molecular biology 183:543-551.

Dittman JS, Regehr WG (1997) Mechanism and kinetics of heterosynaptic depression at a cerebellar synapse. The Journal of neuroscience : the official journal of the Society for Neuroscience 17:9048-9059.

Dittman JS, Kaplan JM (2008) Behavioral impact of neurotransmitter-activated G-protein-coupled receptors: muscarinic and GABAB receptors regulate Caenorhabditis elegans locomotion. The Journal of neuroscience : the official journal of the Society for Neuroscience 28:7104-7112.

Driscoll M, Kaplan J (1997) Mechanotransduction. In: C. elegans II, 2nd Edition (Riddle DL, Blumenthal T, Meyer BJ, Priess JR, eds). Cold Spring Harbor (NY).

Duerr JS, Han HP, Fields SD, Rand JB (2008) Identification of major classes of cholinergic neurons in the nematode Caenorhabditis elegans. The Journal of comparative neurology 506:398-408.

Eastman C, Horvitz HR, Jin Y (1999) Coordinated transcriptional regulation of the unc-25 glutamic acid decarboxylase and the unc-47 GABA vesicular transporter by the Caenorhabditis elegans UNC-30 homeodomain protein. The Journal of neuroscience : the official journal of the Society for Neuroscience 19:6225-6234.

Emmons SW, Hall DH, Brittin C, Cook SJ et al. http://wormwiring.org

Fang-Yen C, Avery L, Samuel AD (2009) Two size-selective mechanisms specifically trap bacteria-sized food particles in Caenorhabditis elegans. Proceedings of the National Academy of Sciences of the United States of America 106:20093-20096.

Fang-Yen C, Gabel CV, Samuel AD, Bargmann CI, Avery L (2012) Laser microsurgery in Caenorhabditis elegans. Methods in cell biology 107:177-206.

Fang-Yen C, Wyart M, Xie J, Kawai R, Kodger T, Chen S, Wen Q, Samuel AD (2010) Biomechanical analysis of gait adaptation in the nematode Caenorhabditis elegans. Proceedings of the National Academy of Sciences of the United States of America 107:20323-20328.

Gray JM, Hill JJ, Bargmann CI (2005) A circuit for navigation in Caenorhabditis elegans. Proceedings of the National Academy of Sciences of the United States of America 102:3184-3191.

Grillner S (2003) The motor infrastructure: from ion channels to neuronal networks. Nature reviews Neuroscience 4:573-586.

Ha HI, Hendricks M, Shen Y, Gabel CV, Fang-Yen C, Qin Y, Colon-Ramos D, Shen K, Samuel AD, Zhang Y (2010) Functional organization of a neural network for aversive olfactory learning in Caenorhabditis elegans. Neuron 68:1173-1186.

Haubert K, Drier T, Beebe D (2006) PDMS bonding by means of a portable, low-cost corona system. Lab on a chip 6:1548-1549.

Hendricks M, Ha H, Maffey N, Zhang Y (2012) Compartmentalized calcium dynamics in a C. elegans interneuron encode head movement. Nature 487:99-103.

Isaacson JS, Solis JM, Nicoll RA (1993) Local and diffuse synaptic actions of GABA in the hippocampus. Neuron 10:165-175.

Jin Y, Jorgensen E, Hartwieg E, Horvitz HR (1999) The Caenorhabditis elegans gene unc-25 encodes glutamic acid decarboxylase and is required for synaptic transmission but not synaptic development. The Journal of neuroscience : the official journal of the Society for Neuroscience 19:539-548.

Jones AK, Sattelle DB (2004) Functional genomics of the nicotinic acetylcholine receptor gene family of the nematode, Caenorhabditis elegans. BioEssays : news and reviews in molecular, cellular and developmental biology 26:39-49.

Jorgensen EM (2005) Gaba. WormBook : the online review of C elegans biology:1-13.

Jospin M, Qi YB, Stawicki TM, Boulin T, Schuske KR, Horvitz HR, Bessereau JL, Jorgensen EM, Jin Y (2009) A neuronal acetylcholine receptor regulates the balance of muscle excitation and inhibition in Caenorhabditis elegans. PLoS biology 7:e1000265.

Karbowski J, Schindelman G, Cronin CJ, Seah A, Sternberg PW (2008) Systems level circuit model of C. elegans undulatory locomotion: mathematical modeling and molecular genetics. Journal of computational neuroscience 24:253-276.

Karbowski J, Cronin CJ, Seah A, Mendel JE, Cleary D, Sternberg PW (2006) Conservation rules, their breakdown, and optimality in Caenorhabditis sinusoidal locomotion. Journal of theoretical biology 242:652-669.

Kiehn O (2006) Locomotor circuits in the mammalian spinal cord. Annual review of neuroscience 29:279-306.

Kindt KS, Viswanath V, Macpherson L, Quast K, Hu H, Patapoutian A, Schafer WR (2007) Caenorhabditis elegans TRPA-1 functions in mechanosensation. Nature neuroscience 10:568-577.

Kocabas A, Shen CH, Guo ZV, Ramanathan S (2012) Controlling interneuron activity in Caenorhabditis elegans to evoke chemotactic behaviour. Nature 490:273-277.

Kohn RE, Duerr JS, McManus JR, Duke A, Rakow TL, Maruyama H, Moulder G, Maruyama IN, Barstead RJ, Rand JB (2000) Expression of multiple UNC-13 proteins in the Caenorhabditis elegans nervous system. Molecular biology of the cell 11:3441-3452.

Komuniecki R, Hapiak V, Harris G, Bamber B (2014) Context-dependent modulation reconfigures interactive sensory-mediated microcircuits in Caenorhabditis elegans. Current opinion in neurobiology 29C:17-24.

Lee H, Choi MK, Lee D, Kim HS, Hwang H, Kim H, Park S, Paik YK, Lee J (2012) Nictation, a dispersal behavior of the nematode Caenorhabditis elegans, is regulated by IL2 neurons. Nature neuroscience 15:107-112.

Leifer AM, Fang-Yen C, Gershow M, Alkema MJ, Samuel AD (2011) Optogenetic manipulation of neural activity in freely moving Caenorhabditis elegans. Nature methods 8:147-152.

Li W, Feng Z, Sternberg PW, Xu XZ (2006) A C. elegans stretch receptor neuron revealed by a mechanosensitive TRP channel homologue. Nature 440:684-687.

Liu Q, Hollopeter G, Jorgensen EM (2009) Graded synaptic transmission at the Caenorhabditis elegans neuromuscular junction. Proceedings of the National Academy of Sciences of the United States of America 106:10823-10828.

MacLeod AR, Waterston RH, Brenner S (1977a) An internal deletion mutant of a myosin heavy chain in Caenorhabditis elegans. Proceedings of the National Academy of Sciences of the United States of America 74:5336-5340.

MacLeod AR, Waterston RH, Fishpool RM, Brenner S (1977b) Identification of the structural gene for a myosin heavy-chain in Caenorhabditis elegans. Journal of molecular biology 114:133-140.

Maguire SM, Clark CM, Nunnari J, Pirri JK, Alkema MJ (2011) The C. elegans touch response facilitates escape from predacious fungi. Current biology : CB 21:1326-1330.

Mann EO, Mody I (2008) The multifaceted role of inhibition in epilepsy: seizure-genesis through excessive GABAergic inhibition in autosomal dominant nocturnal frontal lobe epilepsy. Current opinion in neurology 21:155-160.

McIntire SL, Jorgensen E, Horvitz HR (1993a) Genes required for GABA function in Caenorhabditis elegans. Nature 364:334-337.

McIntire SL, Jorgensen E, Kaplan J, Horvitz HR (1993b) The GABAergic nervous system of Caenorhabditis elegans. Nature 364:337-341.

Mello CC, Kramer JM, Stinchcomb D, Ambros V (1991) Efficient gene transfer in C.elegans: extrachromosomal maintenance and integration of transforming sequences. EMBO J 10:3959-3970.

Miller DM, Stockdale FE, Karn J (1986) Immunological identification of the genes encoding the four myosin heavy chain isoforms of Caenorhabditis elegans. Proceedings of the National Academy of Sciences of the United States of America 83:2305-2309.

Miller KG, Alfonso A, Nguyen M, Crowell JA, Johnson CD, Rand JB (1996) A genetic selection for Caenorhabditis elegans synaptic transmission mutants. Proceedings of the National Academy of Sciences of the United States of America 93:12593-12598.

Nagel G, Szellas T, Huhn W, Kateriya S, Adeishvili N, Berthold P, Ollig D, Hegemann P, Bamberg E (2003) Channelrhodopsin-2, a directly light-gated cation-selective membrane

channel. Proceedings of the National Academy of Sciences of the United States of America 100:13940-13945.

Oblak A, Gibbs TT, Blatt GJ (2009) Decreased GABAA receptors and benzodiazepine binding sites in the anterior cingulate cortex in autism. Autism research : official journal of the International Society for Autism Research 2:205-219.

Okazaki A, Sudo Y, Takagi S (2012) Optical silencing of C. elegans cells with arch proton pump. PloS one 7:e35370.

Peden EM, Barr MM (2005) The KLP-6 kinesin is required for male mating behaviors and polycystin localization in Caenorhabditis elegans. Current biology : CB 15:394-404.

Qin Y (2013) Neural Substrates of Experience in Caenorhabditis elegans Olfactory Learning. In: Organismic and Evolutionary Biology: Harvard University.

Rand JB, Russell RL (1984) Choline acetyltransferase-deficient mutants of the nematode Caenorhabditis elegans. Genetics 106:227-248.

Richmond JE, Jorgensen EM (1999) One GABA and two acetylcholine receptors function at the C. elegans neuromuscular junction. Nature neuroscience 2:791-797.

Richmond JE, Broadie KS (2002) The synaptic vesicle cycle: exocytosis and endocytosis in Drosophila and C. elegans. Current opinion in neurobiology 12:499-507.

Sakata K, Shingai R (2004) Neural network model to generate head swing in locomotion of Caenorhabditis elegans. Network 15:199-216.

Schiavo G, Benfenati F, Poulain B, Rossetto O, Polverino de Laureto P, DasGupta BR, Montecucco C (1992) Tetanus and botulinum-B neurotoxins block neurotransmitter release by proteolytic cleavage of synaptobrevin. Nature 359:832-835.

Schultheis C, Brauner M, Liewald JF, Gottschalk A (2011) Optogenetic analysis of GABAB receptor signaling in Caenorhabditis elegans motor neurons. Journal of neurophysiology 106:817-827.

Schuske K, Beg AA, Jorgensen EM (2004) The GABA nervous system in C. elegans. Trends in neurosciences 27:407-414.

Sgado P, Dunleavy M, Genovesi S, Provenzano G, Bozzi Y (2011) The role of GABAergic system in neurodevelopmental disorders: a focus on autism and epilepsy. International journal of physiology, pathophysiology and pharmacology 3:223-235.

Shingai R, Furudate M, Hoshi K, Iwasaki Y (2013) Evaluation of Head Movement Periodicity and Irregularity during Locomotion of Caenorhabditis elegans. Frontiers in behavioral neuroscience 7:20.

Towers PR, Edwards B, Richmond JE, Sattelle DB (2005) The Caenorhabditis elegans lev-8 gene encodes a novel type of nicotinic acetylcholine receptor alpha subunit. Journal of neurochemistry 93:1-9.

Turek M, Lewandrowski I, Bringmann H (2013) An AP2 transcription factor is required for a sleep-active neuron to induce sleep-like quiescence in C. elegans. Current biology : CB 23:2215-2223.

Vashlishan AB, Madison JM, Dybbs M, Bai J, Sieburth D, Ch'ng Q, Tavazoie M, Kaplan JM (2008) An RNAi screen identifies genes that regulate GABA synapses. Neuron 58:346-361.

Vidal-Gadea A, Topper S, Young L, Crisp A, Kressin L, Elbel E, Maples T, Brauner M, Erbguth K, Axelrod A, Gottschalk A, Siegel D, Pierce-Shimomura JT (2011) Caenorhabditis elegans selects distinct crawling and swimming gaits via dopamine and serotonin. Proceedings of the National Academy of Sciences of the United States of America 108:17504-17509.

Wang X, Zhang W, Cheever T, Schwarz V, Opperman K, Hutter H, Koepp D, Chen L (2008) The C. elegans L1CAM homologue LAD-2 functions as a coreceptor in MAB-20/Sema2 mediated axon guidance. The Journal of cell biology 180:233-246.

Wen Q, Po MD, Hulme E, Chen S, Liu X, Kwok SW, Gershow M, Leifer AM, Butler V, Fang-Yen C, Kawano T, Schafer WR, Whitesides G, Wyart M, Chklovskii DB, Zhen M, Samuel AD (2012) Proprioceptive coupling within motor neurons drives C. elegans forward locomotion. Neuron 76:750-761.

White JG, Southgate E, Thomson JN, Brenner S (1986) The structure of the nervous system of the nematode Caenorhabditis elegans. Philosophical transactions of the Royal Society of London Series B, Biological sciences 314:1-340.

Chapter 3. EOL-1, the homolog of the mammalian Dom3Z, regulates olfactory learning in *C. elegans*

Introduction

Learning is critical for survival in a complex environment. The abilities to update the meaning of an external stimulus based on recent experience and to adjust behavioral responses to it increase animal's fitness. Because of the adaptive values, the molecular mechanisms that underlie experience-dependent neural plasticity are often highly conserved. One example of evolutionarily conserved mechanism is learning-induced activation of key kinase enzymes such as PKA (cAMP-dependent protein kinase A) and transcription factors such as CREB (cAMP-responsive element binding protein). PKA and CREB, initially characterized in the long-term facilitation of the gill-withdrawal reflex in *Aplysia*, are later found to play critical roles in olfactory learning in *Drosophila* and spatial memory in mice (Brunelli et al., 1976; Dash et al., 1990; Yin et al., 1994; Abel et al., 1997; Bartsch et al., 1998; Kandel, 2012). It suggests that studies of molecular mechanisms underlying neural plasticity in model organisms may provide insights into our understanding of the human brain.

In addition to the molecules that facilitate learning and memory, previous studies have also characterized inhibitory factors (Abel et al., 1998). As counteractive enzymes of the protein kinases, synaptic protein phosphatases set constraints of memory formation. For example, calcineurin acts as a memory suppressor for sensitization in the *Aplysia* (Sharma et al., 2003; Kandel, 2012), and protein phosphatase 1 (PP1) limits acquisition in the rodent object recognition task with short intervals between training sessions (Genoux et al., 2002). In addition, the *Drosophila* GABAA receptor Rdl, which is expressed in the mushroom bodies, suppresses olfactory associative learning (Liu et al., 2007). Downstream of the signaling pathway, memory formation is also constrained by suppressor genes. Another CRE-binding protein, CREB2 in *Aplysia,* inhibits long-term facilitation of the gill-withdrawal reflex by interfering with CREB1-

mediated transcription (Bartsch et al., 1995). Inhibiting ATF4, the mammalian homolog of CREB2, in the mouse hippocampus enhances long-term potentiation and spatial memory (Chen et al., 2003). These findings demonstrate that negative regulators are an important part of the molecular machinery underlying learning and memory.

The nematode *Caenorhabditis elegans* provides an opportunity to study molecular underpinnings of learning in greater detail. With a fully sequenced genome encoding about 20,000 genes, many of which have human homologs (Chalfie and Jorgensen, 1998), *C. elegans* is highly accessible by both forward and reverse genetic approaches. Its small nervous system of 302 neurons is well defined (Brenner, 1974; White et al., 1986), allowing characterization of genes in the context of neural circuits. Feeding on bacteria, *C. elegans* responds to the smells of different bacteria via the function of olfactory sensorimotor circuits (Bargmann, 2006b). Previous studies have shown that *C. elegans* reduces its olfactory preference for pathogenic bacteria, such as *Pseudomonas aeruginosa* strain PA14, after ingesting the bacteria for several hours (Zhang et al., 2005; Ha et al., 2010). Using this form of olfactory aversive learning, our lab has identified a neural network that underlies animal's naïve and learned olfactory preferences (Ha et al., 2010). Concurrent studies in the lab have also characterized conserved pathways that mediate the pathogen-induced olfactory learning, including a TGF-β pathway and an insulin/IGF-1 pathway (Zhang and Zhang, 2012; Chen et al., 2013). Intriguingly, while one insulin-like peptide (ILP) INS-6 is required for animals to learn to avoid the smell of pathogenic PA14, another ILP, INS-7, antagonistically disrupts aversive learning (Chen et al., 2013). These results have shown that learning is regulated bi-directionally by the molecular network in *C. elegans*.

In the past two decades, neurogenetics studies in *C. elegans* revealed a number of genes with evolutionarily conserved function in learning. For example, the *C. elegans* DEG/ENaC channel ASIC-1 was found to function in dopaminergic neurons to mediate associative learning (Voglis and Tavernarakis, 2008). The mutant *asci-1* is defective in both chemosensory conditioning and food-dependent thermotaxis, although the sensory perception is unimpaired (Voglis and Tavernarakis, 2008). Overexpressing the human homolog ASIC 1a in mice enhanced fear conditioning (Wemmie et al., 2004), suggesting a conserved role of ASIC-1 in neural plasticity. In addition to the candidate approaches, forward genetic screens have identified multiple new genetic regulators of learning (Morrison et al., 1999; Ishihara et al., 2002; Ikeda et al., 2008). A screen based on the salt chemotaxis learning isolated a mutant in *casy-1*, which encodes an ortholog of Calsyntenin/Alcadein in mammalian brain (Ikeda et al., 2008). The *casy-1* mutants are normal in primary sensory transduction, but exhibit defects in more than one type of higher-order information integration, such as olfactory adaptation and temperature learning (Ikeda et al., 2008). Interestingly, a genome-wide association study suggests that the mammalian homolog of *casy-1*, calsyntenin-2, is implied in human memory performance (Papassotiropoulos et al., 2006). Because it is rather difficult to demonstrate causal relationship between genes and behaviors in human, analysis of conserved molecules in *C. elegans* provides important evidence for the function of learning-related genes *in vivo*.

In this chapter of my dissertation, I characterize a new inhibitor of olfactory learning in *C. elegans,* EOL-1. I isolated the *eol-1* mutant from a forward genetic screen because it displays enhanced olfactory learning. *eol-1* encodes a putative protein that has many homologs in eukaryotes, including the mammalian protein Dom3Z implicated in pre-mRNA quality control (Jiao et al., 2013). *eol-1* acts in the URX sensory neurons to inhibit learning. Expressing the

mouse *Dom3z* in *eol-1*-expressing cells fully rescues the learning phenotype in *eol-1* mutants, indicating that EOL-1 shares functional similarities with Dom3Z in regulating learning. Mutating the residues that are critical for the enzymatic activity of Dom3Z, and the equivalent residues in EOL-1, abolishes the function of these molecules in learning. Together, our findings provide insights into the function of this conserved protein in regulating experience-dependent behavioral plasticity.

Results

A high-throughput genetic screen identified mutants in olfactory learning

As previously shown, we quantify the preference for the smell of *P. aeruginosa* PA14 over the smell of *E. coli* OP50 in *C. elegans* with a microdroplet assay, in which swimming animals are subjected to alternating airstreams odorized with the bacterial cultures (Ha et al., 2010). Swimming *C. elegans* suppresses sharp body bends ("Ω" bends) in response to attractive olfactory stimuli and increases the bending rate upon the removal of the attractants (Luo et al., 2008). Previous work has shown that short-term training with the pathogenic PA14 induces robust aversive olfactory learning, in which PA14-trained animals reduce their preference for the smell of PA14 [(Ha et al., 2010), Materials and Methods].

To identify novel regulators of olfactory learning, I performed a forward genetic screen for mutants with altered learning abilities. I conducted the screen with the microdroplet assay (Ha et al., 2010, Fig. 3. 1), because it provided single-animal resolution, well-controlled odor delivery and semi-automated data processing that allowed us to screen a large number of mutants with high throughput. The workflow of the genetic screen is shown in Fig. 3. 2. In the microdroplet assay, wild-type animals reduce their olfactory preference for PA14 after aversive training; therefore, I screened for mutants that displayed aberrant trained preference index (Fig. 3. 3A). I analyzed 1,072 EMS-mutagenized F2 clones with wild-type controls side-by-side and selected ~90 candidate mutants whose learning ability differed from the wild type mean by at least 2 standard deviations (Table 3. 1). For example, one of the mutants still preferred PA14 to OP50 smells after training, suggesting possible defects in olfactory learning; two others displayed stronger aversion to PA14 smells (Fig. 3. 3B). I further tested these candidate clones to

isolate mutants that displayed normal olfactory preference under the naive condition and defective learning after training (Fig. 3. 2).

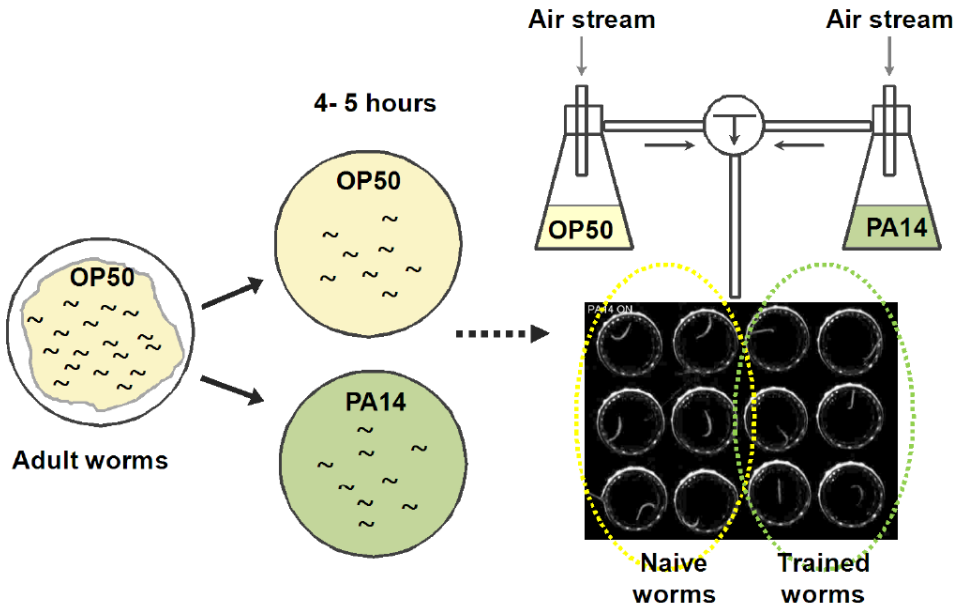

I (Turning frequency) = number of Ω bends/time (second)

Preference index = $(I_{OP50} - I_{PA14})/(I_{OP50} + I_{PA14})$

Learning index = Preference index (naive) – Preference index (trained)

Figure 3. 1 *C. elegans* olfactory aversive learning in the microdroplet assay. Adult animals raised on *E. coli* OP50 were transferred to training plates seeded with either *E. coli* OP50 or *P. aeruginosa* PA14, respectively. After 4-5 hours of training, animals were loaded to microdroplets of NGM buffer and exposed to alternating airstreams odorized by overnight culture of OP50 or PA14. Each assay lasts 10 min (10 "OP50-PA14" cycles). Images were captured at 10 Hz automatically and analyzed by a customized script. Animal's preference index, based on turning frequency under each condition, was used to calculate learning index.

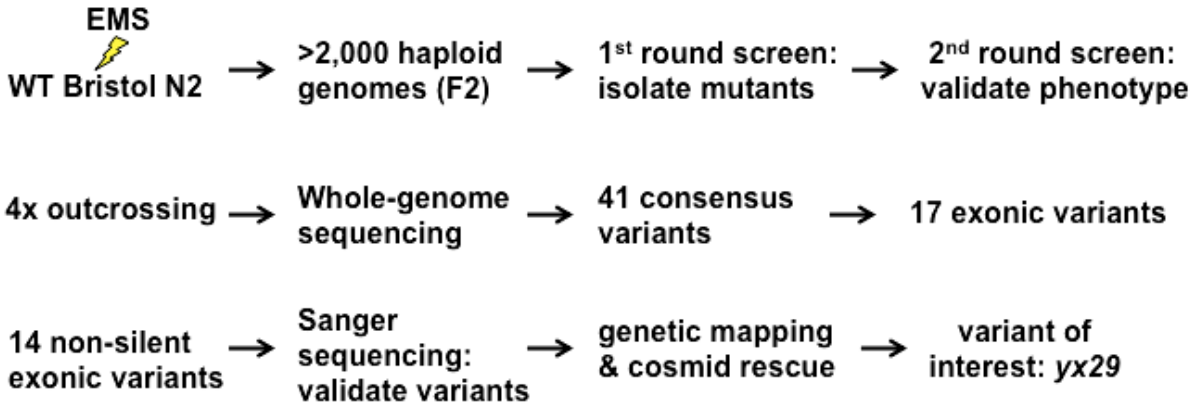

Figure 3. 2 Workflow of the forward genetic screen. First-round screen was performed on trained animals from the F2 clone library with wild-type controls side-by-side. Candidate mutants were outcrossed and sequenced to identify the mutation of interest.

Table 3. 1 Potential hits in the forward genetic screen for learning mutants

	Threshold for Preference Index of Trained mutants	Number of mutant clones	Frequency (out of 1072 F2 clones)
Mean Preference Index of Trained N2 (NCI)	-0.0286	-	-
NCI + 3SD	0.247	6	0.56%
NCI + 2SD	0.155	60	5.60%
NCI - 2SD	-0.211	22	2.05%
NCI - 3SD	-0.303	6	0.56%

Table 3. 1 Preference indexes of trained mutants were normalized to a standardized score based on the deviation of daily averaged preference index of N2 from the mean preference index of N2 (NCI) in all the assays during the first-round screen. After normalization, 3× and 2× standard deviation (SD) among all the preference indexes of trained N2 was calculated to set the thresholds for potential hits. The preference indexes of 12 mutant clones are out of NCI ± 3SD interval, and those of 82 mutant clones are within NCI ± 3SD but out of NCI ± 2SD interval. 8.8% (94 out of 1072) clones were collected from the first round based on the criteria above.

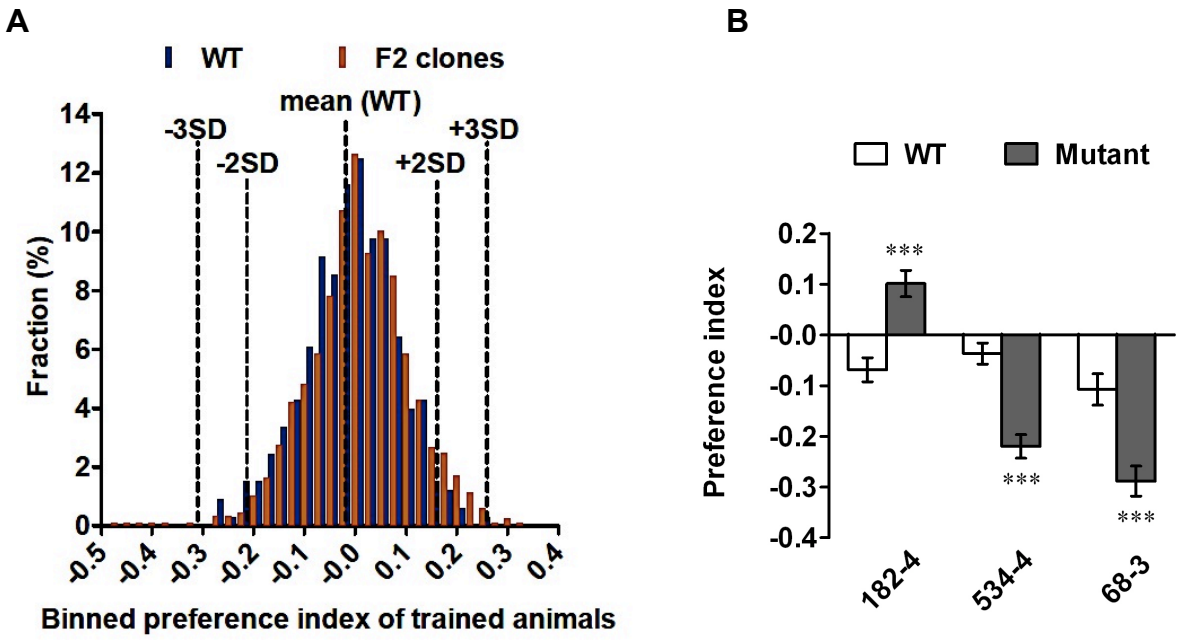

Figure 3. 3 Forward genetic screen isolated candidate mutants for learning. A, Histogram of preference index of trained wild type (WT) and mutagenized F2 clones in the first-round screen. Bin size= 0.025, columns are slightly nudged for a clear display. SD: standard deviation of wild-type preference index. B, Mutants that display aberrant preference index after training. Student's t-test, ***p< 0.001, n≥ 10 assays, Mean ± SEM.

eol-1(yx29) shows enhanced olfactory learning

Among the mutants that I isolated, one allele *yx29* appears to be enhanced in olfactory learning. Under the naive condition, *yx29* animals showed wild-type olfactory preference for PA14. However, after 4-5 hours of training, *yx29* displayed a preference index much lower than that of wild type (Fig. 3. 4A), generating about 50% increase in the learning index (Fig. 3. 4B). Analysis of turning frequency in the microdroplet assay showed that training increased the turning frequency in response to the PA14 smell in *yx29* similarly as in wild type and decreased the turning frequency in response to the OP50 smell in *yx29* (Fig. 3. 5). However, training does not affect the general attraction to bacterial smells in either *yx29* or wild type [(Ha et al., 2010), Fig. 3. 6A]. In addition, *yx29* and wild type respond similarly to the alternating smells of OP50 and NGM buffer (Fig. 3. 6B). Therefore, the changes in the turning rates to the alternating smells of OP50 and PA14 indicate altered olfactory preference between these bacterial strains. Together, these results show that *yx29*, after being trained with the pathogen PA14, reduces its olfactory preference for PA14 over OP50 more than wild type. We named *yx29* as *eol-1* (enhanced olfactory learning).

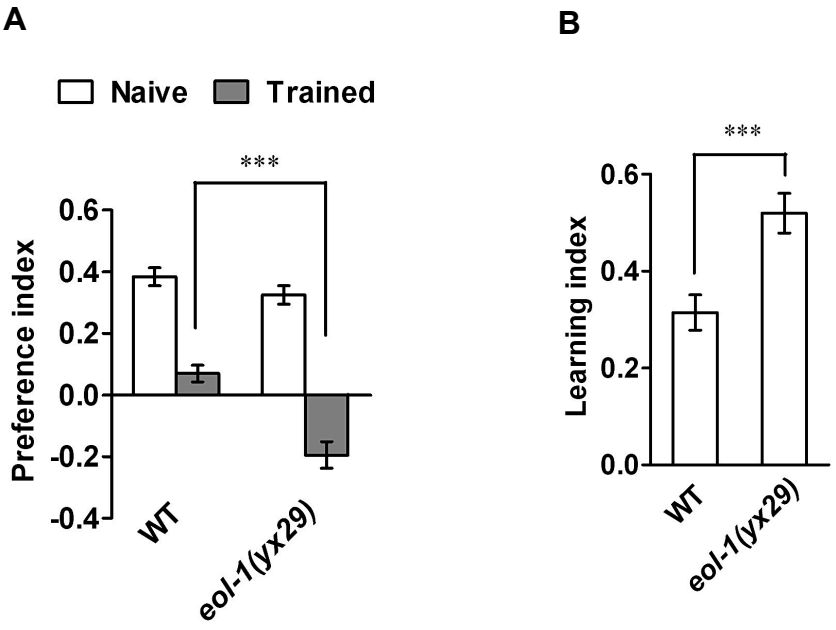

Figure 3. 4 *eol-1(yx29)* displays enhanced olfactory learning. Preference index (A) and learning index (B) of wild type and *eol-1(yx29)* in aversive olfactory learning assay. A, B, two-tailed Student's t-test, ***p< 0.001. n= 23 assays, Mean ± SEM.

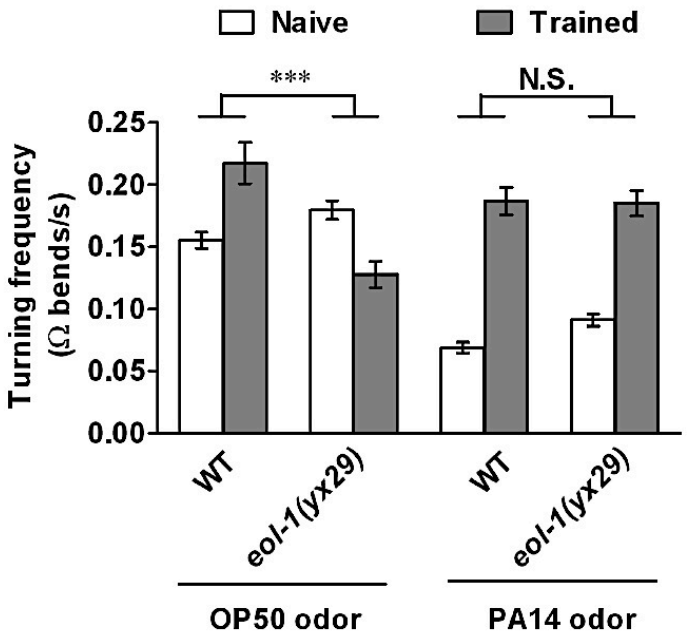

Figure 3. 5 Turning frequency of wild type and *eol-1(yx29)* in response to the alternating smells of *E. coli* OP50 and *P. aeruginosa* PA14. Two-way ANOVA, a significant genotype × treatment interaction (***$p < 0.001$) was detected for responses to OP50 odor (genotype, $p < 0.01$; treatment, $p > 0.05$), but not for responses to PA14 odor (N. S., $p > 0.05$ for genotype × treatment interaction; genotype, $p > 0.05$; treatment, $p < 0.001$). n= 23 assays, Mean ± SEM.

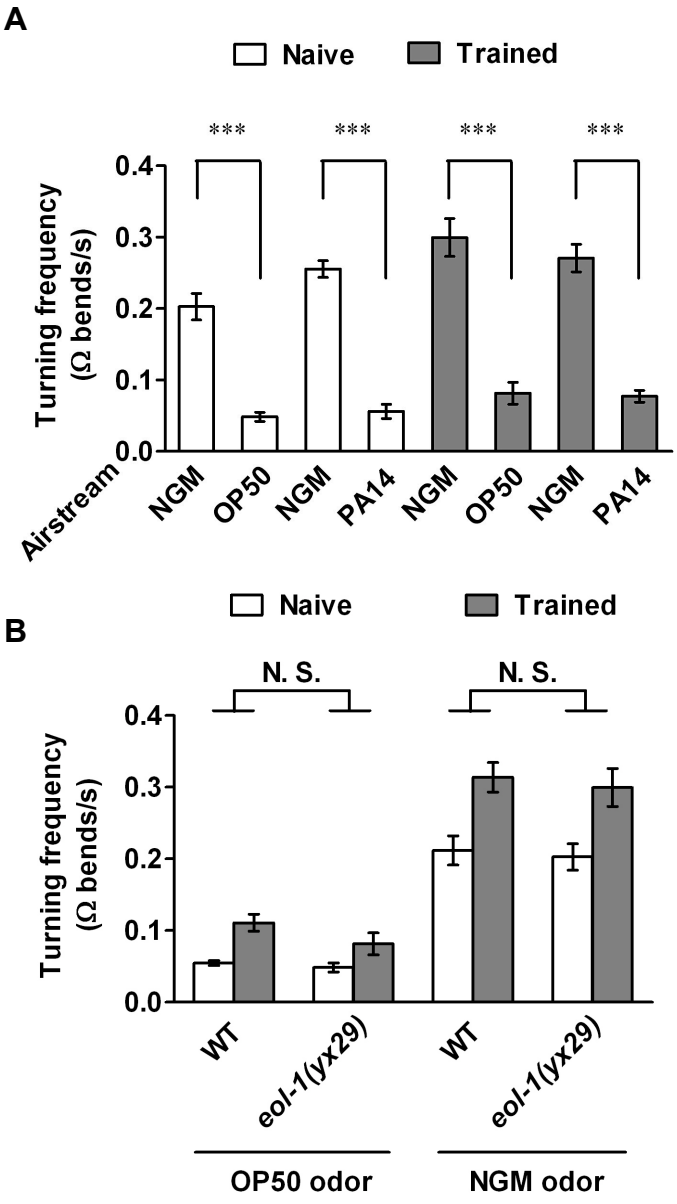

Figure 3. 6 Turning frequency of *eol-1(yx29)* to bacterial odor versus buffer. A, Turning rate of *eol-1(yx29)* to the alternating smells of NGM buffer and bacteria OP50 or PA14 (two-tailed Student's t-test, ***$p < 0.001$). B, WT and *eol-1(yx29)* respond similarly to the alternating smells of OP50 and NGM buffer. Two-way ANOVA (N. S., $p > 0.05$ for genotype × treatment interaction; genotype, $p > 0.05$; treatment, $p < 0.001$). $n \geq 9$ assays, Mean ± SEM.

eol-1 specifically regulates aversive olfactory learning

To test whether the enhanced learning of *eol-1(yx29)* was due to changed resistance to PA14 infection, I performed the slow-killing assays to quantify the survival kinetics. I found that the survival curve of *eol-1(yx29)* was indistinguishable from that of wild type, indicating that *eol-1(yx29)* does not learn more because of altered pathogen resistance (Fig. 3. 7, Materials and Methods). In addition, I evaluated the ability of *eol-1(yx29)* to respond to other repellents. Using previously established assays (Troemel et al., 1997; Chao et al., 2004), I found that *eol-1(yx29)* displayed wild-type response to repulsive odors 2-nonanone and 1-octanol (Fig. 3. 8), indicating the mutation did not alter aversive response in a unspecific manner. These results suggest that the enhance learning in *eol-1(yx29)* is not caused by defects in immunity or olfaction.

To examine the temporal profile of the enhanced learning, I measured learning in *eol-1(yx29)* and wild type at different time points of training on PA14. I found that *eol-1(yx29)* learned faster than wild type, with a learning index after two-hour training comparable to the wild-type learning index induced by five-hour training (Fig. 3. 9). The learning indexes of *eol-1(yx29)* remained higher than wild type throughout the time course, showing about 50% increase at the end (Fig. 3. 9). To evaluate whether the training effects lasts longer in *eol-1(yx29)*, I also measured the olfactory preference of *eol-1(yx29)* after trained animals were transferred from PA14 plates to OP50 lawn or empty NGM plates at different time points. I found the olfactory preference of trained *eol-1(yx29)* returned to naïve-level after 2-3 hours post removal from PA14, indicating that the olfactory memory in *eol-1(yx29)* was short-term, comparable with wild type (Fig. 3. 10, Ha et al. 2010). These results suggest that *eol-1(yx29)* mutants show faster and enhanced olfactory learning, but not memory, induced by the pathogen PA14.

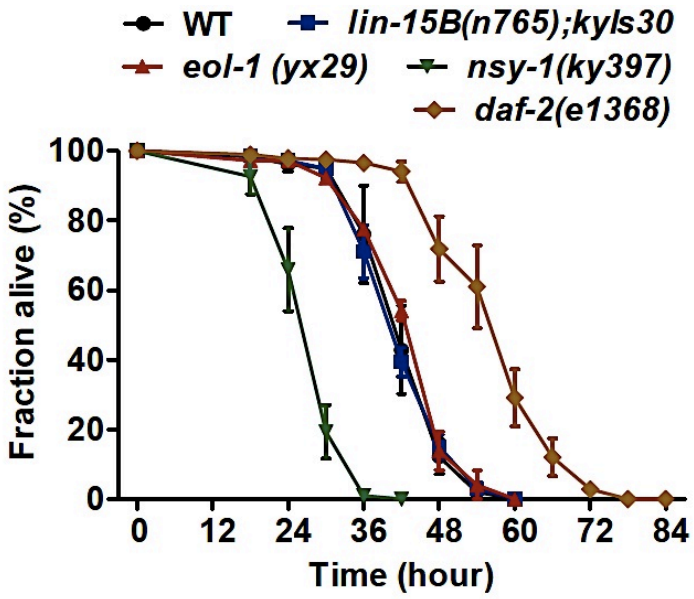

Figure 3. 7 Slow killing assays on *P. aeruginosa* PA14. n= 3 assays each genotype, n≥ 3 replicates per assay, log-rank test with Bonferroni correction, no significant difference between *eol-1(yx29)* and wild type. *nsy-1* and *daf-2* are controls for reduced and enhanced PA14 resistance, respectively. *lin-15B(n765);kyIs30* is a wild-type reporter line used for backcrossing. Error bars, SEM.

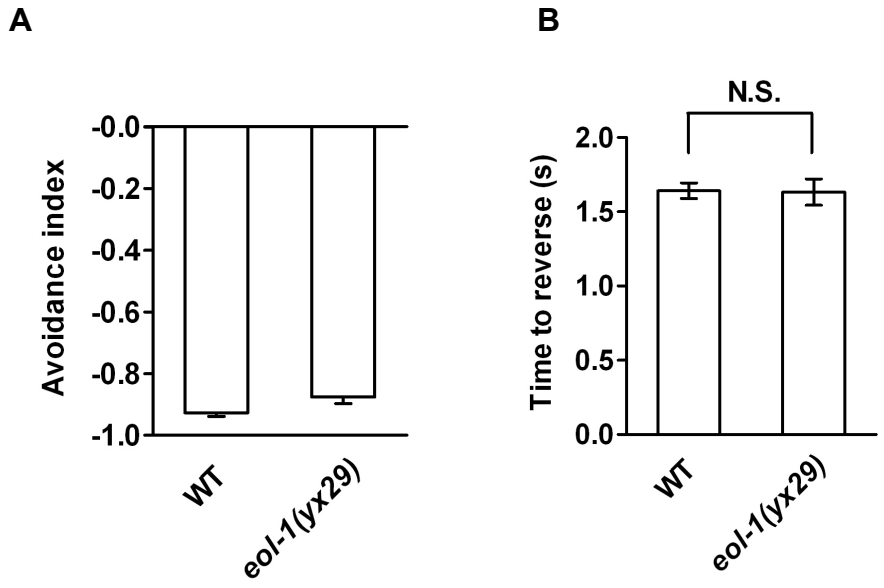

Figure 3. 8 Response of wild type and *eol-1(yx29)* to repellent odors.

A, 2-nonanone avoidance behavior of *eol-1(yx29)* is comparable with wild type. Student's t-test, p= 0.070, n= 4 trials, 3-4 replica per trial, Mean ± SEM. B, *eol-1(yx29)* responds to 1-octanol odor presented to nose similarly as wild type. Student's t-test, p= 0.933, n= 3 trials, > 20 animals per trial. Mean ± SEM.

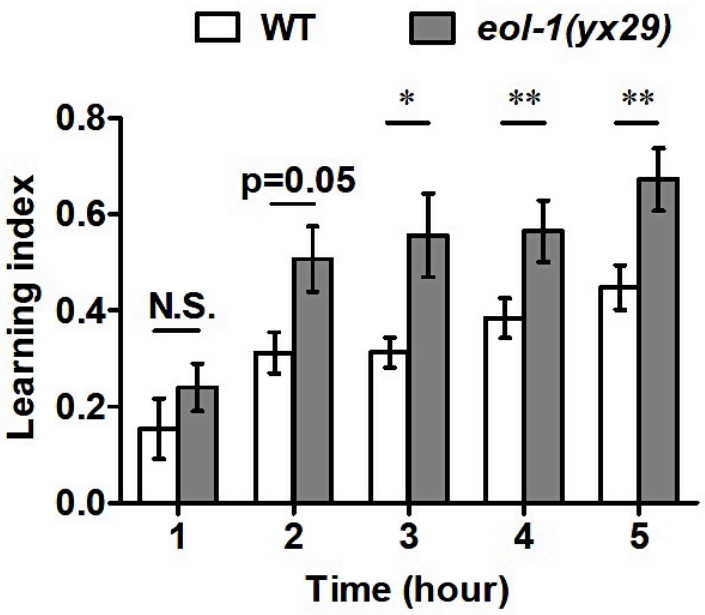

Figure 3. 9 Time course of learning. Animals were trained on PA14 lawn for different time lengths before being tested in droplet assay. *eol-1(yx29)* mutants are compared with wild-type controls at each time point, n≥ 6 assays each. Two-tailed paired t-test, **p< 0.01, *p< 0.05, N.S. not significant, Mean ± SEM.

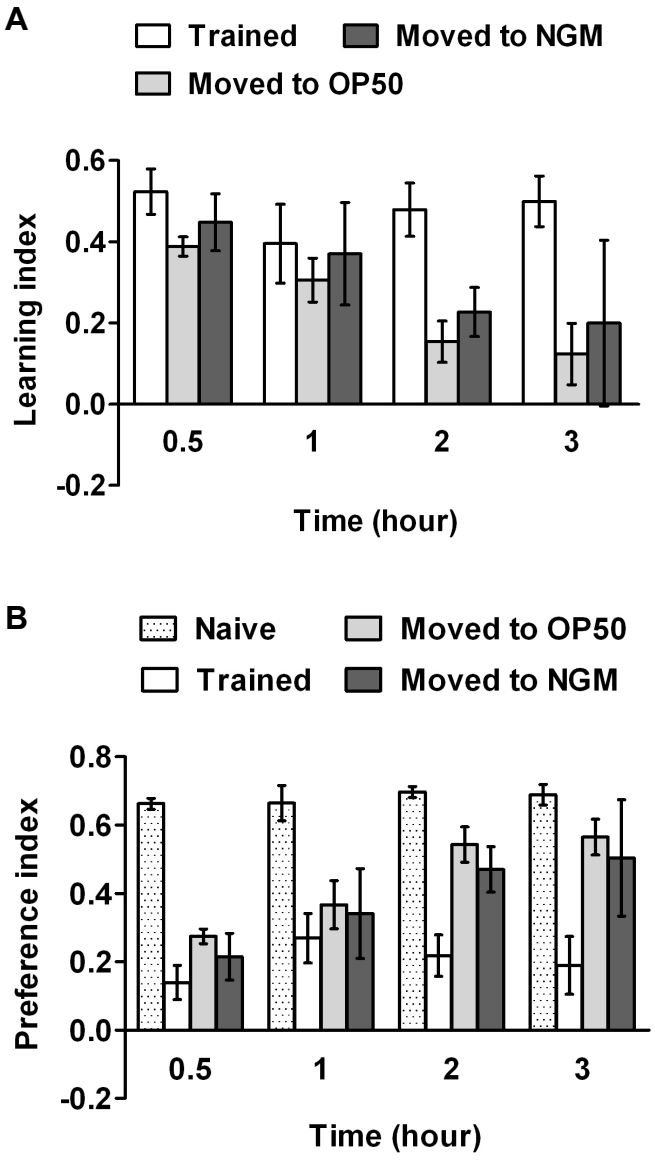

Figure 3. 10 Time course of "forgetting". *eol-1(yx29)* animals trained on PA14 lawn were removed to either OP50 lawn or empty NGM-agar plates and tested after different time points. A, Learning index and B, Preference index of different groups. n≥ 3 assays at each time point. Mean ± SEM.

To evaluate whether *eol-1* regulates other forms of neural plasticity, I tested *eol-1(yx29)* mutants in another short-term olfactory learning, food-enhanced butanone chemotaxis. In this learning paradigm, animals increase attraction to butanone after being exposed to butanone on food (Torayama et al., 2007). I observed no significant difference between *eol-1(yx29)* and wild type in this assay (Fig. 3. 11). Therefore, *eol-1* specifically regulates aversive olfactory learning.

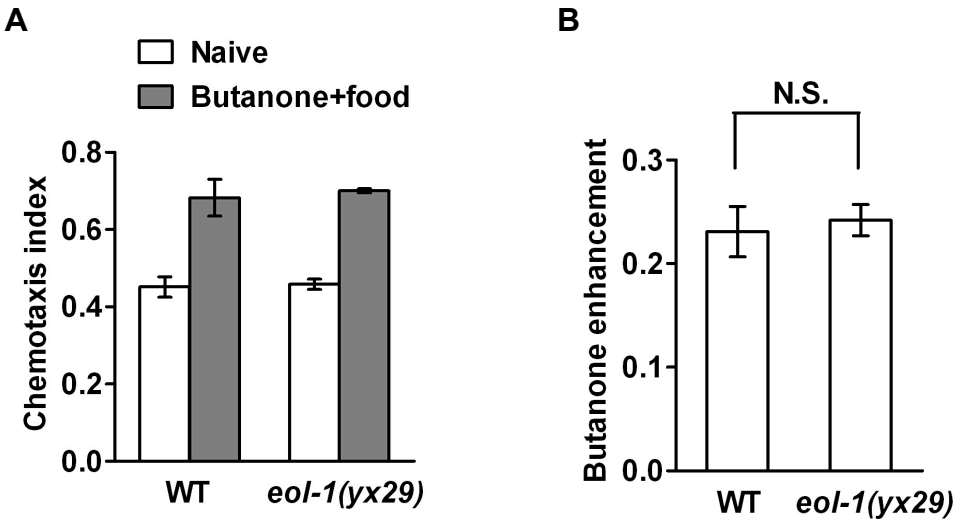

Figure 3. 11 Butanone chemotaxis (A) and butanone enhancement index (B) of wild type and *eol-1(yx29)* in the food-enhanced butanone chemotaxis assay. *eol-1(yx29)* are compared with wild type by two-tailed Student's t-test, N. S.: Not significant, n= 4 assays for each genotype, n≥ 5 replicates in each assay. Mean ± SEM.

The wild-type *T26F2.3* sequence restores normal learning to *eol-1(yx29)*

To identify the genetic lesion(s) underlying the learning phenotype of *eol-1(yx29),* I performed whole-genome sequencing on the 4× outcrossed mutant allele. I confirmed that *yx29* is a recessive allele, because the F1 progeny of *yx29* crossing with wild type showed wild-type learning (Fig. 3. 12). Sequencing analysis with two independent algorithms identified 41 consensus variants in *eol-1(yx29)*, most of which were localized in two regions on Chromosome V and X (Table 3. 2). Non-silent, exonic variants with high confidence were mapped into 13 genes (Table 3. 3). The functions of these genes were tested by cosmid rescue or by assaying learning in independently generated alleles. With the aid of genetic mapping, the mutation in *eol-1(yx29)* was assigned to a 4Mb region on the right arm of chromosome V (Fig. 3. 13). Among all the cosmids tested, T26F2 restored wild-type learning to *eol-1(yx29)* (Fig. 3. 14). *yx29* contains a single-nucleotide mutation in an annotated protein-coding gene *T26F2.3*. A PCR product containing the wild-type *T26F2.3* coding sequence, a 908 bp 5' cis-regulatory sequence and a 3.1 kb 3' cis-regulatory sequence rescued the *eol-1(yx29)* learning phenotype, indicating that the G-to-A transition that changes Serine 285 to a Phenylalanine in *T26F2.3* enhanced learning in *eol-1(yx29)* (Fig. 3. 13-3. 14). Expressing a *T26F2.3::gfp* translational fusion transgene in *eol-1(yx29)* also rescued its learning phenotype (Fig. 3. 14). Thus, *T26F2.3* is sufficient to restore normal learning to *eol-1(yx29)* mutants. Another allele, *tm6514,* containing 668bp deletion of *T26F2.3* also produced an increased learning index (Fig. 3. 15A). In addition, knocking down *T26F2.3* by injecting sense and antisense fusion constructs increased learning index (Fig. 3. 15B). Together, these results show that *T26F2.3* encodes EOL-1. Over-expressing the *T26F2.3::gfp* fusion transgene in wild type decreased the learning index, suggesting that *eol-1* suppresses learning (Fig. 3. 16).

Table 3. 2 Variants identified in *yx29* mutant by whole-genome sequencing

Chromosome	I	IV	V	X
#Variant	1	1	21	18
#Exonic	0	0	11	6
#Non-sildent	0	0	9	5

Table 3. 2 Whole-genome sequencing of 4× outcrossed mutant allele *yx29* and wild-type controls identified 41 variants in *yx29*. Sequencing results were analyzed by ELAND and STAMPY, and consensus variants with high confidence were localized to candidate genes (based on Ensembl Genome Browser, *C. elegans* WS220).

Table 3. 3 Candidate genes with exonic mutations identified in *yx29*

Gene ID	Gene name	Genetic position (cM)	Change	Description
C13C4.1	*nhr-153*	V:3.65 +/- 0.004	G1120A, Glu→Lys	Nuclear hormone receptor
T04H1.6	*lrx-1*	V:3.94 +/- 0.010	G513A, Met→Ile	LDL receptor domain
ZC443.5	*ugt-18*	V:4.71	G1147A, Glu→Lys	UDP-Glucuronosyl Transferase
F53F1.11	*srd-19*	V:5.30	C996T, Ser (silent)	
T01D3.5	*T01D3.5*	V:5.59	C877T, Gln→STOP	ZIP-like zinc transporter protein
T26F2.3	*T26F2.3*	V:5.87	C854T, Ser→Phe	Homolog of dom-3
C53A5.4	*tag-191*	V:6.47 +/- 0.015	G731A, Arg→Gln	Predicted protein kinase
C53A5.5	*C53A5.5*	V:6.47	G949A (form a), Val→Met	Ca^{2+}-activated K^{+} channel proteins
K06B4.5	*nhr-196*	V:8.63 +/- 0.004	C75T, Asn (silent)	
F21H7.7	*srh-104*	V:9.85	G579A, Glu→Lys	Predicted G-protein coupled receptor
T13F3.3	*nhr-127*	V:9.90 +/- 0.008	C190T, His→Tyr	Nuclear hormone receptor
F13C5.6	*unc-96*	X:-19.56 +/- 0.644	C795T, Asp (silent)	
F09E10.8	*toca-1*	X:-17.97 +/- 0.027	C1099T, Arg→Trp	TOCA homolog (Cdc42 pathway)
K06A9.2	*K06A9.2*	X:-17.95	G98A, Arg→Gln	Predicted protein with F-box motif
T10H10.1	*hum-6*	X:-15.83 +/- 0.073	G145A, Ala→Thr	Unconventional myosin
T02C5.5	*unc-2*	X:-13.78 +/- 0.069	C5252T (form b), Ala→Val	Calcium channel α subunit
T02C5.5	*unc-2*	X:-13.78 +/- 0.069	C4372T (form a), Leu→Phe	Calcium channel α subunit

Table 3. 3 Non-silent, exonic variants identified in *yx29* with high confidence were localized into 13 genes based on Ensembl Genome Browser, *C. elegans* WS220.

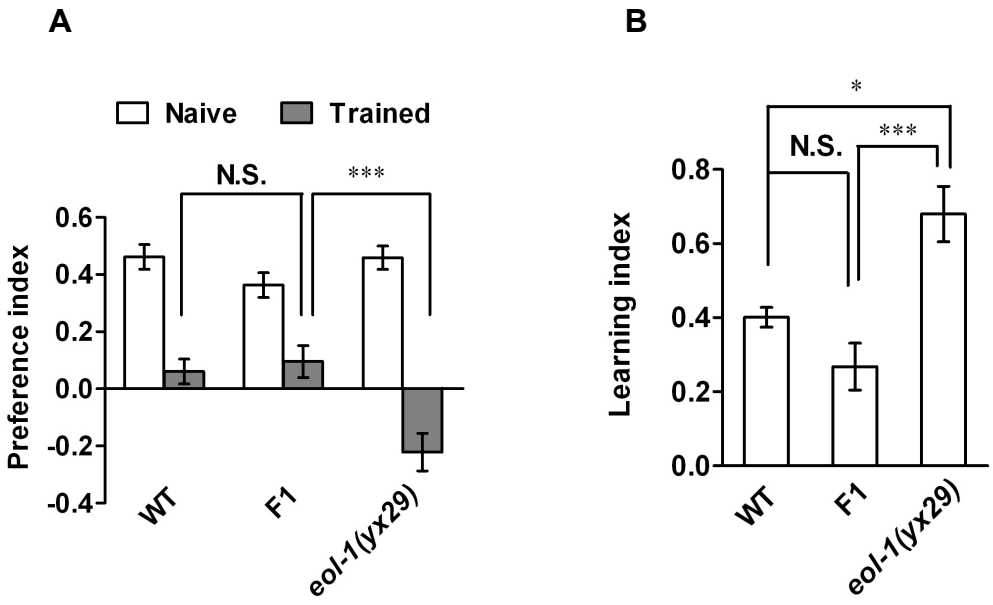

Figure 3. 12 *yx29* is a recessive allele. Preference index (A) and learning index (B) of trained wild type (WT), *yx29* and F1 progeny generated by crossing *yx29* with the otherwise wild-type allele *dpy-5(e61)*. A, Preference index of trained animals were compared by Student's t-test, ***p< 0.001, N.S. not significant. B, One-way ANOVA, *p< 0.05, ***p< 0.001, N.S. not significant. n≥ 6 assays, Mean ± SEM.

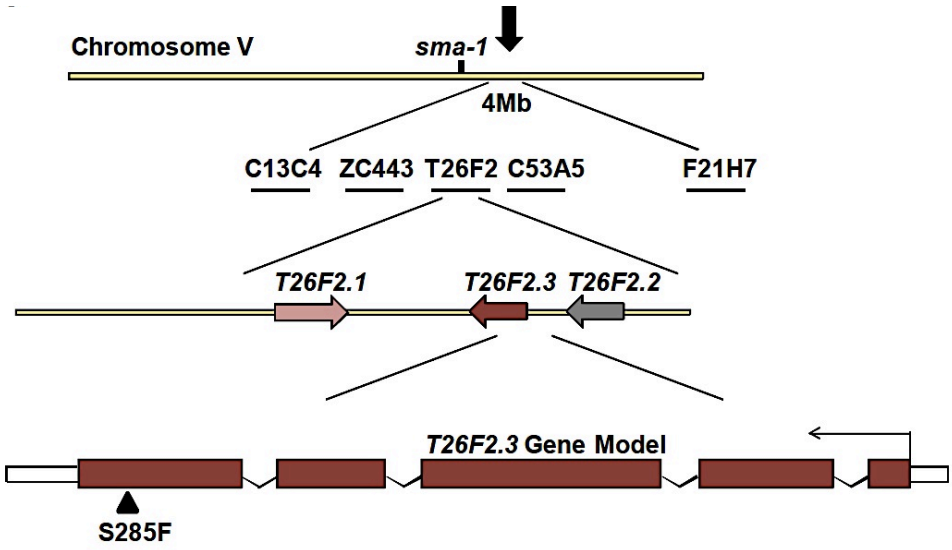

Figure 3. 13 Genomic structure of *T26F2.3* sequence (Ensemble Genome Browser, *C. elegans* WS220). The variation in *yx29* was localized to a 4 Mb region on Chromosome V. *T26F2.2* is a pseudo gene. Filled boxes denote coding exons. Arrow head denotes the S285F mutation in *yx29*. Cosmids tested for rescue are shown and only T26F2 rescued the learning phenotype in *eol-1(yx29)*.

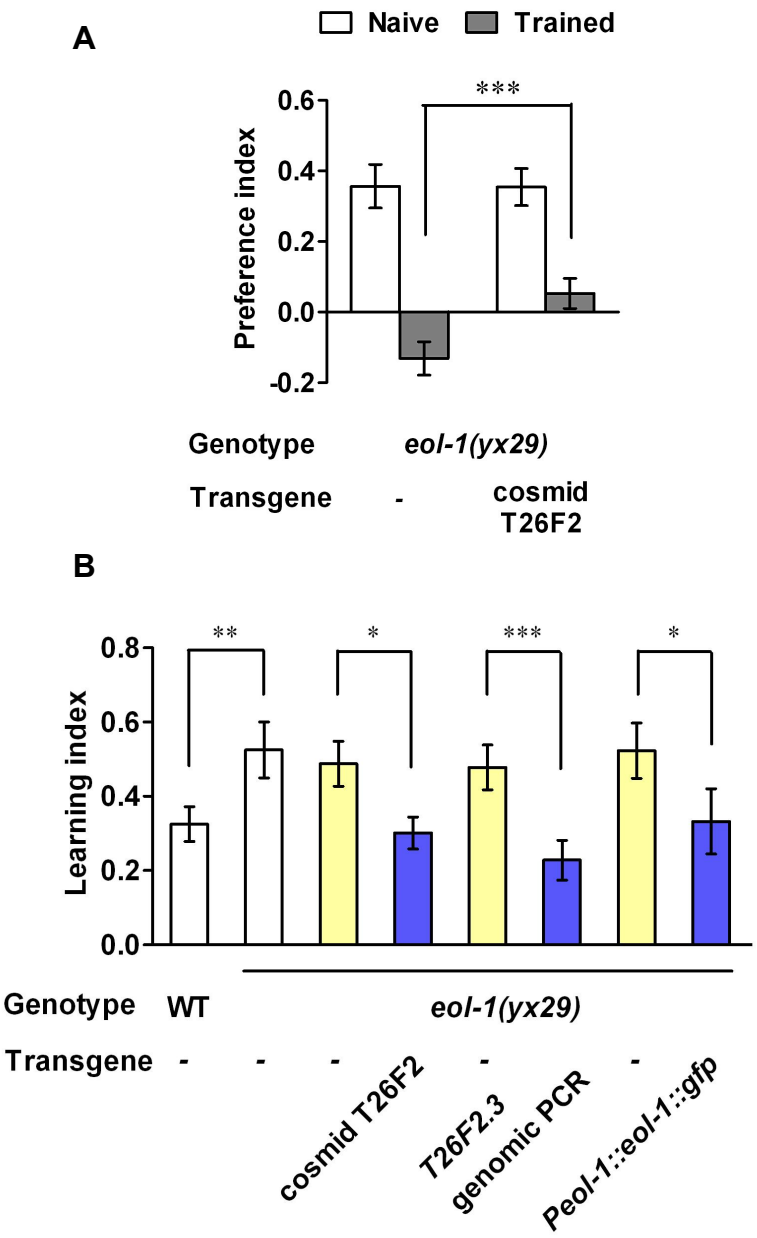

Figure 3. 14 Aversive olfactory learning of wild type, *eol-1(yx29)* and transgenic *eol-1(yx29)* that express wild-type *eol-1* sequence. The learning phenotype was rescued by the cosmid T26F2, genomic PCR of *T26F2.3* as well as the translational fusion clone. Preference indexes of cosmid rescue animals are shown in (A).Transgenic animals are compared with non-transgenic siblings. Two-tailed paired t-test, ***p< 0.001, **p< 0.01, *p< 0.05, n ≥ 12 assays each. Mean ± SEM.

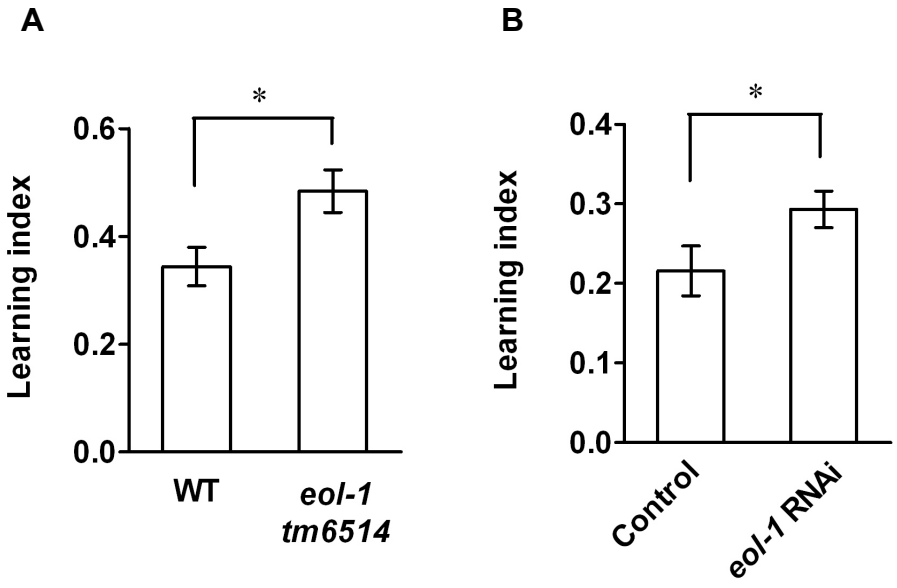

Figure 3. 15 Enhanced learning in an independent allele of *eol-1* and *eol-1* RNAi strain. A. Learning behavior of *T26F2.3(tm6514)*. Student's t-test, p= 0.0118 n= 24 assays. B. Knock-down effect of *eol-1* by RNAi, where the transgenic animals carry sense and anti-sense PCR fusion constructs of *eol-1*. Transgenic animals are compared with non-transgenic siblings. Student's t-test, p= 0.0399. n= 15 assays, Mean ± SEM.

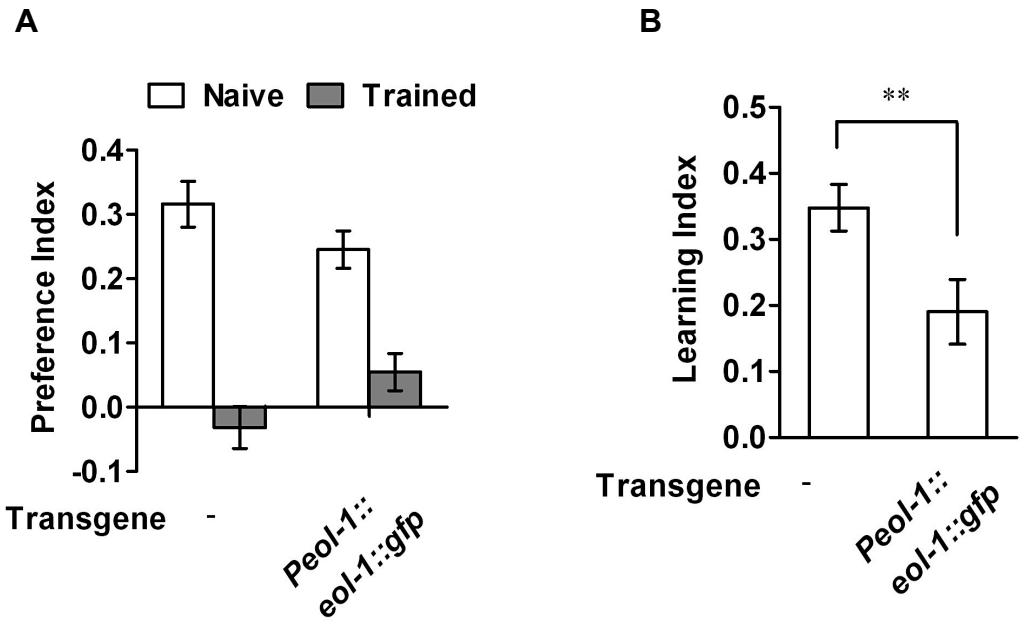

Figure 3. 16 Overexpressing *eol-1* in wild type reduces learning. A, Preference index of naïve and trained animals. B, Learning index of animals over-expressing *eol-1*. Transgenic animals are compared with non-transgenic siblings, n= 13 assays. Two-tailed paired t-test, **$p < 0.01$, Mean ± SEM.

eol-1 functions in the URX neuron to regulate olfactory learning

To understand the function of *eol-1* in regulating the pathogen-induced aversive learning, I first examined the expression pattern of *eol-1* by expressing a GFP or mCherry transcriptional reporter using both the 5' and 3' cis-regulatory sequences of *eol-1*, as well as a translational reporter with GFP fused to the C-terminus of the *eol-1* coding sequence. These transgenes showed consistent expression patterns, and no difference in *eol-1* expression was detected between wild type and *yx29*. In adult hermaphrodites, *Peol-1::gfp* was expressed in a few head and tail neurons, in the reproductive system, and sometimes in intestine (Fig. 3. 17). Dye-fill assay showed the head neuron that expresses *eol-1* was adjacent to ASK (Fig. 3. 18). Using reporters known to express in specific cells (Chou et al., 2001; Lickteig et al., 2001; Macosko et al., 2009), I identified all the *eol-1*-expressing neurons based on co-localization of the fluorescent signals and morphological features of the neurons. The head neurons expressing *eol-1* are URX in the lateral ganglion and AVF in the retrovesicular ganglion, and the tail neuron that expresses *eol-1* is PQR (Fig. 3. 18-3. 19).

A

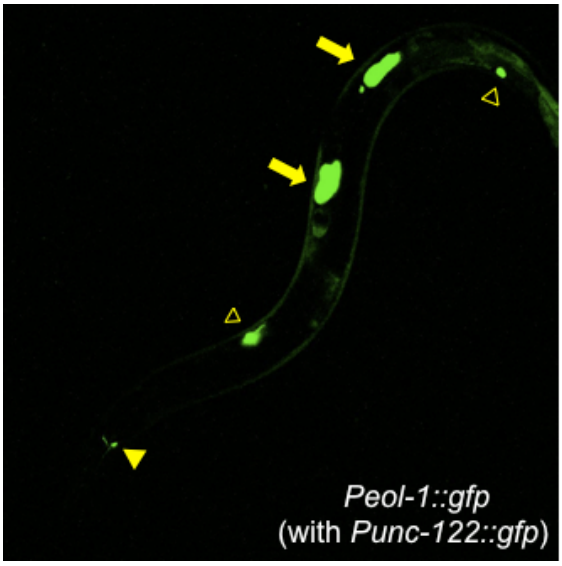

B

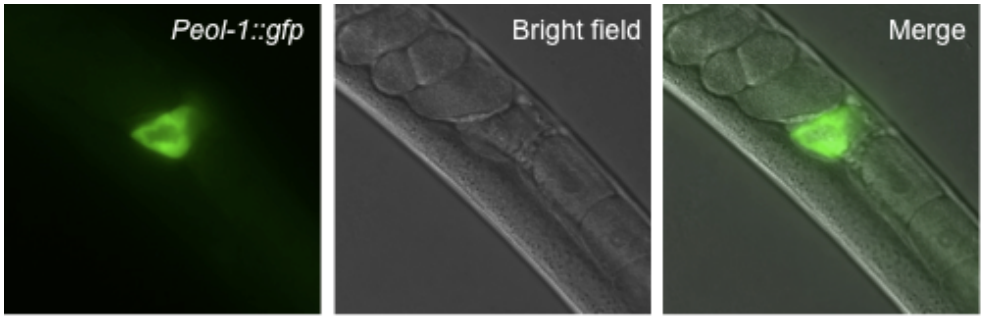

Figure 3. 17 Expression of *Peol-1::gfp* in a wild-type adult hermaphrodite. A, View of *eol-1* expression in a whole animal. Arrows denote reproductive system and arrow heads denote neurons. The transgenic marker *Punc-122::gfp* is expressed in coelomocytes (empty arrow heads). B, Expression of *eol-1* in hermaphrodite reproductive system.

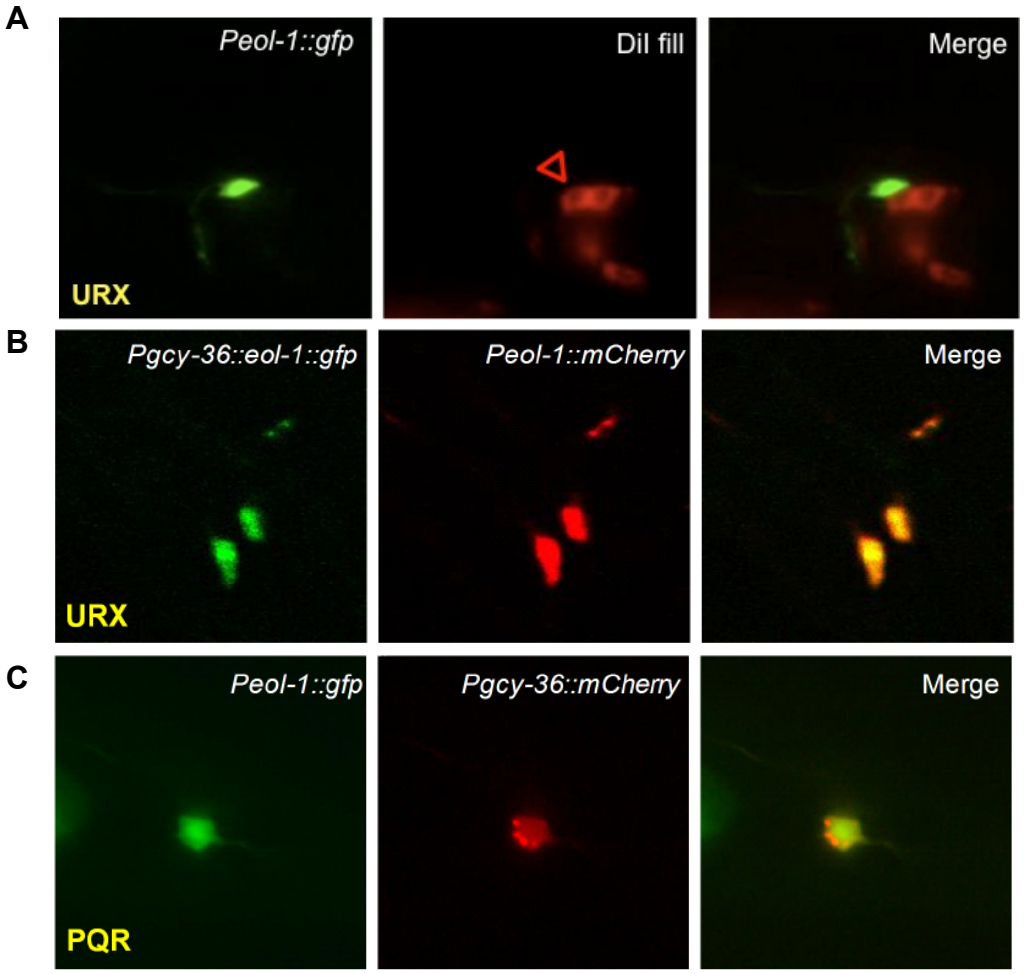

Figure 3. 18 Expression of *eol-1* in the URX and PQR neurons. A, Red dye fill of ciliated neurons ASK, ADL, ASI, AWB, ASH, ASJ. *Peol-1::gfp* is expressed in URX next to ASK (empty arrow head). B, C, *eol-1* expression in URX and PQR demonstrated by fluorescence protein colocalization.

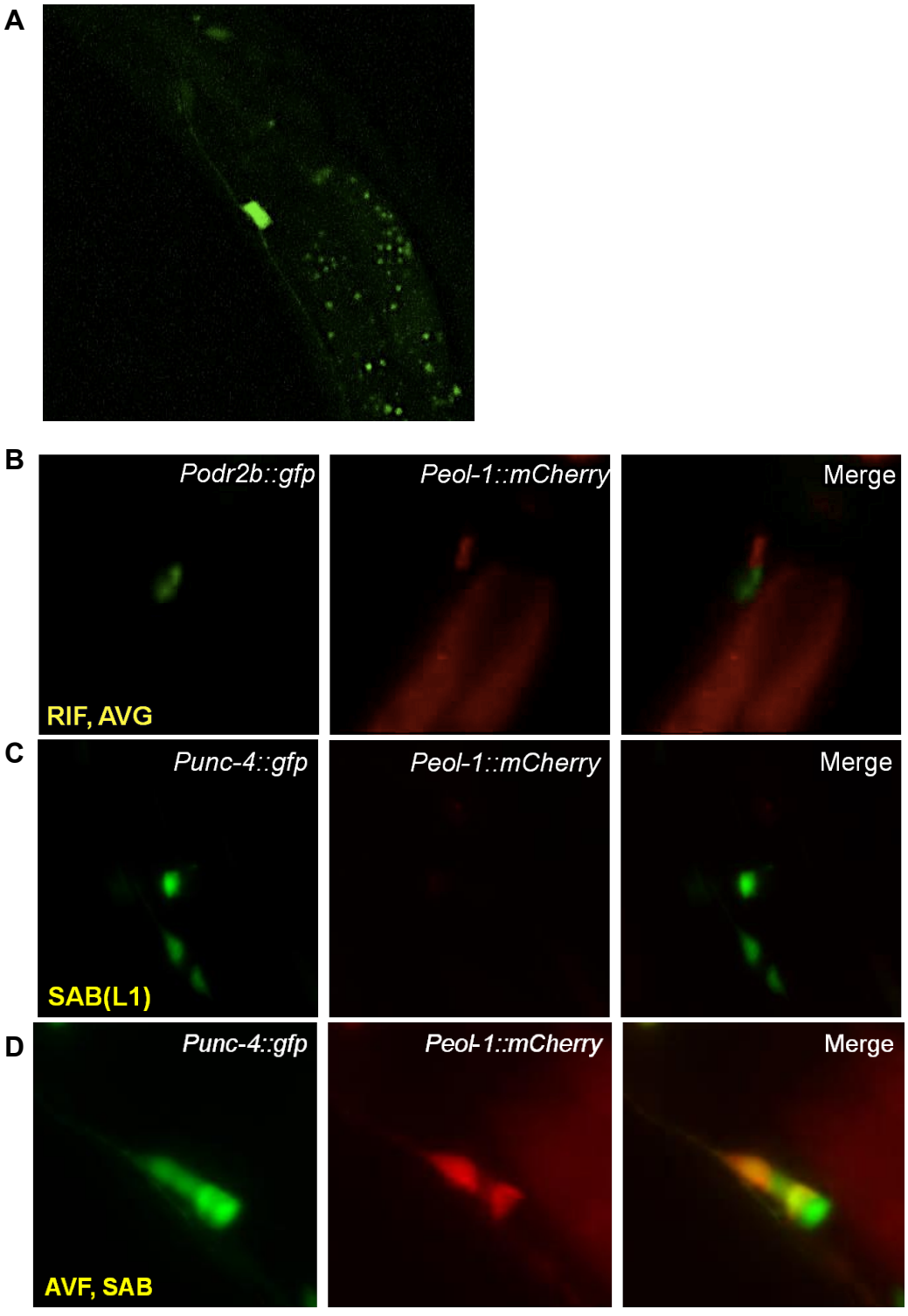

Figure 3. 19 Expression of *eol-1* in the AVF neurons (continue on next page).

Figure 3. 19 (Continued) A, Confocal microscopy shows *Peol-1::gfp* expression in AVF neurons. B, Fluorescence co-localization shows the relative position of AVF to RIF and AVG labeled by *Podr-2b::gfp*. C. In L1 larva, *Punc-4::gfp* is expressed in SAB neurons, and AVF is not present. D. In L4 to adults, *Punc-4::gfp* is expressed in SAB and AVF neurons. Fluorescence co-localization shows *Peol-1::mCherry* is expressed in AVF.

To examine where *eol-1* acts in the nervous system to regulate learning, I used cell-specific promoters to selectively express a gfp-tagged wild-type *eol-1* coding sequence in specific sets of neurons in *eol-1(yx29)*. I found that expressing wild-type *eol-1::gfp* in URX, AQR and PQR neurons using the *gcy-36* promoter (Macosko et al., 2009) completely rescued the learning phenotype in *eol-1(yx29)* (Fig. 3. 20). To narrow down the functional site of *eol-1*, I also expressed the *eol-1::gfp* transgene using the *flp-8* promoter in URX and AUA (Macosko et al., 2009) and observed a similar rescuing effect in the *eol-1(yx29)* mutants. Among the neurons that endogenously express *eol-1*, only the URX neurons express both *gcy-36* and *flp-8*, suggesting *eol-1* expression in URX is sufficient to restore wild-type learning. Killing URX by ectopically expressing a cell death molecule EGL-1 (Chang et al., 2006) significantly decreased the pathogen-induced olfactory learning (Fig. 3. 21), confirming the critical role of URX in acquiring learned olfactory preference. Together, the results show that EOL-1 acts in the URX sensory neurons to play a negative role in aversive olfactory learning.

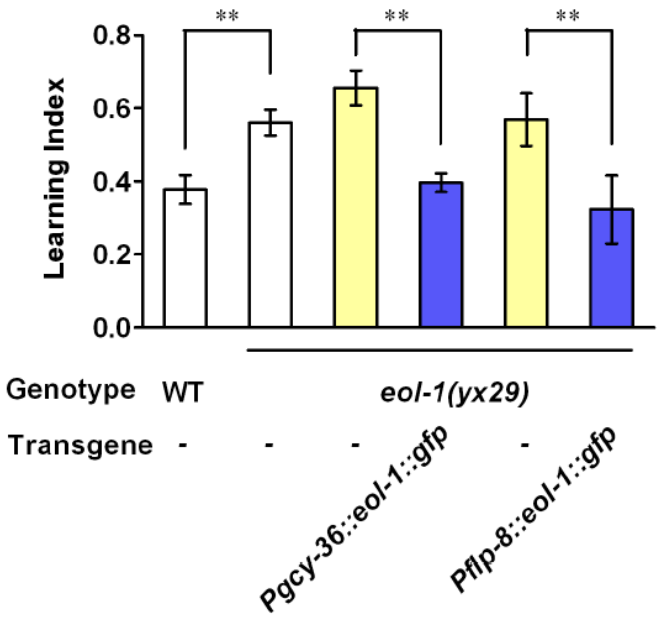

Figure 3. 20 Aversive olfactory learning of wild type, *eol-1(yx29)* and transgenic *eol-1(yx29)* animals that express wild-type *eol-1* gene under cell-specific promoters. Transgenic animals are compared with non-transgenic siblings, two-tailed paired t-test, **p< 0.01, n≥ 10 assays, Mean ± SEM.

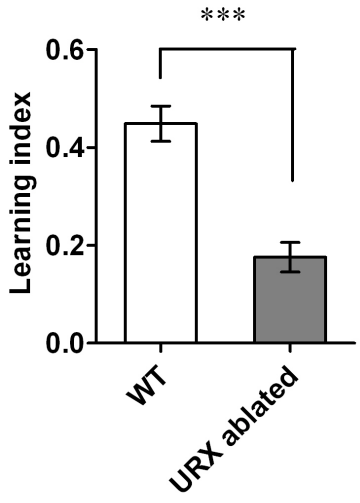

Figure 3. 21 URX ablated animals are defective in learning. Animals expressing the integrated transgene *Pgcy-36::egl-1* are compared with wild type. Student's t-test, ***p< 0.001, n= 18 assays. Mean ± SEM.

The mouse homolog of *eol-1, Dom3z,* rescues the learning phenotype of *eol-1(yx29)*

The EOL-1 protein has several paralogs in *C. elegans* and homologs in other *Caenorhabditis* species, including *C. brenneri, C. remanei* and *C. japonica*. EOL-1 is also homologous to the protein Rai1 and Dox1 in yeast and Dom3Z in mammals (Fig. 3. 22). The closest homolog of Dom3Z in *C. elegans* is DOM-3. However, the deletion allele *dom-3(tm2422)* did not show any defect in olfactory learning (Fig. 3. 23), suggesting the functional specificity of *eol-1* in learning.

Because the protein sequence of EOL-1 is conserved across species, I evaluated its functional conservation. I amplified the cDNA of one isoform of *Dom3z, Dom3z.b,* from a mouse neuronal RNA library and expressed it under the *eol-1* promoter in the *eol-1(yx29)* mutants. Interestingly, the mouse *Dom3z.b* cDNA fully rescued the learning phenotype in *eol-1(yx29)* (Fig. 3. 24), suggesting that EOL-1 and its mammalian homolog Dom3Z share functional similarities in regulating aversive olfactory learning.

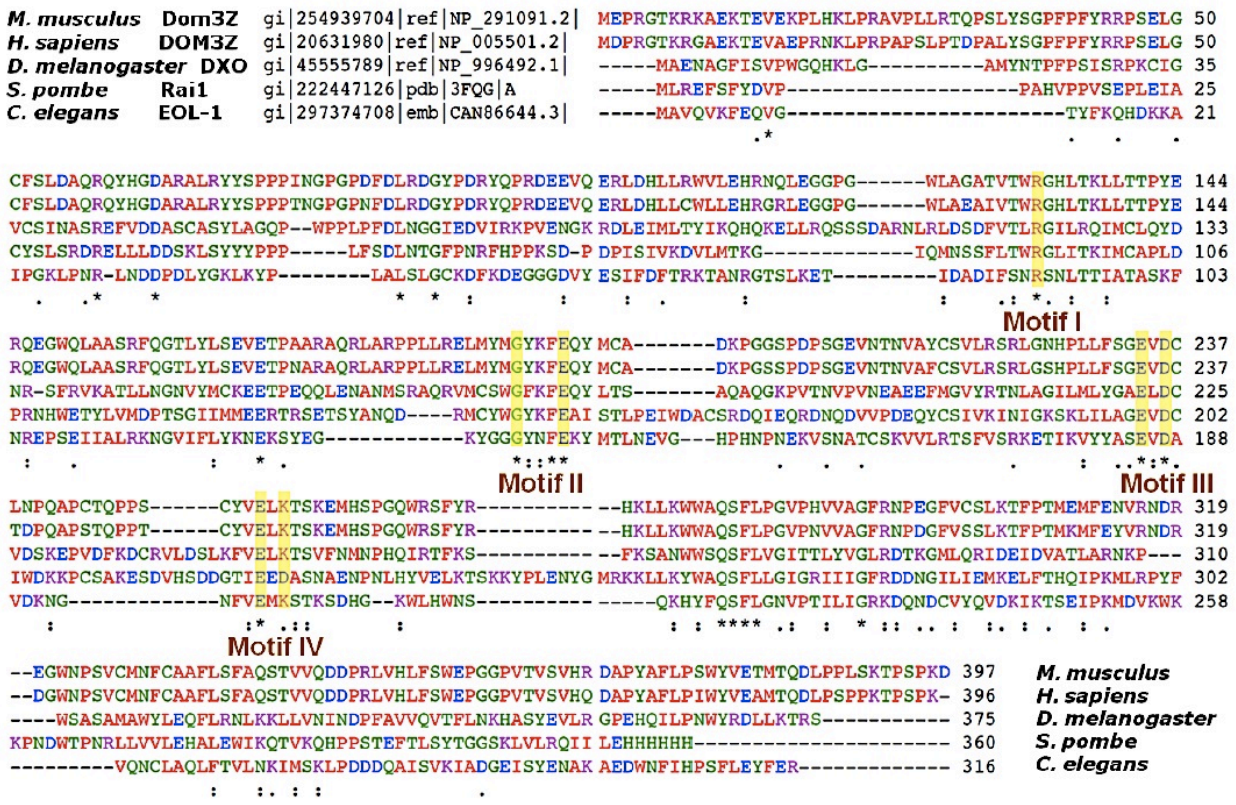

Figure 3. 22 Sequence conservation among EOL-1 homologs. * indicate positions with a single conserved residue, : indicates conservation between groups of strongly similar properties, ● indicates conservation between groups of weakly similar properties. Color code indicates physicochemical properties of amino acids (ClustalW2.1).

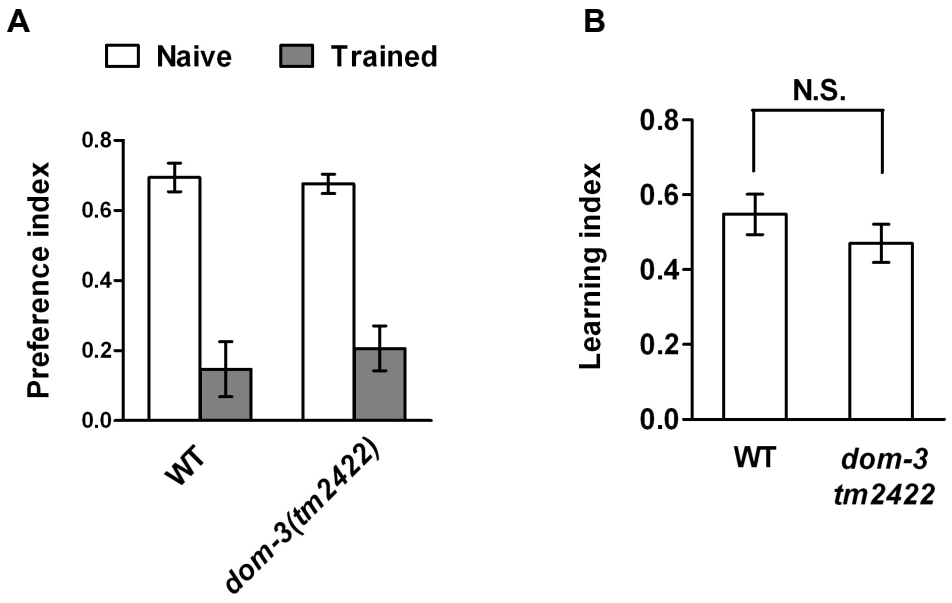

Figure 3. 23 *dom-3(tm2422)* mutants are not defective in olfactory learning.

A, Preference index of wild type and *dom-3(tm2422)*. B, Learning index of wild type and *dom-3(tm2422).* Student's t-test, N.S., not significant. n= 10 assays, Mean ± SEM.

The two yeast homologs of EOL-1, Rai1 and Dxo1, initiate a quality control system to clear pre-mRNAs with aberrant 5' caps, which can be produced under normal conditions and during nutritional stress (Jiao et al., 2010; Chang et al., 2012). Similarly, the mammalian homolog Dom3Z plays a central role in degrading aberrantly capped pre-mRNAs [(Jiao et al., 2013), Table 3. 4]. To examine whether the enzymatic activity of Dom3Z is important for learning, I mutated two residues, E234 and D236, which play critical roles in the exonuclease and de-capping activities of Dom3Z (Chang et al., 2012; Jiao et al., 2013), as well as the equivalent residues in EOL-1, E185 and D187. I found that neither Dom3Z(E234A, D236A) nor EOL-1(E185A, D187A) could rescue the learning phenotype in *eol-1(yx29)* (Fig. 3. 24). Furthermore, no difference was detected in localization or fluorescence intensity between the EOL-1::GFP fusion and the EOL-1(E185A, D187A)::GFP fusion in these transgenic animals (Fig. 3. 25), suggesting the lack of rescue is not caused by changes in localization or expression level of the mutated EOL-1. Thus, the enzymatic activity of EOL-1/Dom3Z is needed for its function in learning.

Table 3. 4 Known catalytic activities of EOL-1 homologs

Organism	EOL-1 homolog	Pyrophospho-hydrolase	5' RNA decapping	5'-3' exo-RNase	Reference
S. pombe	Rai1	Y	Y	N	Xiang et al. 2009; Jiao et al. 2010
K. lactic	Dxo1	N	Y	Y	Chang et al. 2012
M. musculus	Dom3Z	Y	Y	Y	Jiao et al. 2013

Table 3. 4 Homologs of EOL-1 in yeast and mammals have catalytic activities demonstrated by *in vitro* biochemistry assays. Y: possess catalytic activity. N: no catalytic activity.

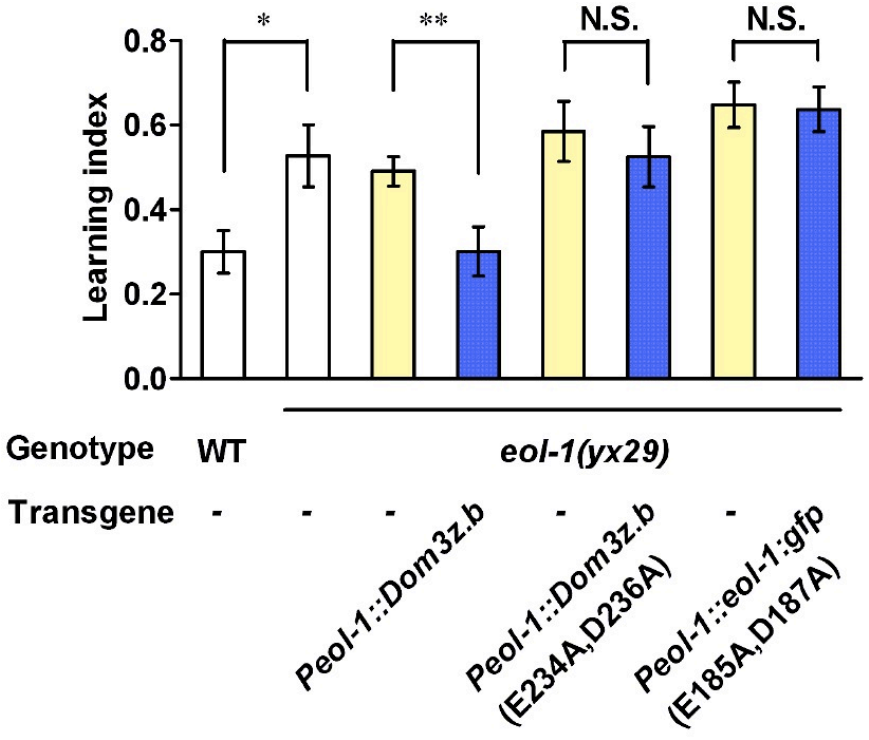

Figure 3. 24 Mouse *Dom3z.b* cDNA rescues aversive olfactory learning of *eol-1(yx29)*, but the mutated isoform *Dom3z.b*(E234A, D236A) or *eol-1*(E185A, D187A) does not. Wild type and *eol-1(yx29)* are compared using two-tailed Student's t-test, n≥ 4 assays, *p< 0.05. Transgenic animals are compared with non-transgenic siblings with two-tailed paired t-test, n= 14 assays, **p< 0.01, N.S., not significant, Mean ± SEM.

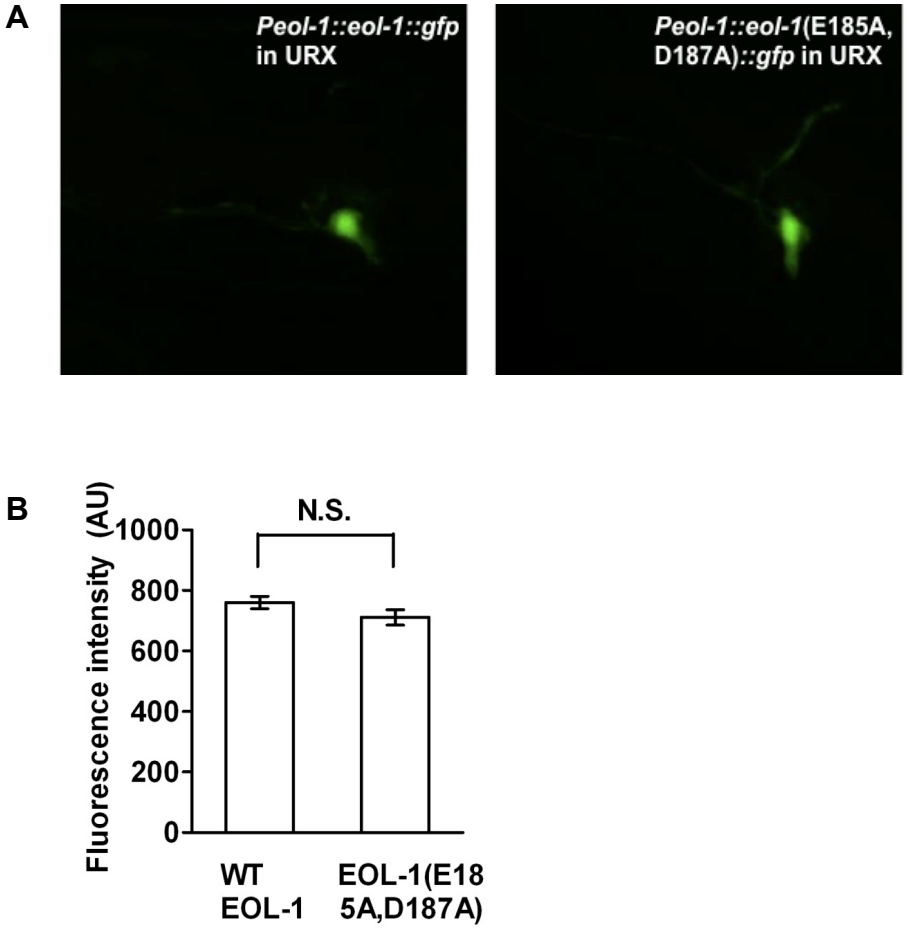

Figure 3. 25 Localization (A) and expression level (B) of *Peol-1::eol-1::gfp* wild-type or mutant proteins in URX. n= 50 transgenic animals each. Student's t-test, p= 0.137. N.S., not significant, Mean ± SEM.

EOL-1 does not form protein complex with XRN-2

The homolog of EOL-1 in *S. pombe*, Rai1, is a protein partner that stabilizes and activates the exoribonuclease Rat1 (Stevens and Poole, 1995; Xue et al., 2000; Xiang et al., 2009). Previous studies have reported the crystal structure of Rai1 in complex with Rat1, and Rai1 increases the efficiency of Rat1 to degrade RNA substrates (Xiang et al., 2009). The closest homolog of Rat1 in *C. elegans* is XRN-2, a 5'-3' exoribonuclease that is required for regulation of levels of mature microRNAs (Frand et al., 2005; Chatterjee and Grosshans, 2009). *xrn-2* is expressed in the pharyngeal myoepithelium, intestine, and neurons including URX (Frand et al., 2005; Fig. 3. 26). To examine whether EOL-1 interacts with XRN-2, I expressed GFP-tagged EOL-1 and 3×HA-tagged XRN-2 in wild-type animals, respectively, and performed co-immunoprecipitation (co-IP) of the two fusion proteins. Using antibodies against either GFP or 3×HA, I did not detect protein complex of EOL-1 and XRN-2 in the co-IP assays (Fig. 3. 27), suggesting that EOL-1 may not interact with XRN-2.

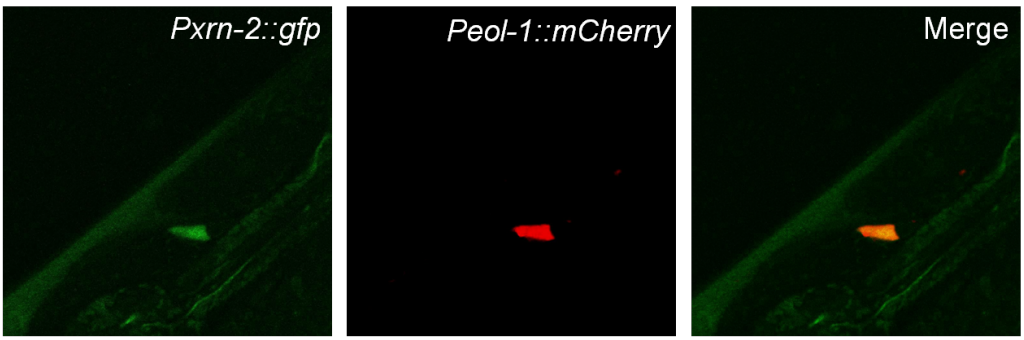

Figure 3. 26 Expression of *xrn-2* in *C. elegans*. *Pxrn-2::gfp* is expressed in intestine, pharyngeal cells and neurons, including URX that expresses *Peol-1::mCherry*.

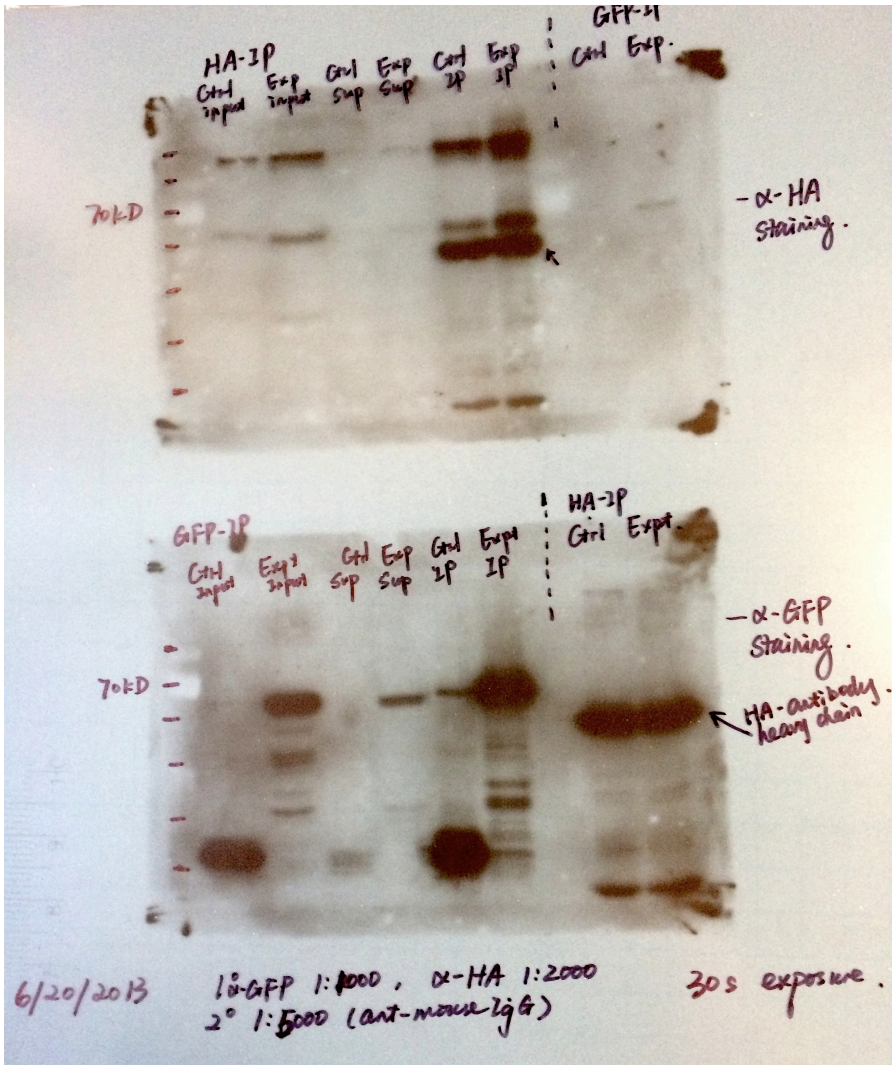

Figure 3. 27 EOL-1 does not form protein complex with XRN-2. co-IP assay using antibodies against GFP or 3×HA did not detect protein complex of GFP-tagged EOL-1 and 3×HA-tagged XRN-2 in wild-type animals.

Discussion

Protein homologs of EOL-1 play key roles in pre-mRNA quality control

The 5' end capping and decapping of eukaryotic messenger RNAs (mRNAs) are critical for mRNA synthesis, splicing, export, translation and stability (Shatkin, 1976; Merrick, 2004; Meyer et al., 2004; Liu and Kiledjian, 2006; Ghosh and Lima, 2010; Topisirovic et al., 2011). The methyl group on the 7-methylguanosine (m^7G) cap is recognized by the cap-binding proteins CBP20 and eIF4E (Gingras et al., 1999; Goodfellow and Roberts, 2008; Fischer, 2009), and the removal of the 5' end cap is catalyzed by decapping enzymes such as Dcp2 and Nudt16 (Dunckley and Parker, 1999; Song et al., 2010). After decapping, the 5' monophosphorylated RNA is subjected to degradation by the 5'-to-3' exoribonuclease (Decker and Parker, 1993); in contrast, capped transcripts or capping intermediates are thought to be exempted from decay mediated by the 5'-to-3' exoribonuclease (Jiao et al., 2013).

Recent biochemistry research on the homologs of EOL-1, such as the yeast Rai1 and Dxo1 (Ydr370C) and the mammalian Dom3Z, has revealed new enzymatic activities targeting mRNAs with incomplete cap structures (Xiang et al., 2009; Jiao et al., 2010; Chang et al., 2012; Jiao et al., 2013). Instead of being merely a stabilizing and activating partner of the exoribonuclease Rat1, Rai1 has RNA 5' pyrophosphohydrolase (PPH) activity (Xiang et al., 2009) and decapping activity on unmethyl-capped RNAs (Jiao et al., 2010). Its homolog Dxo1 possesses decapping activity on RNAs with both methylated and unmethylated 5' caps, but lacks PPH activity (Chang et al., 2012). The mammalian homolog Dom3Z, in comparison, has PPH, decapping and 5'-to-3' exoribonuclease activities (Jiao et al., 2013). It is proposed that Dom3Z and the other homologs in its family play key roles in a pre-mRNA quality control system, detecting and degrading incompletely 5'-capped pre-mRNAs generated in nutritional stress

(Chang et al., 2012; Jiao et al., 2013). Such a surveillance mechanism may help prevent the accumulation of potentially deleterious RNA products with aberrant caps (Jiao et al., 2013), yet the function of Dom3Z-like proteins in whole organism physiology remains largely unknown. By analyzing the *C. elegans* homolog EOL-1, this project provides insights into the function of Dom3Z and the pre-mRNA quality control system in regulating neural plasticity.

EOL-1 shares functional similarity with its mammalian homolog Dom3Z

In search of new molecular regulators of learning, I identified a mutant allele of *eo-1*, *yx29,* that displays increased learning induced by pathogens (Fig. 3. 4). Although EOL-1 and Dom3Z share weak sequence similarity, the four sequence motifs shared by Rai1, Dxo1 and Dom3Z in the putative active site region (Chang et al., 2012; Jiao et al., 2013) are conserved in EOL-1 (Fig. 3. 22). Expressing a cDNA of mouse *Dom3z* in the *eol-1*-expressing cells fully rescues the learning phenotype in *eol-1(yx29)* mutants (Fig. 3. 24), suggesting EOL-1 and Dom3Z are functionally interchangeable in this context. Based on biochemistry assays *in vitro*, several key amino acids in the highly conserved motifs are required for decapping and 5'-to-3' exoribonuclease activities. Strikingly, mutating two of these residues in Dom3Z and the equivalent residues in EOL-1 abolishes their function in learning (Fig. 3. 24), suggesting the predicted catalytic activities of EOL-1 are required for its role in neural plasticity. In fact, EOL-1 is more likely to catalyze RNA substrates on its own than to act as an activating partner of another exoribonuclease. Several key residues in the yeast Rai1-Rat1 interface, which are important for the stability of the Rai1-Rat1 complex, are not present in either EOL-1 or Dom3Z (Xiang et al., 2009). No evidence has shown Dom3Z associates with mammalian XRN2 by gel

filtration (Xiang et al., 2009). Consistently, I did not detect protein complex of EOL-1 and XRN-2 in *C. elegans* (Fig. 3. 27).

EOL-1 may suppress learning by tuning down stress signals in URX

The homologs of EOL-1 are capable of degrading incompletely 5'-capped pre-mRNAs generated in normal conditions as well as during nutritional stress (Jiao et al., 2013). Given that EOL-1 functions in URX to inhibit learning, I propose that aversive training with the pathogenic bacteria *P. aeruginosa* PA14 poses a condition that may increase the amount of abnormally 5' capped pre-mRNAs in the URX neurons, which can serve as a form of cellular stress that induces change in olfactory preference for bacterial foods. These potentially deleterious RNA products can be cleared by EOL-1 or Dom3Z (Fig. 3. 28). Defective EOL-1 would result in accumulation of excessive aberrantly capped pre-mRNAs, thus amplify the stress signal and enhance learning; in contrast, overexpression of EOL-1 would mitigate training effect and inhibit learning. This model proposes that the molecular machinery in URX equilibrates pathogen-induced molecular changes before signaling to the rest of the neural network. Consistently, ablating URX by an apoptosis activator EGL-1 strongly reduces learning (Fig. 3. 21).

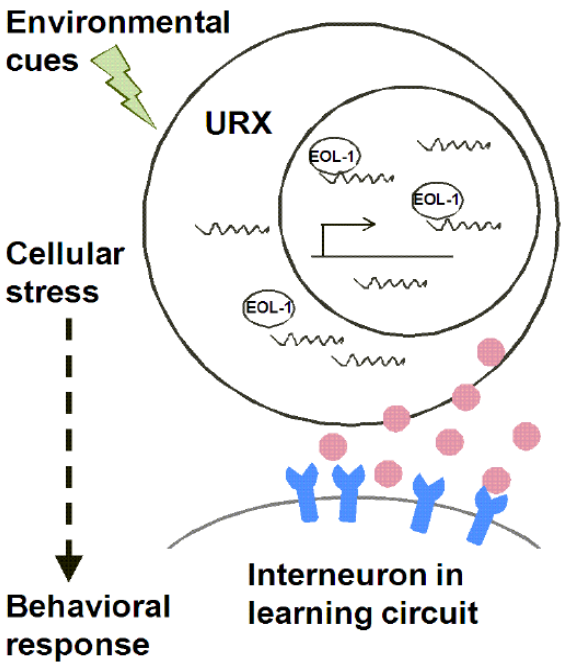

Figure 3. 28 Model of EOL-1 function in aversive olfactory learning. Aversive training on pathogenic bacteria may induce cellular stress in the URX neurons, which signals to key interneurons in the circuit underlying olfactory learning. EOL-1 may function in URX to clear away potentially deleterious aberrantly capped pre-mRNAs.

Previously work in the lab has mapped a sensorimotor circuit underlying the aversive olfactory learning induced by pathogenic bacteria (Ha et al., 2010). In this circuit, the interneuron RIA plays an essential role, because animals lacking RIA completely lose the learning ability without compromising their olfactory or immune response to the training pathogen (Ha et al., 2010). The URX neuron, the functional site of EOL-1 in regulating learning, is the major presynaptic neuron of RIA (White et al., 1986), providing a circuit base for URX to signal training effects to RIA and to induce learned olfactory preference. Although URX was characterized in aerotaxis primarily (Gray et al., 2004; Zimmer et al., 2009), a recent study in our lab has found the insulin-like peptide INS-7 secreted from URX inhibits olfactory learning via the DAF-2 receptor in RIA (Chen et al., 2013). It is unclear whether EOL-1 interacts with the insulin/IGF-1 pathway to regulate molecular signals from URX to the RIA-centered learning circuit. Quantitative profiling of RNA substrates in URX pre- and post-training, as well as *in vitro* analysis of the enzymatic activities of EOL-1, may help understanding the nature of the signal and how it derives from the EOL-1-mediated RNA processing.

Learning is a balancing act in *C. elegans*

Decades of research have revealed an amazingly rich repertoire of *C. elegans* behavior, many of which show experience-dependent plasticity (Ardiel and Rankin, 2010; Sasakura and Mori, 2013). It is no surprise that various genes and signaling pathways are required for learning to occur (Zhang, 2008; Ardiel and Rankin, 2010; Sasakura and Mori, 2013), and it is equally interesting, if not more, that a number of genes have been identified as negative regulators of learning (Yamada et al., 2010; Chen et al., 2013; Sasakura and Mori, 2013). As mentioned previously, the insulin-like peptide INS-7 antagonizes the insulin receptor-like homolog DAF-2

to inhibit learning (Chen et al., 2013); in a different behavior assay, a peptide SNET-1 suppresses the neprilysin homolog NEP-2 and negatively regulates olfactory plasticity in population density-dependent response to pheromone (Yamada et al., 2010). Here, I characterize another molecule, EOL-1, that suppresses learning induced by pathogenic bacteria. These and more examples suggest that inhibition in *C. elegans*, similar as in other organisms (Abel et al., 1998), serves as an important part of the regulatory mechanism underlying neural plasticity.

It might not be obvious why an animal with only 302 neurons would develop a complex molecular network that regulates learning bi-directionally. In particular, since learning to avoid the smells of pathogenic bacteria appears to improve animal's fitness, why were the negative regulators not selected against as deleterious alleles? This may be explained by the sophisticated interaction between the genome and the environment: In its natural habitat soil or compost, *C. elegans* relies on chemosensation to detect and choose different bacteria foods (Bargmann, 2006b; Zhang, 2008). Some bacteria are potentially harmful and consumption of them causes infection (Zhang et al., 2005; Zhang, 2008), but the benefit of learning to avoid such hazardous foods depends on the availability of alternative food sources, the often-dynamic environmental condition, severity of infection, and the status of the animal population. For example, when a high-density population of animals encounters a harsh environment with very limited benign food, developing a strong aversion to mildly toxic food sources too early may not be the best strategy for survival. It is partially illustrated by the differential expression of learning-related ILPs under different conditions: the expression of learning-enabling INS-6 in ASI is switched off by dauer-inducing cues, whereas the expression of learning-inhibiting INS-7 in URX is increased (Cornils et al., 2011; Chen et al., 2013). Thus, the ASI and URX neurons may signal differently,

depending on the environmental cues, to the learning circuit to guide animal's olfactory response.

Likewise, the inhibitory role of EOL-1 may add an additional dimension of flexibility in regulating learning. In a complex environment, enhanced learning does not always equal to enhanced fitness. A lesson learned from experience would have little adaptive value unless the present context is taken into consideration.

Materials and Methods

Strains

C. elegans strains were maintained under standard conditions at 20ºC (Brenner, 1974). Hermaphrodites were used in the study. The strains used in this study include: N2, ZC1063 *dol-1(yx14)*, ZC1064 *eol-2(yx15)*, ZC1279 *eol-1(yx29)*V*,* ZC361 *lin-15B(n765)*X; *kyIs30*, QZ120 *daf-2(e1368)*III, CX4998 *kyIs140*I; *nsy-1(ky397)*II, CB61 *dpy-5(e61)*I, NC300 *dpy-20(e1282)*IV; *wdIs5*[*Punc-4::gfp*; *dpy-20(+)*], CX3300 *lin-15 (n765ts)*X; *kyIs51*[*Podr-2b::gfp; lin-15(+)*], FX06514 *T26F2.3(tm6514)*V, FX02422 *dom-3(tm2422)*I, ZC1533 *yxIs13; yxEx744*[*Pgcy-36::mCherry*; *Punc-122::gfp*], ZC1683 *eol-1(yx29)*V; *yxEx858*[cosmid T26F2; *Punc-122::gfp*], ZC1726 *eol-1(yx29)*V; *yxEx891*[genomic PCR *T26F2.3*; *Punc-122::gfp*], ZC1925 *yxEx970*[*Peol-1::gfp*; *Punc-122::dsred*], ZC1957 *yxEx744*; *yxEx970*, ZC2027 *eol-1(yx29)*V; *yxEx1058*[*Peol-1::eol-1::gfp*; *Punc-122::gfp*], ZC2039 *eol-1(yx29)*V; *yxEx1067*[*Pgcy-36::eol-1::gfp*; *Punc-122::gfp*], ZC2046 *wdIs5*; *yxEx1018*[*Peol-1::mCherry*; *Punc-122::gfp*], ZC2053 *yxEx1068*[*Pgcy-36::eol-1::gfp*; *Punc-122::gfp*]; *yxEx1018*[*Peol-1::mCherry*; *Punc-122::gfp*], ZC2124 *yxEx1129*[*Peol-1::eol-1::gfp*], ZC2157 *yxEx1137*[*Pxrn-2::gfp; Punc-122::dsred*]; *yxEx1018*[*Peol-1::mCherry; Punc-122::gfp*], ZC2172 *yxEx1161*[*Peol-1::eol-1RNAi*; *Punc-122::gfp*], ZC2243 *eol-1(yx29)*V; *yxEx1183*[*Pflp-8::eol-1::gfp*; *Punc-122::gfp*], CX7102 *lin-15(n765)*X; *qaIs2241*[*Pgcy-36::egl-1*; *Pgcy-35::gfp*; *lin-15(+)*]X, ZC2202 *yxEx1171*[*Peol-1::gfp*], ZC2353 *eol-1(yx29)*V; *yxEx1224*[*Peol-1::Dom3z.b* cDNA; *Punc-122::gfp*], ZC2456 *eol-1(yx29)*V; *yxEx1268*[*Peol-1::eol-1*(E185A, D187A)*::gfp*; *Punc-122::gfp*], ZC2459 *eol-1(yx29)*V; *yxEx1274*[*Peol-1::Dom3z.b*(E234A, D236A); *Punc-122::gfp*].

Molecular biology and germ-line transformation

For rescue experiments, cosmids C13C4, ZC443, T26F2, C53A5 and F09E10 (Wellcome Trust Sanger Institute) were injected into *yx29* at 15 ng/µl. Full-length genomic sequences were amplified from the wild-type genome by polymerase chain reaction (PCR) and injected at 23ng/µl (*srh-104*) or 15ng/µl (*eol-1*). Microinjection was performed as described (Mello et al., 1991) with either *Punc-122::gfp* or *Punc-122::dsred* as a co-injection marker.

To clone *eol-1*, the *unc-54* 3'UTR in *pPD95.77* was replaced by the *eol-1* 3' cis-regulatory sequence and a Gateway recombination cassette (rfB) (Invitrogen) was ligated upstream of GFP to produce *pPD95.77-rfB-gfp*. The coding sequence of *eol-1* was amplified and cloned into this vector to produce *pPD95.77-rfB-eol-1-gfp*. The 908 bp 5' region upstream of *eol-1* was amplified from N2 genomic DNA and cloned into *pCR8* to generate the entry clone. Recombination reactions were performed according to the manufacturer's instructions, producing *Peol-1::gfp*, *Peol-1::eol-1::gfp*, *Pgcy-36::eol-1::gfp* and *Pflp-8::eol-1::gfp*. For the mouse *Dom3z* cDNA rescue, *Dom3z.b* cDNA sequence was reverse transcribed from the mouse neuronal RNA library and cloned to generate *Peol-1::Dom3z.b*. Nucleotide mutations were introduced using QuickChange® Site-Directed Mutagenesis Kit (Life Technologies). Plasmids were injected at 10 ng/µl unless otherwise specified to generate transgenic lines.

Cell-specific RNAi constructs were generated as described (Esposito et al., 2007). In brief, the 5' region upstream of *eol-1* was fused to an axon-rich region of the *eol-1* gene to generate sense and anti-sense PCR fusion constructs. The fusion products were injected at 50 ng/µl with 25 ng/µl *Punc-122::gfp* into wild-type germ line.

Aversive olfactory learning assay

Control and training plates were prepared by inoculating 10-cm NGM-agar (nematode growth medium) plates with 0.5 ml overnight NGM culture of *E. coli* OP50 or *P. aeruginosa* PA14, respectively, and incubating at 26 °C for 40-45 hours. On the day of assay, adult animals were transferred onto a control plate or a training plate for 4-5 hours at room temperature. Animals were then washed briefly in NGM buffer and tested in the microdroplet assay.

Microdroplet assay was performed as previously described (Ha, 2010). In brief, 12 adult animals were placed individually into microdroplets of NGM buffer and subjected to alternating airstreams odorized with over-night culture of OP50 or PA14. The behavioral responses were recorded by a CCD camera at 10 Hz and analyzed by a machine-vision software written in MATLAB (MathWorks, Natick, MA). The average turning rate (frequency of "Ω" bends) of three animals of the identical genotype and treatment in each assay was used to generate the following indexes. The indexes from multiple assays were used for statistical analysis.

I (Turning frequency) = number of Ω bends/time (second)

Preference index = $(I_{OP50} - I_{PA14})/(I_{OP50} + I_{PA14})$

Learning index = Preference index (naive) – Preference index (trained)

Mutagenesis, screen and mutant identification

Wild-type hermaphrodites enriched at L4 stage (P0) were soaked in 0.5% ethanemethylsulfonate (EMS)- M9 solution for 4 hours and then washed 5 times with M9 buffer. After recovering for 24 hours on a regular culture plate, 100 EMS-treated P0s were transferred to a fresh plate to reproduce. 600 F1 (*i.e.* progeny of P0) animals were isolated and about 2,300 F2 (*i.e.* progeny of F1) were individually isolated to generate a clonal mutant library. Mutants that were lethal, sterile, morphologically deformed or severely uncoordinated in locomotion were

excluded; olfactory learning was analyzed in the remaining 1,072 F2 clones with the microdroplet assay.

The allele *yx29* was one of the several mutant clones isolated from the screen. It was 4× outcrossed with an essentially wild-type strain ZC361 that expresses a GFP reporter and sequenced by Illumina Hi-Seq2000 (paired-ends, 100bp read length). Sequencing reads were aligned to the WS220 reference genome by ELAND and STAMPY; 41 consensus variants were identified in *yx29* using the reads from the parental wild type and ZC361 as controls. The variants of confidence were annotated based on the online Ensembl Genome Browser, *C. elegans* WS220; variants localized to coding regions were prioritized in further analysis.

Fluorescence microscopy

Fluorescent images were collected with a Nikon Eclipse TE2000-U at 40× magnification or with an Olympus FV1000A confocal microscope at 20× or 60× magnification. For cell ID, animals expressing *Peol-1::gfp*, *Peol-1::eol-1::gfp* or *Peol-1::mCherry* were crossed with transgenic animals expressing a different fluorescence reporter under cell-specific promoters. Images were processed with Image J (NIH).

Slow killing assay

The pathogen resistance of *C. elegans* strains to *P. aeruginosa* PA14 was determined using a slow killing assay essentially as described (Tan et al., 1999) with minor modifications. Briefly, 50 µl of overnight lysogeny broth (LB) culture of PA14 was spread onto a 5-cm NGM-agar plate and incubated at 37°C for 24 hours. 15-20 L4-stage hermaphrodites were placed on each plate, kept at 25°C and scored every 6-7 hours. Animals that escaped or died on the wall of the plates were censored.

Chemotaxis assay

2-nonanone avoidance assay was performed as previously described (Troemel et al., 1997; Chao et al., 2004). In brief, synchronized adults were washed off and seeded to the center of a square NGM plate with either pure 2-nonanone or dissolvent control at each end. Animals were let move freely for 1 hour before counting. 1-octanol avoidance assay was performed as described (Chao et al., 2004; Harris et al., 2009). Adult animals were individually transferred to an OP50 assay plate and presented with pure 1-octanol on the tip of a brush hair (Loew-Cornell 9000 Kolinsky 8 paintbrush) during forward movement. Time to reverse was measured for each animal.

Food-enhanced butanone chemotaxis assay was performed essentially as described (Torayama et al., 2007). Synchronized adults were transferred to *E. coli* OP50 plates with or without exposure to 10^{-2} butanone; after 2 hours, animals were tested in standard chemotaxis assays with 10^{-4} butanone.

Biochemistry

Lysates of *C. elegans* animals were prepared as follows: animals grown on 10-cm plates were washed off with ice-cold M9 buffer and resuspended in ice-cold homogenization buffer [100 mM NaCl; 25 mM HEPES, pH 7.5; 250 µM EDTA, pH 8.0; 0.1% (w/v) NP-40; 2 mM DTT, 1 tablet per 10 mL buffer of Complete Mini Protease Inhibitor (Roche)]. The mixture was sonicated with 10× 0.5 second pulses and 10× 0.5 second rests for 12 rounds. Lysates were spinned at 16,000× g for 15 min at 4 ºC and the supernatant was collected and frozen at -80 ºC.

co-Immunoprecipitation (co-IP) was performed using standard protocols. In brief, magnetic beads conjugated with antibodies against 3× HA tags or GFP were pre-washed in

homogenization buffer and incubated with the supernatant of worm lysates for 2 hours at 4 ºC. After incubation, 20 µl of supernatant was taken from each sample as controls, and the beads were washed 3× with PNK buffer (50 mM Tris pH7.4; 10 mM $MgCl_2$; 0.5% NP-40). Beads were then resuspended in sample buffer and boiled at 95ºC for 5 minutes. The samples were spinned again, and supernatants were analyzed by SDS-PAGE and western blot.

For western blot, PVDF membranes were blocked with 5% milk for 30 min and incubated with monoclonal antibodies against GFP (1:1000) or 3× HA (1:2000) at 4 ºC overnight. Membranes were then washed in PBS and incubated with anti-mouse IgG (1:5000) at room temperature for 1 hour. Protein signals were detected by the HRP-ECL system with Kodak film. The 3×HA tag was optimized for *C. elegans* by the Henikoff lab.DNA sequence: tacccatacgacgttccagactatgccggctacccctatgatgtcccggactatgcaggatcttatccatatgacgtcccagattacgct Protein sequence: YPYDVPDYAGYPYDVPDYAGSYPYDVPDYA.

Acknowledgements

I thank the *Caenorhabditis* Genetics Center (funded by NIH Office of Research Infrastructure Programs P40 OD010440) and the *C. elegans* Gene Knockout Consortium for strains, the Wellcome Trust Sanger Institute for cosmids, Dr. C. Daly for whole-genome sequencing, Dr. J. Zhang for sequencing data analysis, Drs. V. Poon, P. McGrath, B. Lesch, A. Boyanov, C. Fang-Yen and C. Gabel for sharing protocols and programs, Dr. S. Sarin for the mouse neuronal RNA library, Dr. J. Calarco for assistance in biochemistry experiments, C. Zhong for assistance in behavioral assays, and the Zhang lab members for discussion. J.A.C. is supported by an NIH Early Independence Award and Harvard University. Y.Z. is supported by The Esther A. and Joseph Klingenstein Fund, March of Dimes Foundation, The Alfred P. Sloan Foundation, The John Merck Fund and NIH.

References

Abel T, Martin KC, Bartsch D, Kandel ER (1998) Memory suppressor genes: inhibitory constraints on the storage of long-term memory. Science 279:338-341.

Abel T, Nguyen PV, Barad M, Deuel TA, Kandel ER, Bourtchouladze R (1997) Genetic demonstration of a role for PKA in the late phase of LTP and in hippocampus-based long-term memory. Cell 88:615-626.

Ardiel EL, Rankin CH (2010) An elegant mind: learning and memory in Caenorhabditis elegans. Learning & memory 17:191-201.

Bargmann CI (2006) Chemosensation in C. elegans. WormBook:1-29.

Bartsch D, Casadio A, Karl KA, Serodio P, Kandel ER (1998) CREB1 encodes a nuclear activator, a repressor, and a cytoplasmic modulator that form a regulatory unit critical for long-term facilitation. Cell 95:211-223.

Bartsch D, Ghirardi M, Skehel PA, Karl KA, Herder SP, Chen M, Bailey CH, Kandel ER (1995) Aplysia CREB2 represses long-term facilitation: relief of repression converts transient facilitation into long-term functional and structural change. Cell 83:979-992.

Brenner S (1974) The genetics of Caenorhabditis elegans. Genetics 77:71-94.

Brunelli M, Castellucci V, Kandel ER (1976) Synaptic facilitation and behavioral sensitization in Aplysia: possible role of serotonin and cyclic AMP. Science 194:1178-1181.

Chalfie M, Jorgensen EM (1998) C. elegans neuroscience: genetics to genome. Trends Genet 14:506-512.

Chang AJ, Chronis N, Karow DS, Marletta MA, Bargmann CI (2006) A distributed chemosensory circuit for oxygen preference in C. elegans. PLoS Biol 4:e274.

Chang JH, Jiao X, Chiba K, Oh C, Martin CE, Kiledjian M, Tong L (2012) Dxo1 is a new type of eukaryotic enzyme with both decapping and 5'-3' exoribonuclease activity. Nat Struct Mol Biol 19:1011-1017.

Chao MY, Komatsu H, Fukuto HS, Dionne HM, Hart AC (2004) Feeding status and serotonin rapidly and reversibly modulate a Caenorhabditis elegans chemosensory circuit. Proc Natl Acad Sci U S A 101:15512-15517.

Chatterjee S, Grosshans H (2009) Active turnover modulates mature microRNA activity in Caenorhabditis elegans. Nature 461:546-549.

Chen A, Muzzio IA, Malleret G, Bartsch D, Verbitsky M, Pavlidis P, Yonan AL, Vronskaya S, Grody MB, Cepeda I, Gilliam TC, Kandel ER (2003) Inducible enhancement of memory storage and synaptic plasticity in transgenic mice expressing an inhibitor of ATF4 (CREB-2) and C/EBP proteins. Neuron 39:655-669.

Chen Z, Hendricks M, Cornils A, Maier W, Alcedo J, Zhang Y (2013) Two insulin-like peptides antagonistically regulate aversive olfactory learning in C. elegans. Neuron 77:572-585.

Chou JH, Bargmann CI, Sengupta P (2001) The Caenorhabditis elegans odr-2 gene encodes a novel Ly-6-related protein required for olfaction. Genetics 157:211-224.

Cornils A, Gloeck M, Chen Z, Zhang Y, Alcedo J (2011) Specific insulin-like peptides encode sensory information to regulate distinct developmental processes. Development 138:1183-1193.

Dash PK, Hochner B, Kandel ER (1990) Injection of the cAMP-responsive element into the nucleus of Aplysia sensory neurons blocks long-term facilitation. Nature 345:718-721.

Decker CJ, Parker R (1993) A turnover pathway for both stable and unstable mRNAs in yeast: evidence for a requirement for deadenylation. Genes & development 7:1632-1643.

Dunckley T, Parker R (1999) The DCP2 protein is required for mRNA decapping in Saccharomyces cerevisiae and contains a functional MutT motif. EMBO J 18:5411-5422.

Esposito G, Di Schiavi E, Bergamasco C, Bazzicalupo P (2007) Efficient and cell specific knock-down of gene function in targeted C. elegans neurons. Gene 395:170-176.

Fischer PM (2009) Cap in hand: targeting eIF4E. Cell cycle 8:2535-2541.

Frand AR, Russel S, Ruvkun G (2005) Functional genomic analysis of C. elegans molting. PLoS Biol 3:e312.

Genoux D, Haditsch U, Knobloch M, Michalon A, Storm D, Mansuy IM (2002) Protein phosphatase 1 is a molecular constraint on learning and memory. Nature 418:970-975.

Ghosh A, Lima CD (2010) Enzymology of RNA cap synthesis. Wiley Interdiscip Rev RNA 1:152-172.

Gingras AC, Raught B, Sonenberg N (1999) eIF4 initiation factors: effectors of mRNA recruitment to ribosomes and regulators of translation. Annual review of biochemistry 68:913-963.

Goodfellow IG, Roberts LO (2008) Eukaryotic initiation factor 4E. The international journal of biochemistry & cell biology 40:2675-2680.

Gray JM, Karow DS, Lu H, Chang AJ, Chang JS, Ellis RE, Marletta MA, Bargmann CI (2004) Oxygen sensation and social feeding mediated by a C. elegans guanylate cyclase homologue. Nature 430:317-322.

Ha HI, Hendricks M, Shen Y, Gabel CV, Fang-Yen C, Qin Y, Colon-Ramos D, Shen K, Samuel AD, Zhang Y (2010) Functional organization of a neural network for aversive olfactory learning in Caenorhabditis elegans. Neuron 68:1173-1186.

Harris GP, Hapiak VM, Wragg RT, Miller SB, Hughes LJ, Hobson RJ, Steven R, Bamber B, Komuniecki RW (2009) Three distinct amine receptors operating at different levels within the locomotory circuit are each essential for the serotonergic modulation of chemosensation in Caenorhabditis elegans. J Neurosci 29:1446-1456.

Ikeda DD, Duan Y, Matsuki M, Kunitomo H, Hutter H, Hedgecock EM, Iino Y (2008) CASY-1, an ortholog of calsyntenins/alcadeins, is essential for learning in Caenorhabditis elegans. Proc Natl Acad Sci U S A 105:5260-5265.

Ishihara T, Iino Y, Mohri A, Mori I, Gengyo-Ando K, Mitani S, Katsura I (2002) HEN-1, a secretory protein with an LDL receptor motif, regulates sensory integration and learning in Caenorhabditis elegans. Cell 109:639-649.

Jiao X, Chang JH, Kilic T, Tong L, Kiledjian M (2013) A mammalian pre-mRNA 5' end capping quality control mechanism and an unexpected link of capping to pre-mRNA processing. Mol Cell 50:104-115.

Jiao X, Xiang S, Oh C, Martin CE, Tong L, Kiledjian M (2010) Identification of a quality-control mechanism for mRNA 5'-end capping. Nature 467:608-611.

Kandel ER (2012) The molecular biology of memory: cAMP, PKA, CRE, CREB-1, CREB-2, and CPEB. Mol Brain 5:14.

Lickteig KM, Duerr JS, Frisby DL, Hall DH, Rand JB, Miller DM, 3rd (2001) Regulation of neurotransmitter vesicles by the homeodomain protein UNC-4 and its transcriptional corepressor UNC-37/groucho in Caenorhabditis elegans cholinergic motor neurons. J Neurosci 21:2001-2014.

Liu H, Kiledjian M (2006) Decapping the message: a beginning or an end. Biochem Soc Trans 34:35-38.

Liu X, Krause WC, Davis RL (2007) GABAA receptor RDL inhibits Drosophila olfactory associative learning. Neuron 56:1090-1102.

Luo L, Gabel CV, Ha HI, Zhang Y, Samuel AD (2008) Olfactory behavior of swimming C. elegans analyzed by measuring motile responses to temporal variations of odorants. J Neurophysiol 99:2617-2625.

Macosko EZ, Pokala N, Feinberg EH, Chalasani SH, Butcher RA, Clardy J, Bargmann CI (2009) A hub-and-spoke circuit drives pheromone attraction and social behaviour in C. elegans. Nature 458:1171-1175.

Mello CC, Kramer JM, Stinchcomb D, Ambros V (1991) Efficient gene transfer in C.elegans: extrachromosomal maintenance and integration of transforming sequences. EMBO J 10:3959-3970.

Merrick WC (2004) Cap-dependent and cap-independent translation in eukaryotic systems. Gene 332:1-11.

Meyer S, Temme C, Wahle E (2004) Messenger RNA turnover in eukaryotes: pathways and enzymes. Crit Rev Biochem Mol Biol 39:197-216.

Morrison GE, Wen JY, Runciman S, van der Kooy D (1999) Olfactory associative learning in Caenorhabditis elegans is impaired in lrn-1 and lrn-2 mutants. Behavioral neuroscience 113:358-367.

Papassotiropoulos A, Stephan DA, Huentelman MJ, Hoerndli FJ, Craig DW, Pearson JV, Huynh KD, Brunner F, Corneveaux J, Osborne D, Wollmer MA, Aerni A, Coluccia D, Hanggi J, Mondadori CR, Buchmann A, Reiman EM, Caselli RJ, Henke K, de Quervain DJ (2006) Common Kibra alleles are associated with human memory performance. Science 314:475-478.

Sasakura H, Mori I (2013) Behavioral plasticity, learning, and memory in C. elegans. Curr Opin Neurobiol 23:92-99.

Sharma SK, Bagnall MW, Sutton MA, Carew TJ (2003) Inhibition of calcineurin facilitates the induction of memory for sensitization in Aplysia: requirement of mitogen-activated protein kinase. Proc Natl Acad Sci U S A 100:4861-4866.

Shatkin AJ (1976) Capping of eucaryotic mRNAs. Cell 9:645-653.

Song MG, Li Y, Kiledjian M (2010) Multiple mRNA decapping enzymes in mammalian cells. Mol Cell 40:423-432.

Stevens A, Poole TL (1995) 5'-exonuclease-2 of Saccharomyces cerevisiae. Purification and features of ribonuclease activity with comparison to 5'-exonuclease-1. J Biol Chem 270:16063-16069.

Tan MW, Mahajan-Miklos S, Ausubel FM (1999) Killing of Caenorhabditis elegans by Pseudomonas aeruginosa used to model mammalian bacterial pathogenesis. Proc Natl Acad Sci U S A 96:715-720.

Topisirovic I, Svitkin YV, Sonenberg N, Shatkin AJ (2011) Cap and cap-binding proteins in the control of gene expression. Wiley Interdiscip Rev RNA 2:277-298.

Torayama I, Ishihara T, Katsura I (2007) Caenorhabditis elegans integrates the signals of butanone and food to enhance chemotaxis to butanone. J Neurosci 27:741-750.

Troemel ER, Kimmel BE, Bargmann CI (1997) Reprogramming chemotaxis responses: sensory neurons define olfactory preferences in C. elegans. Cell 91:161-169.

Voglis G, Tavernarakis N (2008) A synaptic DEG/ENaC ion channel mediates learning in C. elegans by facilitating dopamine signalling. EMBO J 27:3288-3299.

Wemmie JA, Coryell MW, Askwith CC, Lamani E, Leonard AS, Sigmund CD, Welsh MJ (2004) Overexpression of acid-sensing ion channel 1a in transgenic mice increases acquired fear-related behavior. Proc Natl Acad Sci U S A 101:3621-3626.

White JG, Southgate E, Thomson JN, Brenner S (1986) The structure of the nervous system of the nematode Caenorhabditis elegans. Philos Trans R Soc Lond B Biol Sci 314:1-340.

Xiang S, Cooper-Morgan A, Jiao X, Kiledjian M, Manley JL, Tong L (2009) Structure and function of the 5'-->3' exoribonuclease Rat1 and its activating partner Rai1. Nature 458:784-788.

Xue Y, Bai X, Lee I, Kallstrom G, Ho J, Brown J, Stevens A, Johnson AW (2000) Saccharomyces cerevisiae RAI1 (YGL246c) is homologous to human DOM3Z and encodes a protein that binds the nuclear exoribonuclease Rat1p. Mol Cell Biol 20:4006-4015.

Yamada K, Hirotsu T, Matsuki M, Butcher RA, Tomioka M, Ishihara T, Clardy J, Kunitomo H, Iino Y (2010) Olfactory plasticity is regulated by pheromonal signaling in Caenorhabditis elegans. Science 329:1647-1650.

Yin JC, Wallach JS, Del Vecchio M, Wilder EL, Zhou H, Quinn WG, Tully T (1994) Induction of a dominant negative CREB transgene specifically blocks long-term memory in Drosophila. Cell 79:49-58.

Zhang X, Zhang Y (2012) DBL-1, a TGF-beta, is essential for Caenorhabditis elegans aversive olfactory learning. Proc Natl Acad Sci U S A 109:17081-17086.

Zhang Y (2008) Neuronal mechanisms of Caenorhabditis elegans and pathogenic bacteria interactions. Curr Opin Microbiol 11:257-261.

Zhang Y, Lu H, Bargmann CI (2005) Pathogenic bacteria induce aversive olfactory learning in Caenorhabditis elegans. Nature 438:179-184.

Zimmer M, Gray JM, Pokala N, Chang AJ, Karow DS, Marletta MA, Hudson ML, Morton DB, Chronis N, Bargmann CI (2009) Neurons detect increases and decreases in oxygen levels using distinct guanylate cyclases. Neuron 61:865-879.

Appendix

Publications

Shen Y, Zhang J, Calarco J, Zhang Y. EOL-1, the homolog of the mammalian Dom3Z, regulates olfactory learning in *C. elegans*. *The Journal of Neuroscience*, 2014 Oct 1;34(40):13364-70

Harris G, **Shen Y**, Ha H, Donato A, Wallis S, Zhang X, Zhang Y. Dissecting the signaling mechanisms underlying recognition and preference of food odors. *The Journal of Neuroscience*. 2014 Jul 9;34(28):9389-403

Fernandes de Abreu DA, Caballero A, et al. **Shen Y**, Fontana W, Lu H, Csikasz-Nagy A, Murphy CT, Antebi A, Blanc E, Apfeld J, Zhang Y, Alcedo J, Ch'ng Q. An insulin-to-insulin regulatory network orchestrates phenotypic specificity in development and physiology. *PLoS Genetics.* 2014 Mar 27;10(3):e1004225.

Ma X, **Shen Y**. Structural basis for degeneracy among thermosensory neurons in *Caenorhabditis elegans*. *The Journal of Neuroscience*. 2012 Jan 4;32(1):1-3.

Ha HI, Hendricks M, **Shen Y**, Gabel CV, Fang-Yen C, Qin Y, Colón-Ramos D, Shen K, Samuel AD, Zhang Y. Functional organization of a neural network for aversive olfactory learning in *Caenorhabditis elegans. Neuron.* 2010 Dec 22;68(6):1173-86.

Shen Y*, Wen Q*, Zhong C, Qin Y, Kawano T, Samuel ADT, Zhang Y. A gain control mechanism in *C. elegans* locomotory gait. Manuscript in preparation. *: co-first author

Conference Abstracts

Shen Y, Wen Q, Zhong C, Qin Y, Samuel ADT, Zhang Y. Oral presentation at the *C. elegans* Neurobiology Meeting, July 7-10, 2014, Madison, WI, USA.

Shen Y, Zhang J, Calarco J, Zhang Y. Oral presentation at the 19th International *C. elegans* Meeting, June 26-30, 2013, Los Angles, CA, USA.

Shen Y, Ha HI, Zhang Y. Poster presentation at the Cold Spring Harbor Laboratory meeting *"Synapses: From Molecules to Circuits & Behavior"* April 12-16, 2011, NY, USA

Shen Y, Zhang J, Calarco J, Zhang Y. Poster presentation at the *C. elegans* Neurobiology Meeting, June 27-30, 2010, Madison, WI, USA.